63-2-3

1 December 1962

Report No. 0162-01TN-16

ANALYSIS OF THE FLOW OF GAS-PARTICLE MIXTURES IN TWO-DIMENSIONAL AND AXISYMMETRIC NOZZLES

AFBSD Technical Note BSD-TDR-62-144

Contract No. AF 33(600)-36610

AEROJET-GENERAL CORPORATION
SOLID ROCKET PLANT • SACRAMENTO, CALIFORNIA
A SUBSIDIARY OF THE GENERAL TIRE & RUBBER COMPANY

COPY NO. 23

W. O. 0380

TECHNICAL NOTE
AFBSD-TDR-62-144
AFBM Exhibit 58-1

1 December 1962

ANALYSIS OF THE FLOW OF GAS-PARTICLE MIXTURES IN TWO-DIMENSIONAL AND AXISYMMETRIC NOZZLES

Aerojet-General Report No. 0162-01TN-16

AEROJET-GENERAL CORPORATION
Sacramento, California

AFBSD Technical Note BSD-TDR-62-144

Contract No. AF 33(600)-36610

Prepared for

HQ., AIR FORCE BALLISTIC SYSTEMS DIVISION
AIR FORCE SYSTEMS COMMAND, USAF
AIR FORCE UNIT POST OFFICE
Los Angeles 45, California
Atten: Tech Data Center

Approved by:

C. C. Conway, Manager
Minuteman Program

AEROJET GENERAL

SOLID ROCKET PLANT SACRAMENTO, CALIFORNIA

A SUBSIDIARY OF THE GENERAL TIRE & RUBBER COMPANY

PREFACE

Acknowledgment is made to J.D. Hoffman, Development Engineer, author of this report, and to O.J. Demuth, Manager, Aerophysics Department, and S.A. Lorenc, Supervisor, Fluid Mechanics and Special Studies Section, for their assistance in the preparation of material; and to R.R. Edminster, Computing Analyst, for assistance in the development of the digital computer program. Technical editors were L.O. Fagan Jr., and D.P. Campbell.

ABSTRACT

From theoretical studies of two-phase flow of gas-particle mixtures in rocket nozzles, the governing equations for two-dimensional and axisymmetrical flows have been derived. Characteristic equations have been put into finite difference form and a mathematical model has been developed for a general interior point in the supersonic flow field. The subsonic and transonic flow fields have been investigated. To integrate the subsonic, transonic, and supersonic solutions, a mathematical model will be programed for the IBM 7090 computer that will determine nozzle performance for given nozzle contour and motor conditions.

TABLE OF CONTENTS

		Page No.
I.	Introduction	1
II.	Summary	1
III.	Technical Discussion	2
	A. Equations Governing Gas-Particle Mixtures	2
	B. Characteristic Equations	6
	C. Subsonic Solution	7
	D. Transonic Solution	12
	E. Supersonic Solution	19
	F. Finite-Difference Equations	22
	G. Interior Point Numerical Example	23
IV.	Conclusions	24
V.	Recommendations For Future Work	25
VI.	Nomenclature	26
VII.	Bibliography	34

FIGURE LIST

	Figure No.
One-Dimensional Sink-Flow Model	1
Constant-Lag Transonic Flow Model	2
Transonic Characteristic Curves	3
Special Cases of Supersonic Flow	4
Interior Point Characteristic Net	5

APPENDIXES

	Appendix
Derivation of Equations Governing Gas-Particle Mixtures	A
Method of Characteristics	B
Determination of the Characteristics of a Gas-Particle Mixture	C
General One-Dimensional Flow of a Gas-Particle Mixture	D
Constant-Lag One-Dimensional Flow of a Gas-Particle Mixture	E
Transonic Flow Approximation	F
Derivation of the Finite-Difference Equations	G
Numerical-Solution Procedure for Computer Program	H
Example Calculation for Verification of Computer Program	I

I. INTRODUCTION

Liquid or solid particles, or a combination of the two, exist in the exhaust products of solid propellants when powdered metals are used as fuel additives. These additives are included in the propellant formula for several reasons, the foremost being to increase the energy release of the propellant and to prevent combustion instability.

However, several important deleterious effects occur when condensable products are formed in the exhaust gases as a result of having metal additivies in the propellant. Significant performance losses occur because the drag of the gas on the particles is irreversible; the thermal-energy content of the particles transfers to the gas by convection and, to some degree, by radiation, which requires a finite amount of time. Since the particles pass through the nozzle very rapidly, this energy transfer does not have time to take place completely, and a significant amount of the thermal energy of the particles is lost. Impingement of particles on the nozzle wall, affecting the heat transfer rates and causing erosion of the wall, alters the internal configuration of the nozzle and results in a change in performance.

To minimize these effects, it is necessary to predict the effects of various geometric and gas-dynamic parameters on the performance of a gas-particle mixture. The objective of this study was to develop an analytical technique for determining the effects of particles on nozzle performance and design.

II. SUMMARY

This report presents a theoretical discussion of the two-phase flow of gas-particle mixtures in rocket nozzles and shows the derivation of the governing equations for two-dimensional and axisymmetric flows. Characteristic

II, Summary (cont.)

equations are put into finite-difference form. A numerical solution procedure, developed for a general interior point in the supersonic flow field, has been programed for the IBM 7090 computer. Correctness of the computer program has been verified through hand calculation of the numerical solution derived for the IBM 7090.

A method has been developed for determining the subsonic flow field on the basis of a one-dimensional sink-flow approximation. The transonic flow field has been approximated by a power-series solution of the linearized system equations for constant kinetic and thermal lags of the particles.

A method is then suggested for integrating the subsonic, transonic, and supersonic solutions into a computer program with which nozzle performance for given chamber conditions and nozzle contour can be determined.

This report indicates that status of gas-particle-flow studies as of February 1962. Since that date significant progress has been made on a program that integrates the subsonic, transonic, and supersonic solutions into one IBM 7090 computer program with which overall nozzle performance can be evaluated. The program enables study of several particle sizes and chemical species. The thermodynamic and flow properties of the gas and particles are evaluated as a function of temperature. Frozen or shifting chemical equilibrium can be studied by specifying the appropriate speed of sound as a function of gas temperature. Studies can be made at any point in the nozzle if a supersonic starting line can be determined by the use of other techniques. Currently, this program has been limited to conventional de Laval nozzles.

III. TECHNICAL DISCUSSION

A. EQUATIONS GOVERNING GAS-PARTICLE MIXTURES

1. Basic Assumptions

III, A, Equations Governing Gas-Particle Mixtures (cont.)

Derivation of the equations governing gas-particle mixtures is given in Appendix A. These equations were derived on the basis of the following assumptions:

a. The particles are spherical and all the same size.

b. The total mass of the gas-particle mixture is constant.

c. The total energy of the gas-particle mixture is constant.

d. The internal temperature of the particle is uniform, and the particle specific heat is constant.

e. The gas and particles exchange thermal energy by convection only.

f. The gas obeys the perfect-gas law, has a constant molecular weight, and has constant specific heats.

g. All external forces except pressure of the gas and drag of the particles are neglected.

h. The gas is inviscid except for the drag it exerts on the particles.

i. The particles do not interact with each other.

j. The volume occupied by the particles is negligible.

III, A, Equations Governing Gas-Particle Mixtures (cont.)

2. Governing Equations

For two-dimensional ($\sigma = 1, \sigma_y = 0$) and axisymmetric ($\sigma = y, \sigma_y = 1$) steady flows, the governing equations are:

$$\rho_g(u_g)_x + \rho_g(v_g)_y + u_g(\rho_g)_x + v_g(\rho_g)_y = -\sigma_y \frac{\rho_g v_g}{\sigma} \tag{1}$$

$$\rho_p(u_p)_x + \rho_p(v_p)_y + u_p(\rho_p)_x + v_p(\rho_p)_y = -\sigma_y \frac{\rho_p v_p}{\sigma} \tag{2}$$

$$\rho_g \left[u_g(u_g)_x + v_g(u_g)_y \right] + A\rho_p(u_g - u_p) + (P_g)_x = 0 \tag{3}$$

$$\rho_g \left[u_g(v_g)_x + v_g(v_g)_y \right] + A\rho_p(v_g - v_p) + (P_g)_y = 0 \tag{4}$$

$$u_g(P_g)_x + v_g(P_g)_y - a^2 \left[u_g(\rho_g)_x + v_g(\rho_g)_y \right] - A\rho_p B = 0 \tag{5}$$

$$u_p(u_p)_x + v_p(u_p)_y = A(u_g - u_p) \tag{6}$$

$$u_p(v_p)_x + v_p(v_p)_y = A(v_g - v_p) \tag{7}$$

$$u_p(h_p)_x + v_p(h_p)_y = -\frac{2}{3} AC(T_p - T_g) \tag{8}$$

$$P_g = \rho_g R T_g \tag{9}$$

III, A, Equations Governing Gas-Particle Mixtures (cont.)

$$T_p = f(h_p) \quad \text{Tabulated,} \tag{10}$$

$$a^2 = \gamma_g R T_g \tag{11}$$

$$M^2 = \frac{(u_g^2 + v_g^2)}{a^2} \tag{12}$$

$$\mu_g = \mu_o T_g^{\alpha} \tag{13}$$

$$A = \frac{9}{2} \frac{\mu_g f}{m_p r_p^2} \tag{14}$$

$$B = (\gamma_g - 1)\left[(u_g - u_p)^2 + (v_g - v_p)^2 + \frac{2}{3} C (T_p - T_g) \right] \tag{15}$$

$$C = \frac{g}{f} \frac{C_{pg}}{Pr} \tag{16}$$

III, Technical Discussion (cont.)

B. CHARACTERISTIC EQUATIONS

By the use of the method of characteristics as discussed in Appendix B and developed in detail in Appendix C, the characteristic equations for the above system of quasi-linear partial differential equations (equation 1 through 8) were found to be:

1. Along Gas Streamlines

$$\frac{dy}{dx} = \frac{v_g}{u_g} \tag{17}$$

$$\rho_g\left[u_g du_g + v_g dv_g\right] + dP_g = -A\rho_p\left[(u_g - u_p)\,dx + (v_g - v_p)\,dy\right] \tag{18}$$

$$\frac{dP_g}{P_g} - \gamma_g \frac{d\rho_g}{\rho_g} = \frac{A\rho_p B\,dx}{P_g u_g} \tag{19}$$

2. Along Gas Mach Lines

$$\frac{dy}{dx} = \frac{u_g v_g \pm a^2\sqrt{M^2-1}}{u_g^2 - a^2} \tag{20}$$

$$(u_g dy - v_g dx)\left[A\rho_p B dx - u_g dP_g\right] + a^2\left\{A\rho_p\left[(u_g - u_p)dy - (v_g - v_p)dx\right]dx\right.$$

$$\left.+\rho_g\left[v_g du_g - u_g dv_g - \sigma_y \frac{v_g}{\sigma}(u_g dy - v_g dx)\right]dx + dP_g\,dy\right\} = 0 \tag{21}$$

III, Technical Discussion (cont.)

B. CHARACTERISTIC EQUATIONS

By the use of the method of characteristics as discussed in Appendix B and developed in detail in Appendix C, the characteristic equations for the above system of quasi-linear partial differential equations (equation 1 through 8) were found to be:

1. Along Gas Streamlines

$$\frac{dy}{dx} = \frac{v_g}{u_g} \tag{17}$$

$$\rho_g\left[u_g du_g + v_g dv_g\right] + dP_g = -A\rho_p\left[(u_g - u_p)\,dx + (v_g - v_p)\,dy\right] \tag{18}$$

$$\frac{dP_g}{P_g} - \gamma_g \frac{d\rho_g}{\rho_g} = \frac{A\rho_p B\,dx}{P_g u_g} \tag{19}$$

2. Along Gas Mach Lines

$$\frac{dy}{dx} = \frac{u_g v_g \pm a^2\sqrt{M^2-1}}{u_g^2 - a^2} \tag{20}$$

$$(u_g dy - v_g dx)\left[A\rho_p B dx - u_g dP_g\right] + a^2\left\{A\rho_p\left[(u_g - u_p)dy - (v_g - v_p)dx\right]dx + \rho_g\left[v_g du_g - u_g dv_g - \sigma_y \frac{v_g}{\sigma}(u_g dy - v_g dx)\right]dx + dP_g\,dy\right\} = 0 \tag{21}$$

III, B, Characteristic Equations (cont.)

3. Along Particle Streamlines

$$\frac{dy}{dx} = \frac{v_p}{u_p} \tag{22}$$

$$u_p du_p = A(u_g - u_p)\, dx \tag{23}$$

$$v_p dv_p = A(v_g - v_p)\, dy \tag{24}$$

$$u_p dh_p = -\frac{2}{3} AC\,(T_p - T_g)\, dx \tag{25}$$

$$d\psi_p = 0 \tag{26}$$

$$(\psi_p)_y = \sigma \rho_p u_p \tag{27}$$

$$(\psi_p)_x = -\sigma \rho_p v_p \tag{28}$$

This system of characteristics is totally hyperbolic if the flow is supersonic (M>1), and partially hyperbolic when the flow is subsonic. Hence, the flow in the supersonic portion of the nozzle may be obtained by use of a numerical procedure based on the above system of characteristic equations. However, the subsonic and transonic flow must be obtained differently, since the characteristics are only partially hyperbolic in such regions.

C. SUBSONIC SOLUTION

Because of the elliptic nature of the governing equations for gas-particle mixtures in subsonic flow, a solution could not be obtained for the two-dimensional and axisymmetric flow equations. In approximation, the subsonic flow was assumed to be one dimensional. The following system of equations was then derived (Appendix D), subject to the same assumptions as for the two-dimensional and axisymmetric cases.

III, C, Subsonic Solution (cont.)

$$\frac{du_p}{dx} = A \left(\frac{u_g - u_p}{u_p}\right) \tag{29}$$

$$\frac{dh_p}{dx} = -\frac{2}{3} AC \left(\frac{T_p - T_g}{u_p}\right) \tag{30}$$

$$\frac{du_g}{dx} = \left(\frac{1}{M^2 - 1}\right) \left\{ \frac{u_g}{\text{Area}} \frac{d(\text{area})}{dx} - \left(\frac{\dot{w}_p}{\dot{w}_g}\right)\left(\frac{u_g}{u_p}\right)\frac{1}{a^2}\left[\frac{2}{3}(\gamma_g - 1)AC(T_p - T_g) + A\left\{\gamma_g (u_g - u_p)^2 + u_p (u_g - u_p)\right\}\right]\right\} \tag{31}$$

$$M^2 = \frac{u_g^2}{a^2} \tag{32}$$

$$T_g = T_{go} - \left(\frac{\dot{w}_p}{\dot{w}_g}\right)\frac{1}{c_{pg}}\left[(h_p - h_{po}) + \frac{1}{2} u_p^2\right] - \frac{1}{2}\frac{u_g^2}{c_{pg}} \tag{33}$$

$$\rho_g = \frac{\dot{w}_g}{u_g \text{ area}} \tag{34}$$

$$P_g = \rho_g R T_g \tag{35}$$

$$\rho_p = \frac{\dot{w}_p}{u_p \text{ area}} \tag{36}$$

$$T_p = f(h_p) \text{ Tabulated,} \tag{37}$$

$$\text{area} = f(x) \tag{38}$$

III, C, Subsonic Solution (cont.)

The first three differential expressions can be solved by techniques such as the Adams or Runge-Kutta methods once starting values are assumed at some location where the flow velocities are small and gas-particle equilibrium may be assumed.

Since lines of constant properties in the subsonic portion of a de Laval nozzle are concave downstream, the area in these equations should be based on the spherical sector determined by the distance to the vertex of an equivalent cone which is tangential to the wall of the nozzle at each point. This is equivalent to a sink-flow solution, where the location of the sink varies with the position in the nozzle and the slope of the nozzle wall, as illustrated in Figure 1.

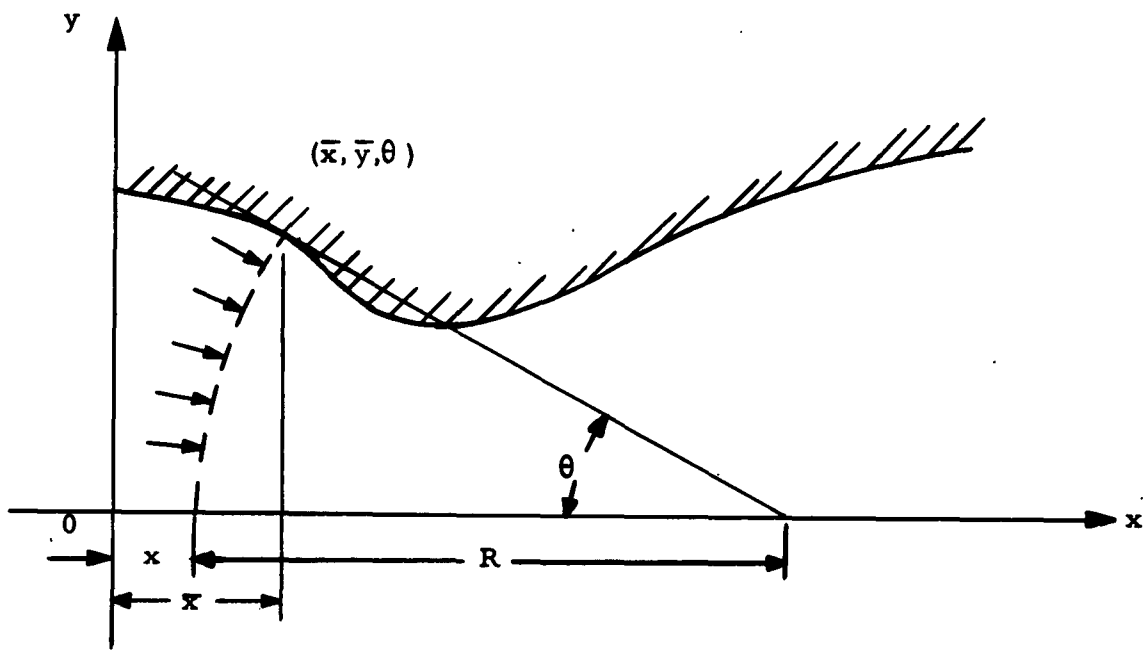

Figure 1. One-Dimensional Sink-Flow Model

Thus, the subsonic geometry would be specified by giving the wall location $\bar{y}$ and slope θ as a tabulated function of $\bar{x}$. The area as a function of x is determined as follows:

$$R = \frac{\bar{y}}{\sin \theta} \tag{39}$$

III, C, Subsonic Solution (cont.)

$$x = \bar{x} - R(1 - \cos\theta) \tag{40}$$

$$\text{area} = 2\pi R^2 (1 - \cos\theta) \tag{41}$$

By using the above relationship between x and area, the subsonic solution may be carried out to a point where the solution begins to diverge because of the $\left(\frac{1}{M^2 - 1}\right)$ term. To perform this solution, the total mass flow must be estimated and must subsequently be corrected after the starting line in the supersonic region is determined.

$$\dot{w} = \dot{w}_g + \dot{w}_p \tag{42}$$

The gas mass-flow rate may be estimated from the chamber stagnation conditions by assuming that the gas-particle mixture is in equilibrium and by using the constant-lag one-dimensional analysis presented in Appendix E to determine the velocity and density at some downstream cross section, such as the nozzle throat, of an equivalent perfect-gas flow.

$$\dot{w}_g = \rho_g u_g \, \text{area} \tag{43}$$

$$\frac{T_{go}}{T_g} = \left[1 + \frac{\bar{\gamma}_g - 1}{2} \bar{M}^2\right] \tag{44}$$

$$\frac{\rho_{go}}{\rho_g} = \left[1 + \frac{\bar{\gamma}_g - 1}{2} \bar{M}^2\right]^{\frac{1}{\bar{\gamma}_g - 1}} \tag{45}$$

III, C, Subsonic Solution (cont.)

$$u_g^2 = \frac{\gamma_g R T_g \overline{M}^2}{E} \tag{46}$$

$$\frac{(area)}{(area)^*} = \frac{1}{\overline{M}}\left[\frac{2}{\overline{\gamma}_g + 1}\left(1 + \frac{\overline{\gamma}_g - 1}{2}\overline{M}^2\right)\right]^{\frac{(\overline{\gamma}_g + 1)}{2(\overline{\gamma}_g - 1)}} \tag{47}$$

$$\overline{\gamma}_g = 1 + (\gamma_g - 1)\frac{D}{E} \tag{48}$$

$$D = \frac{1 + \frac{\dot{w}_p}{\dot{w}_g} K^2}{1 + \frac{\dot{w}_p}{\dot{w}_g}\frac{c_{pl}}{c_{pg}} L} \tag{49}$$

$$E = 1 + \frac{\dot{w}_p}{\dot{w}_g}\left\{K\left[\gamma_g (1-K) + K\right] + (\gamma_g - 1)\frac{c_{pl}}{c_{pg}} LD\right\} \tag{50}$$

$$L = \frac{1}{1 + 3\frac{c_{pl}}{c_{pg}}\left(\frac{1-K}{K}\right)} \tag{51}$$

If the nozzle throat is chosen as the reference cross section, then $\overline{M}_t = \overline{M}^* = 1$ and $(area)_t = (area)^*$. Equations (43) through (46) then reduce to

$$T_g^* = \frac{2}{\overline{\gamma}_g + 1} T_{go} \tag{52}$$

$$\rho_g^* = \rho_{go}\left[\frac{2}{\overline{\gamma}_g + 1}\right]^{\frac{1}{\overline{\gamma}_g - 1}} \tag{53}$$

$$u_g^* = \left[\frac{2\gamma_g R T_{go}}{(\overline{\gamma}_g + 1) E}\right]^{\frac{1}{2}} \tag{54}$$

$$\dot{w}_g = \rho_{go} A_t \left[\frac{2}{\overline{\gamma}_g + 1}\right]^{\frac{1}{\overline{\gamma}_g - 1}} \left[\frac{2\gamma_g R T_{go}}{(\overline{\gamma}_g + 1) E}\right]^{\frac{1}{2}} \tag{55}$$

III, C, Subsonic Solution (cont.)

To evaluate the above expressions, a value for the kinetic lag, K, must be assumed. With some experience, a reasonable average value of K between the entrance and throat may be chosen. However, as a first approximation, K may be chosen as unity. Since $\frac{\dot{w}_p}{\dot{w}_g}$ is known, $\dot{w}_p$ can be calculated when $\dot{w}_g$ is known. Hence, all the parameters necessary for the subsonic solution can be determined.

D. TRANSONIC SOLUTION

The one-dimensional sink flow solution does not converge near Mach 1, and the method of characteristics cannot be used where the Mach number is less than 1. Thus, a different approach was necessary in the transonic flow regime. The particle kinetic and thermal lags were assumed to be constant, and the analysis shown in Appendix E for a constant-lag one-dimensional gas-particle mixture was used to obtain a modified specific heat ratio, $\overline{\gamma}_g$, and Mach number, $\overline{M}$, of the gas, which includes the effects of the particles on the gas. The Sauer transonic flow approximation discussed in Appendix F was then used to obtain the gas velocity components in the supersonic regime where the Mach number is only slightly greater than 1. The other gas and particle properties can then be found along this starting line by the use of the following procedure. A starting line having all properties known is available for use in the supersonic characteristic solution.

The transonic flow regime was broken into two regions of constant lag: the first from the end of the sink-flow regime to the throat, and the second from the throat to the starting line. This is illustrated in Figure 2.

III, D, Transonic Solution (cont.)

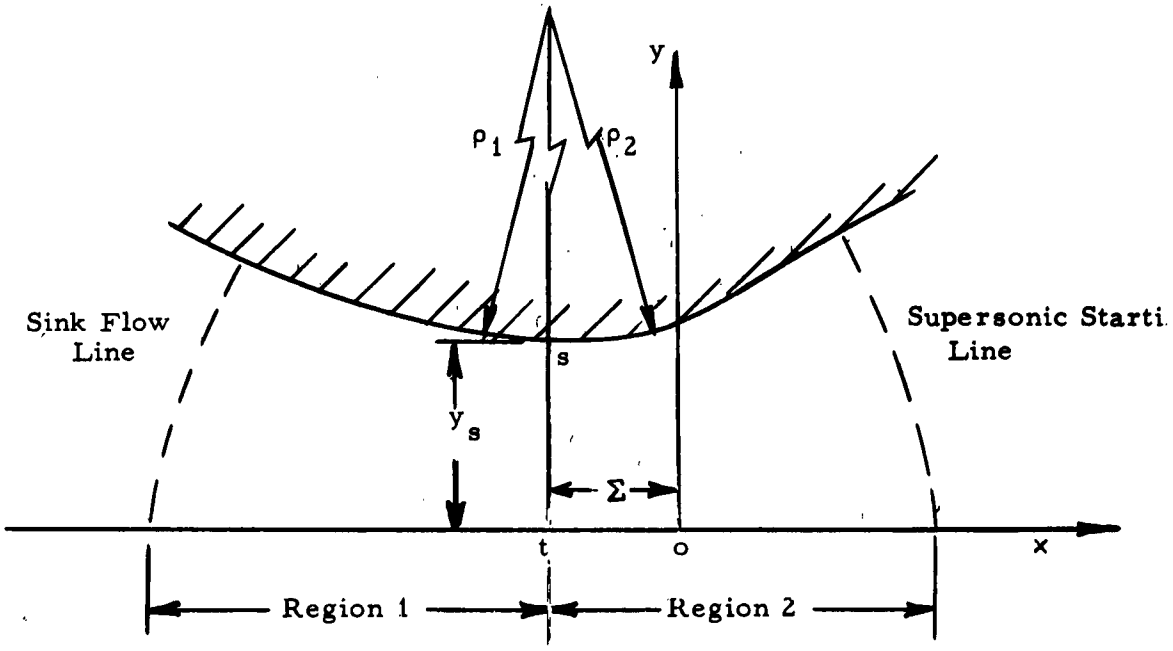

Figure 2. Constant-Lag Transonic Flow Model

This model permits different wall radii of curvature to be used upstream, ρ_1, and downstream, ρ_2, of the throat. In Appendix F, the gas flow field near Mach 1 is described by the following relationships.

$$u(x,y) = a\,x + \frac{(\bar{\gamma}_g + 1)a^2}{2(1+\delta)}y^2 \tag{56}$$

$$v(x,y) = \frac{(\bar{\gamma}_g + 1)\,ax}{(1+\delta)}\,y + \frac{(\bar{\gamma}_g + 1)^2 a^3}{2(1+\delta)(3+\delta)}\,y^3 \tag{57}$$

$$\varepsilon = -\frac{y_s}{2(3+\delta)}\sqrt{\frac{(\bar{\gamma}_g + 1)(1+\delta)\,y_s}{\rho_s}} \tag{58}$$

$$a = \sqrt{\frac{(1+\delta)}{(\bar{\gamma}_g + 1)\,\rho_s y_s}} \tag{59}$$

III, D, Transonic Solution (cont.)

where $\delta = 0$ for two-dimensional flow and $\delta = 1$ for axisymmetric flow, and u and v are nondimensional perturbation velocities. The actual velocity components of the modified gas flow are given by the following expressions containing u and v.

$$\tilde{u}(x,y) = a^*(1 + u) \tag{60}$$

$$\tilde{v}(x,y) = a^* v \tag{61}$$

$$a^{*2} = \frac{2\bar{\gamma}_g}{(\bar{\gamma}_g + 1)} R T_{go} \tag{62}$$

The actual velocity components of the gas in the gas-particle mixture are determined from the following relationship, wherein E is defined as a one-dimensional flow parameter with constant lag:

$$u_g = E^{-\frac{1}{2}} \tilde{u} \tag{63}$$

$$v_g = E^{-\frac{1}{2}} \tilde{v} \tag{64}$$

The value of K (one-dimensional particle velocity lag) used in Region 1 (Figure 2) is determined from the sink-flow solution along the sink flow line. When the entire gas-particle flow field is finally determined at the throat, the value of K at the throat may be found. An average value on K between the sink flow line and the throat can then be established, thus determining the Region 1 flow field more accurately. This procedure should be repeated until the average value of K no longer varies from trial to trial. Region 2 can be solved in the same manner by first choosing K as the value at the throat from the Region 1 solution. When the starting line is determined, an average value of K in

III, D, Transonic Solution (cont.)

Region 2 can be repeated in the same manner as for Region 1. When the flow fields in Regions 1 and 2 are completely determined, the gas velocity components on the supersonic starting line are determined.

Next, it is necessary to make the total mass flow assumed in the sink-flow solution compatible with the total mass flow in the supersonic region. This may be done by integrating the total mass flow across the starting line to obtain the supersonic mass flow. The assumed total mass flow in the subsonic sink-flow solution should then be set equal to the calculated total mass flow in the supersonic region, and the entire subsonic and transonic solutions should be repeated to obtain a new starting line and supersonic total mass flow. This procedure should be repeated until the subsonic and supersonic total mass flows become equal; the supersonic solution may then be initiated.

The particle velocity components in the transonic region may be found by using the method of characteristics, since the particle streamlines, which are also characteristics, exist in subsonic as well as supersonic flow. By choosing several points on the sink flow line as starting points, the particle properties along the streamlines through these points may be found by using numerical techniques. The geometry for this procedure is illustrated in Figure 3.

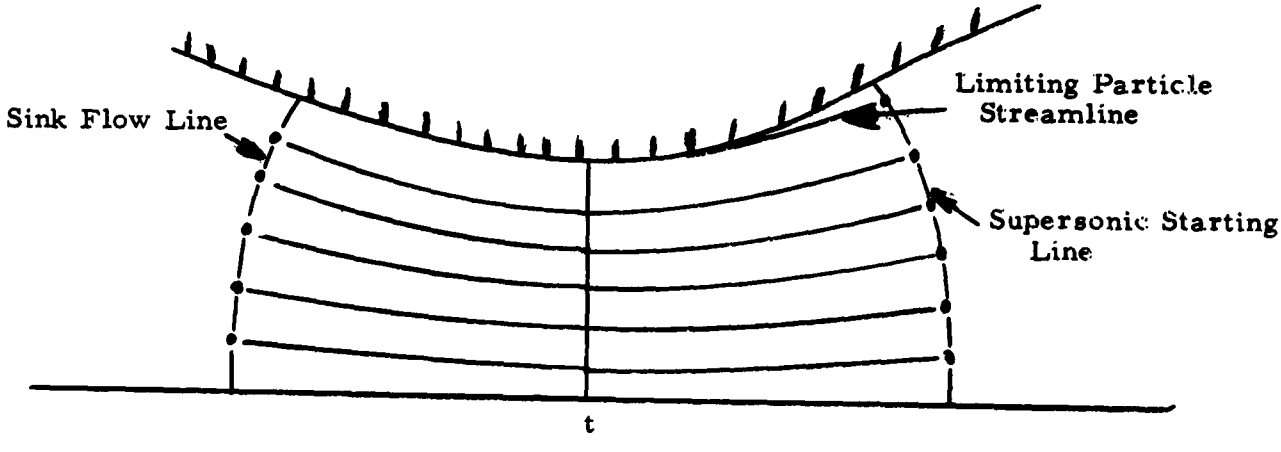

Figure 3. Transonic Characteristic Curves

III, D, Transonic Solution (cont.)

The derivation of the characteristic equations for the determination of the particle properties along the streamlines is shown in Appendix C, where Ψ_p is the particle-stream function.

$$\frac{dy}{dx} = \frac{v_p}{u_p}$$

$$u_p du_p = A(u_g - u_p)\,dx \tag{65}$$

$$v_p dv_p = A(v_g - v_p)\,dy \tag{66}$$

$$u_p dh_p = -\frac{2}{3} AC\,(T_p - T_g)\,dx \tag{67}$$

$$d\Psi_p = 0 \tag{68}$$

This system of equations can be solved by assuming that all variable coefficients are average values and by putting the equations into the following finite difference form suitable for computer evaluation:

$$\frac{\Delta y}{\Delta x} = \frac{\bar{v}_p}{\bar{u}_p} \tag{69}$$

$$\Delta u_p = A\left(\frac{\bar{u}_g - \bar{u}_p}{\bar{u}_p}\right)\Delta x \tag{70}$$

$$\Delta v_p = A\left(\frac{\bar{v}_g - \bar{v}_p}{\bar{v}_p}\right)\Delta y \tag{71}$$

$$\Delta h_p = -\frac{2}{3} AC\left(\frac{\bar{T}_p - \bar{T}_g}{\bar{u}_p}\right)\Delta x. \tag{72}$$

III, D, Transonic Solution (cont.)

Ψ_p may be evaluated along the sink flow line to establish a value of Ψ_p, which, from equation (68), remains constant along the streamline, thus determining Ψ_p along the supersonic starting line. By using the procedure shown in Appendix C, Ψ_p along the sink flow line may be evaluated as follows.

$$d\Psi_p = (\Psi_p)_x\, dx + (\Psi_p)_y\, dy \tag{73}$$

$$d\Psi_p = \sigma \rho_p \left(u_p dy - v_p dx \right) \tag{74}$$

The value of ρ_p along the sink flow line may be found by using the sink-flow solution, and u_p and v_p may be determined by

$$u_p = K u_g \tag{75}$$

$$v_p = K v_g \tag{76}$$

where u_g and v_g are determined from the transonic approximation along the sink flow line, and K is derived from the sink-flow solution along the sink flow line. The value of ρ_p along the supersonic starting line may be found by solving (74) for ρ_p.

$$\rho_p = \frac{d\Psi_p}{\sigma (u_p dy - v_p dx)} \tag{77}$$

The values of P_g and ρ_g along the supersonic starting line can be found by numerically integrating the two characteristic equations which are valid along the gas streamlines from the sink flow line to the starting line. This will establish

III, D, Transonic Solution (cont.)

a system of gas streamlines in the transonic region in the same manner as the particle streamlines illustrated in Figure 3 are established. By using the derivation of the characteristic equations in Appendix C, the equations necessary to determine P_g and ρ_g are

$$\frac{dy}{dx} = \frac{v_g}{u_g} \tag{78}$$

$$\rho_g\left[u_g du_g + v_g dv_g\right] + dP_g = -A\rho_p\left[(u_g - u_p)\,dx + (v_g - v_p)\,dy\right] \tag{79}$$

$$\frac{dP_g}{P_g} - \gamma_g \frac{d\rho_g}{\rho_g} = \frac{A\rho_p B dx}{P_g u_g} \tag{80}$$

For the gas in transonic flow, the equations in finite-difference form are

$$\frac{\Delta y}{\Delta x} = \frac{\bar{v}_g}{\bar{u}_g} \tag{81}$$

$$\Delta P_g = -A\bar{\rho}_p\left[(\bar{u}_g - \bar{u}_p)\,\Delta x + (\bar{v}_g - \bar{v}_p)\,\Delta y\right] - \bar{\rho}_g\left[\bar{u}_g\,\Delta u_g + \bar{v}_g\,\Delta v_g\right] \tag{82}$$

$$\Delta\rho_g = \frac{1}{\bar{a}^2}\Delta P_g - \frac{A\bar{\rho}_p B\bar{\rho}_g \Delta x}{\gamma_g \bar{P}_g \bar{u}_g} \tag{83}$$

Thus P_g and ρ_g can be determined along the starting line to the same order of approximation as was involved in finding u_g and v_g.

Once all the flow properties have been found on the starting line, the total mass flow across the starting line may be found by integration. If this total mass flow is different from the assumed subsonic total mass flow, the subsonic total

III, D, Transonic Solution (cont.)

mass flow should be set equal to the total mass flow through the starting line, and the entire subsonic and transonic solution should be repeated. When the total mass flow through the starting line finally equals the subsonic total mass flow, the supersonic starting line is sufficiently determined to continue with the supersonic solution by the characteristic method.

E. SUPERSONIC SOLUTION

In supersonic flow, the equations are totally hyperbolic, and the characteristic curves are all real. Hence, the flow field can be determined by a numerical technique based on the characteristic equations derived earlier. As discussed in Appendix B, to obtain the solution in a region of a flow field, an initial data line that is nowhere characteristic and along which all the flow properties are known must be determined. This line is the supersonic starting line discussed in section III, D and must be determined in a region where the Mach number is greater than 1.

Once the starting line has been determined, the supersonic solution can be initiated. There are several types of flow regions within the supersonic regime, and each must be handled differently. Points near the axis must be treated in a special manner because of the term (1/y) in several of the equations. Solid and free boundaries must satisfy the added condition of known flow angle and known pressure, respectively. In the region between the limiting particle streamline and the nozzle wall, no particles are present and the gas flow reduces to the case of rotational perfect-gas flow. The flow near a limiting particle streamline must also be handled differently, since $\rho_p = 0$ on one side of this streamline and is finite on the other side. The final type of flow is that of a general interior point where none of the above special situations prevail. The procedure for determining the flow in the neighborhood of an interior point is developed in detail in this study. The types of points discussed are illustrated in Figure 4.

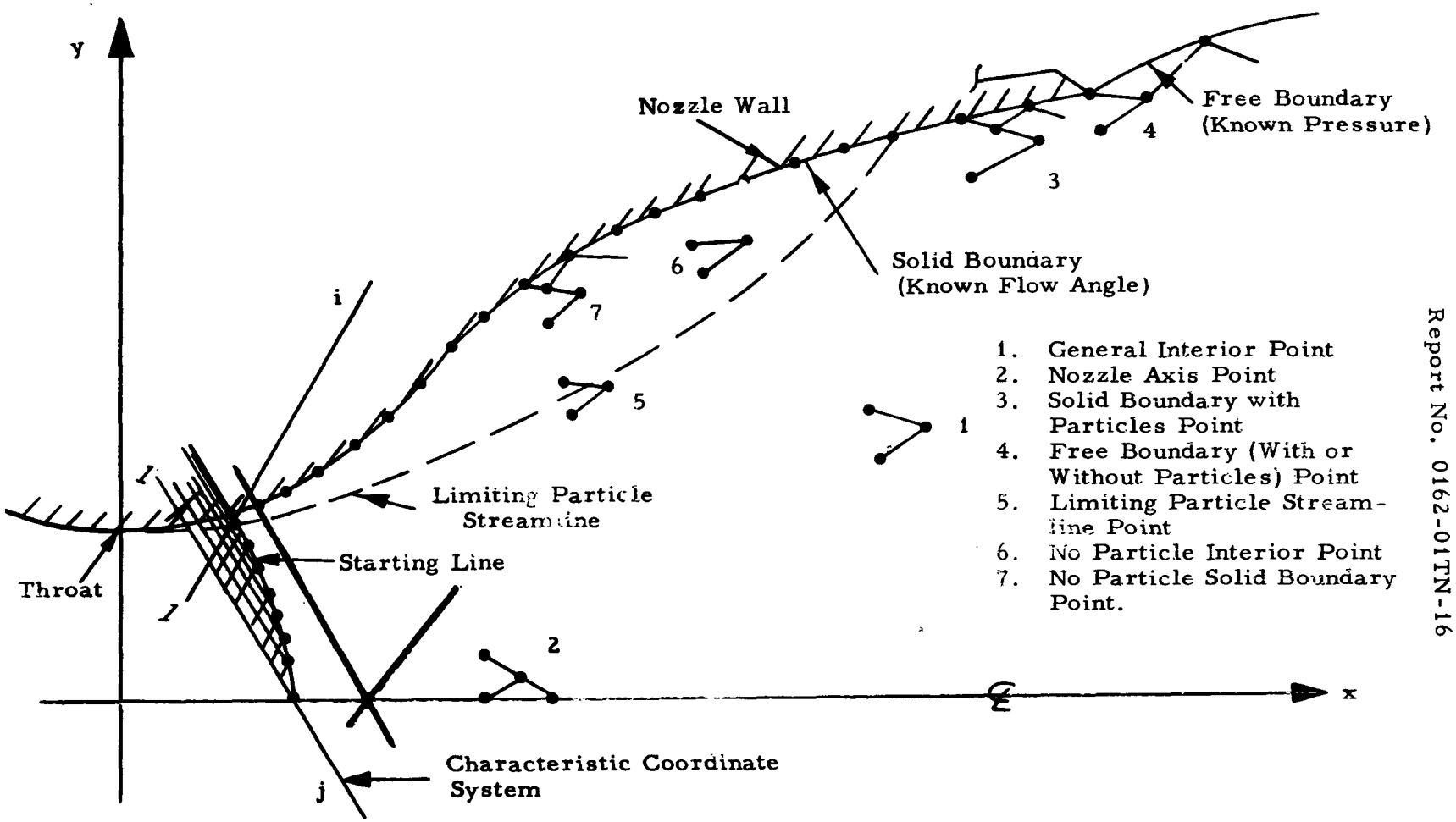

Figure 4. Special Cases of Supersonic Flow

III, E, Supersonic Solution (cont.)

The nozzle wall is determined by specifying x and y coordinates and the slope at a discrete number of points, as illustrated in Figure 4. A left Mach line is then forced to go through each wall point to determine the flow properties at the wall point, as illustrated at point 3 for a solid boundary with particles and at point 7 for a solid boundary with no particles. A right Mach line is then projected out into the flow field from each wall point to continue the solution. The size of the characteristic net can be regulated by varying the spacing of the specified wall points.

The starting line is broken up into several discrete points from which the characteristic solution is initiated. The size of the intervals chosen along the starting line determines the size of the characteristic net near the nozzle throat where property gradients are generally large. A relatively small interval is required along the starting line.

A characteristic coordinate system is indicated in Figure 4 for the solution as it proceeds down the nozzle. As indicated, right Mach lines are numbered from 1 through i, and left Mach lines are numbered from 1 through j. Right Mach line 1 initiates on the starting line at the nozzle axis, and a right Mach line of increasing number initiates from each point on the starting line up to the wall, where a right Mach line then initiates from each wall point. Left Mach line 1 initiates on the starting line at the wall, and a left Mach line of increasing number passes through each point on the starting line until the nozzle axis is reached. Left Mach lines then are initiated at each point on the nozzle axis where a right Mach line from a nozzle wall point intersects the axis, as indicated in Figure 4. Thus, every point in the characteristic solution can be specified by a coordinate (i, j) in the characteristic coordinate system.

Now that the characteristic nets in the supersonic region are specified, it is necessary to develop a numerical solution procedure for each of

III, E, Supersonic Solution (cont.)

the points discussed above and an overall calculation scheme for determining the flow field in the entire nozzle. Point 1, the general interior point, has been considered in great detail, and the finite-difference equations necessary to solve for such a point are discussed in section III, F.

F. FINITE-DIFFERENCE EQUATIONS

As discussed in Appendix C, it was necessary to solve the particle continuity equation by a mass balance on the characteristic control volume. The remaining equations were found to constitute a characteristic system that is hyperbolic. The finite-difference form of these characteristic equations was derived in Appendix G for the characteristic net shown in Figure 5. Points 3, 4, and 5 were located by geometric considerations of the characteristic curves, as discussed in Appendix H.

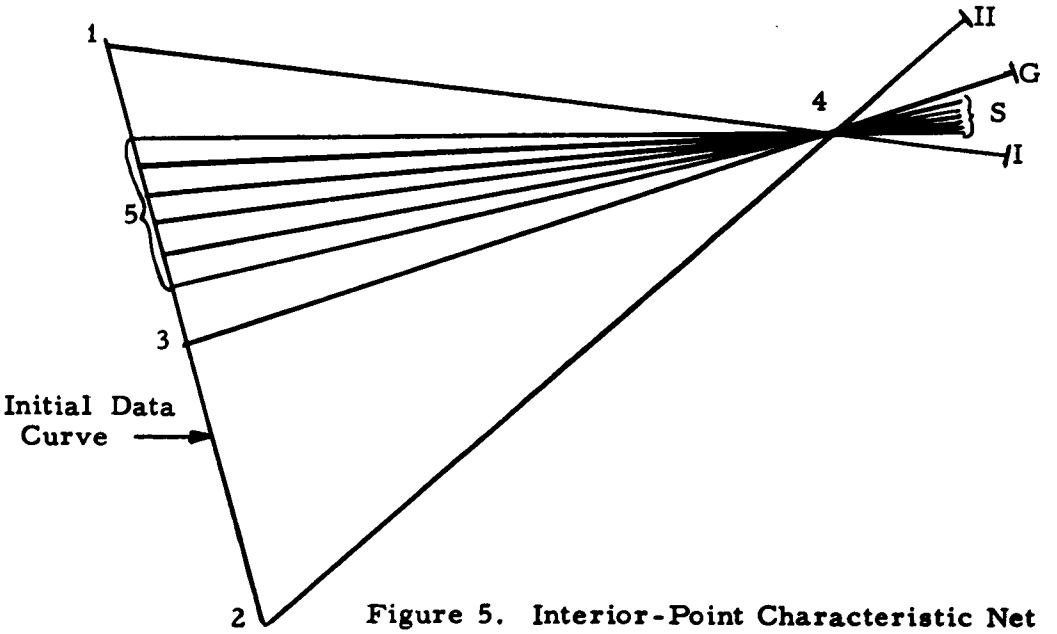

Figure 5. Interior-Point Characteristic Net

III, F, Finite-Difference Equations (cont.)

To account for more than one size or species of particle, six discrete particles were accounted for by introducing the streamline of each additional particle as a characteristic curve along which the particle compatibility equations are valid. Particle parameters appearing in gas compatibility equations were summed for the six particles to account for their effects on these equations.

The equations necessary to calculate the gas and particle properties at point 4 were derived as shown in Appendix G and are discussed in detail for a general interior point in Appendix H. These equations include the properties at point 4, which, as a first approximation, were assumed to be the same as the properties at the intersection of the initial data line and the characteristic line along which the particular parameter was evaluated. For subsequent calculations, the properties at point 4 were considered to be equal to the results of the previous calculations at point 4. In this manner, an iteration procedure was developed for the flow properties at point 4. A numerical example also was derived, as shown in Appendix I, to demonstrate the procedure for determining a general interior point.

G. INTERIOR POINT NUMERICAL EXAMPLE

To check the validity of the theory and the correctness of the IBM 7090 computer program, a numerical example was calculated for a general interior point (Appendix I). A solid propellant containing aluminum was selected as a sample for this calculation. The particles in the exhaust stream contained aluminum oxide particles of six different sizes. The calculation was made for a point 1 ft downstream of the nozzle throat and 0.5 ft from the nozzle axis in an axisymmetric nozzle.

Tabulated values of f and g as functions of Reynolds number are valid for spheres of any chemical species and size and may be considered to be

III, G, Interior Point Numerical Example (cont.)

the proper relationship for future calculations. The values of γ_g and c_{pg} as functions of gas temperature were estimated for this particular gas and should be re-evaluated for future cases. The temperature-enthalpy relationship for the aluminum oxide shown in Appendix I may be used for future calculations involving aluminum oxide particles. The remaining flow properties were estimated to allow a numerical calculation to be made and are not indicative of the type of flow field that would normally occur.

The numerical-solution procedure shown in Appendix H was followed in achieving both the calculated and the IBM 7090 computer solutions. The results obtained through the two methods were in agreement, indicating that the computer solution is correctly programed. The flow properties calculated at the new point were all found to be of the correct order of magnitude and changing in the proper direction for flow down a diverging supersonic nozzle. Therefore, the theoretical development appears accurate and the computer program appears to correctly calculate the flow field at a general interior point.

IV. CONCLUSIONS

The model developed in this Technical note for the two-dimensional and axisymmetric flow of gas-particle mixtures appears to adequately represent the actual flow field for spherical particles inthe exhaust gases. Such is the case when the particles are aluminum oxide. However, not all particles are necessarily spherical, or even approach it, and care must be exercised when considering such flows.

The theory developed here, when completed, will enable the determination of the performance characteristics of conventional de Laval nozzles and

IV, Conclusions (cont.)

unconventional nozzles, such as the plug nozzle. Particle trajectories and impingement points can be accurately determined. Nozzle thrust and specific impulse can be calculated, thus allowing nozzle evaluation studies to be made to determine how to design nozzles for gas-particle mixtures.

V. RECOMMENDATIONS FOR FUTURE WORK

The work described herein is the result of a study of the flow of gas-particle mixtures in two-dimensional and asixymmetric rocket nozzles. The program is far from complete, however. Further work needs to be programed for the following specific items:

1. A more detailed analysis of the subsonic solution.
2. A more detailed analysis of the transonic solution.
3. Development of a solution procedure for the special cases of supersonic flow mentioned in section III, E.
4. Development of a computer program for subsonic, transonic, and supersonic flow, uniting into one program the solutions relating to the entire nozzle.
5. Analysis of particle trajectories.
6. Development of an analysis procedure for unconventional nozzles.
7. Consideration of heat transfer to the wall.
8. Consideration of chemical nonequilibrium in the gas phase.
9. A systematic computer analysis of the effects of nozzle geometry.
10. A systematic computer analysis of the effects of gas-dynamic parameters.
11. Correlation with an experimental program.
12. Re-evaluation of the theoretical analysis based on the experimental comparison.
13. Development of a complete method for designing any type of nozzle for gas-particle systems.

VI. NOMENCLATURE

A. ENGLISH SYMBOLS

A	Particle parameter in characteristic equations
$\overline{A}_S$	Parameter in particle finite-difference equations
area	Area of one-dimensional gas-particle system nozzle
a	Speed of sound in a perfect gas
a*	Speed of sound at sonic conditions
a_{ij}	Coefficient of system of quasi-linear partial-differential equations
B	Parameter in gas characteristic equations
$\overline{B}_S$	Parameter in particle finite-difference equations
b_{ij}	Coefficient of system of quasi-linear partial-differential equations
C	Parameter in characteristic equations
C_D	Drag coefficient
$\overline{C}_S$	Parameter in particle finite-difference equations
$C(\sigma)$	Characteristic curve parametric representation
c_i	Coefficient of system of quasi-linear partial-differential equations
c_{pg}	Specific heat at constant pressure of the gas
c_{pl}	Specific heat at constant pressure of the particles
D	Constant-lag one-dimensional flow parameter
$\overline{D}_f$	Vector drag force
D_G	Parameter in gas finite-difference equations
D_i	Parameter in characteristic compatibility equations derivation
ds	Differential arc length in radius of curvature calculation
dx	Differential distance along nozzle axis

VI, A, English Symbols (cont.)

dy	Differential distance normal to nozzle axis
d( )	Total differential of a quantity
E	Constant-lag one-dimensional flow parameter
$\overline{F}$	Vector force
f	Ratio of C_D to C_D for Stokes' flow
$f_o(x)$	Coefficient in power series solution for ϕ (x, y) in transonic flow
$f_2(x)$	Coefficient in power series solution for ϕ (x, y) in transonic flow
$f_4(x)$	Coefficient in power series solution for ϕ (x, y) in transonic flow
g	Ratio of Nu to Nu for Stokes' flow
h	Particle heat-transfer film coefficient
h_g	Enthalpy of the gas
h_p	Enthalpy of the particles
K	One-dimensional particle velocity lag
K_I, K_{II}	Parameters in gas finite-difference equations
k_g	Thermal conductivity of the gas
k_i	Parameter in characteristic compatibility equations derivation
L	One-dimensional particle thermal lag
L_i	Notation for a system of quasi-linear partial-differential equations
L_1	Parameter in particle mass balance
L_2	Parameter in particle mass balance
M	Mach number
$\overline{M}$	One-dimensional constant-lag modified Mach number
M_I, M_{II}	Parameters in gas finite-difference equations

VI, A, English Symbols (cont.)

m	Slope of a line in geometrical characteristic net
m_p	Density of a particle per unit volume of particle
Nu	Nussult number
n	Index in system of quasi-linear partial-differential equations
$\bar{n}$	Unit normal vector
n_i	Unit vector in ith direction
P_g	Gas pressure
P_i	Any property in finite-difference equations
Pr	Prandtl Number
Q	Heat added to gas-particle system control volume
Q_I, Q_{II}	Parameters in gas finite-difference equations
$\bar{q}$	Velocity vector
R	Gas constant
Re	Reynolds number
R_I, R_{II}	Parameters in gas finite-difference equations
r_p	Particle radius
S_I, S_{II}	Parameters in gas finite-difference equations
s	Throat wall location in transonic flow model
T_G	Parameter in gas finite-difference equations
T_g	Gas temperature
T_{go}	Gas stagnation chamber temperature in one-dimensional model
T_p	Particle temperature
T_{po}	Particle stagnation chamber temperature in one-dimensional model
t	Time

VI, A, English Symbols (cont.)

$\bar{U}$	Parameter in gas finite-difference equations, and nondimensional x-direction velocity component in transonic flow
u	Perturbation x-direction velocity component in transonic flow
$\tilde{u}$	x-direction velocity component in transonic flow
u_g	x-direction gas velocity component
u_{gi}	Gas velocity component in ith direction
u_p	x-direction particle velocity component
u_{pi}	Particle velocity component in ith direction
u^j	Flow property in system of quasi-linear partial-differential equations
u^j_{n+1}	Value of u^j after n + 1th iteration
u^j_n	Value of u^j after nth iteration
$\bar{V}$	Parameter in gas finite-difference equations and nondimensional y-direction velocity component in transonic flow
V	Volume of gas-particle system control volume
v	Perturbation y-direction velocity component in transonic flow
$\tilde{v}$	y-direction velocity component in transonic flow
v_g	y-direction gas-velocity component
v_p	y-direction particle-velocity component
$\dot{w}_g$	One-dimensional gas mass-flow rate
$\dot{w}_p$	One-dimensional particle mass-flow rate
X	Parameter in gas finite-difference equations
x	Coordinate along nozzle axis
x_σ	Direction cosine of characteristic curve
Y	Parameter in gas finite-difference equations
y	Coordinate normal to nozzle axis

VI, A, English Symbols (cont.)

y_S	Radius of nozzle throat in transonic flow model
y_σ	Direction cosine of characteristic curve
Z	Parameter in gas finite-difference equations
z	Coordinate normal to x-y plane in nozzle

B. GREEK SYMBOLS

α	Mach angle, gas viscosity parameter, or Sauer-line velocity gradient
Γ_o	Initial data curve in method of characteristics
Γ_1	Solution curve in method of characteristics
γ_g	Specific heat ratio of the gas
$\bar{\gamma}_g$	One-dimensional constant-lag modified specific heat ratio
$\Delta( )$	Finite difference of a quantity
Δx	Finite change along nozzle axis
Δy	Finite change normal to nozzle axis
δ	Denotes two-dimensional or axisymmetric flow in Sauer's approximation
ε	Location of coordinate system in transonic flow
ζ_+	Slope of characteristic curve for two variables
ζ_-	Slope of characteristic curve for two variables
ζ_n	Slope of characteristic curve for n variables
θ_g	Angle of the tangent to a gas streamline
θ_p	Angle of the tangent to a particle streamline

VI, B, Greek Symbols (cont.)

λ	Linear multiplying factors in method of characteristics
μ	Angle of a line in geometrical characteristics net
μ_g	Gas viscosity
μ_o	Gas viscosity parameter
π	3.14159...
ρ_g	Gas density per unit volume of gas
ρ_p	Particle density per unit volume of gas
ρ_s	Radius of curvature in transonic flow
$\sum$	Indicates a summation
σ	Denotes type of flow, two dimensional or axisymmetric
σ_y	Denotes type of flow, two dimensional or axisymmetric
τ	Angle for determining radius of curvature
$\phi(x, y)$	Gas velocity potential function in transonic flow
Ψ_p	Particle stream function

C. SUBSCRIPTS

G	Gas streamline
g	Gas property
go	Gas property at stagnation chamber conditions
i	Index
ij	Index
j	Index
m	Midpoint of initial data line

VI, C, Subscripts (cont.)

p	Particle property
po	Particle property at stagnation chamber conditions
S	Particle streamline
Stokes'	Stokes' flow regime where $R_e \leq 1$
t	Nozzle throat
I	Right running Mach line
II	Left running Mach line

D. SUPERSCRIPTS

j	Index for flow variables
*	Sonic conditions
-	Average value of a quantity, or a vector quantity
~	Velocity components in transonic flow model

E. OTHER

div	Vector operator
$\frac{d}{dt}( )$	Total derivative with respect to time
$\frac{\partial}{\partial t}$	Partial derivative with respect to time
$\frac{dy}{dx}$	Slope of a line in x-y plane
ln	Natural logarithm
$( )_x$	Partial derivative with respect to x
$( )_y$	Partial derivative with respect to y
$\Delta\bar{q}$	Relative velocity vector between gas and particle $\sim(\bar{q}_g - \bar{q}_p)$
$\lvert( )\rvert$	Absolute value of a quantity

VI, Nomenclature (cont.)

F. UNITS OF PHYSICAL PARAMETERS

C_p	Specific heat at constant pressure	Btu/lbm-°R
f	Ratio of C_D to C_D for Stokes' flow	dimensionless
g	Ratio of Nu to Nu for Stokes' flow	dimensionless
h_p	Particle enthalpy	Btu/lbm
m_p	Particle density per unit volume of particle	lbm/cu ft
P_g	Gas static pressure	lbf/sq in.
Pr	Prandtl number	dimensionless
r_p	Particle radius, based on spherical particles	microns
R	Gas constant	Btu/lbm-°R
Re	Reynolds number	dimensionless
T_g	Gas static temperature	°R
T_p	Particle static temperature	°R
u_g	Axial gas-velocity component	ft/sec
u_p	Axial particle-velocity component	ft/sec
v_g	Normal or radial gas-velocity component	ft/sec
v_p	Normal or radial particle-velocity component	ft/sec
x	Axial coordinate	ft
y	Normal coordinate	ft
α	Exponent of gas-viscosity expression	dimensionless
γ_g	Specific heat ratio of the gas	dimensionless
μ_g	Gas viscosity	lbm/ft-sec
μ_o	Coefficient of gas-viscosity expression	lbm/ft-sec-$(°R)^{\alpha}$

VI, F, Units of Physical Parameters (cont.)

ρ_g	Gas density	lbm/cu ft
ρ_p	Particle density per unit volume of gas	lbm/cu ft

VII. BIBLIOGRAPHY

Higher Order Approximations to the Transonic Flow in a Nozzle Throat, STL Report 7106-0016-RU-000, March 1961, by Kliegel, J.R.

One Dimensional Flow of a Gas-Particle System, IAS Preprint No. 60-5, January 1960, by Kliegel, J.R.

Flow of Gas-Particle Mixtures in Axially Symmetric Nozzles, STL Report 7106-0017-RU-000, March 1961, by Kliegel, J.R., and Nickerson, G.R. (Preprint 1713-61 presented at the Propellants Combustion and Rockets Conference, 26-28 April 1961.

Flow Pattern in a Converging-Divergine Nozzle, NACA TM No. 1215, March 1949, by Oswatitsch, K. and Rothstein, W.

General Characteristics of the Flow Through Nozzles at Near Critical Speeds, NACA TM No. 1147, June 1947, by Sauer, R.

APPENDIX A

DERIVATION OF EQUATIONS GOVERNING GAS-PARTICLE MIXTURES

A gas-particle mixture is described by the equations for conservation of mass, conservation of energy, momentum balance, equation of state for the gas, particle drag, particle heat balance, and particle enthalpy-temperature relationships. This appendix derives these equations on the basis of following assumptions:

1. Only one particle size is present, or some type of integrated particle distribution is performed, and the particles are spherical.
2. The total mass of the gas-particle mixture is constant.
3. The total energy of the gas-particle mixture is constant.
4. The internal temperature of the particles is uniform, and the particle specific heat is constant.
5. The gas and particles exchange thermal energy by convection only.
6. The gas obeys the perfect-gas law, has a constant molecular weight, and constant specific heats.
7. All external forces except pressure of the gas and drag of the particles are neglected.
8. The gas is inviscid except for the drag it exerts on the particles.
9. The particles do not interact with each other.
10. The volume occupied by the particles is negligible.

The following derivations of the equations are based on studies by Kliegel:*

* Kliegel, J. R. and G. R. Nickerson, Flow of Gas-Particle Mixtures in Axially Symmetric Nozzles, STL TM-7106-0023-MU-000; also ARS preprint 1713-61, presented at the Propellants Combustion and Rockets Conference, April 26-28, 1961.

To begin the derivation, a control volume V enclosed by a surface A is considered. This control volume is illustrated by Figure A-1 below.

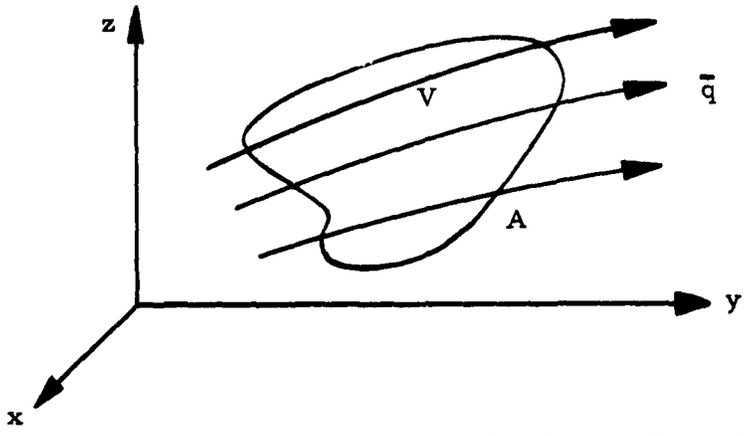

Figure A-1 Control Volume for System Equations

The control volume is fixed in space and the gas-particle mixture flows through it. The mass flux through the surface A is

$$\int_A \left[\rho_g \bar{q}_g \cdot \bar{n} + \rho_p \bar{q}_p \cdot \bar{n} \right] dA \qquad (A-1)$$

where ρ_p is the mass of particles per unit volume of gas. The time rate of change of mass in V is

$$\int_V \left[\frac{\partial \rho_g}{\partial t} + \frac{\partial \rho_p}{\partial t} \right] dV \qquad (A-2)$$

A mass balance for V results in

$$\int_V \left[\frac{\partial \rho_g}{\partial t} + \frac{\partial \rho_p}{\partial t} \right] dV + \int_A \left[\rho_g \bar{q}_g \cdot \bar{n} + \rho_p \bar{q}_p \cdot \bar{n} \right] dA = 0 \qquad (A-3)$$

When the divergence theorem is used, the surface integral of Equation A-3 can be transformed to a volume integral, and Equation A-3 becomes

$$\int_V \left[\frac{\partial \rho_g}{\partial t} + \frac{\partial \rho_p}{\partial t} + \text{div} \left(\rho_g \bar{q}_g + \rho_p \bar{q}_p \right) \right] dV = 0 \qquad \text{(A-4)}$$

Since this equation must be true for any size volume, it can be written as

$$\left[\frac{\partial \rho_g}{\partial t} + \text{div} \left(\rho_g \bar{q}_g \right) \right] + \left[\frac{\partial \rho_p}{\partial t} + \text{div} \left(\rho_p \bar{q}_p \right) \right] = 0$$

However, there is no mass interchange between the gas and particles in V; consequently, each member of Equation A-5 must be identically zero. Thus, the conservation of mass equation for V take the form

$$\frac{\partial \rho_g}{\partial t} + \text{div} \left(\rho_g \bar{q}_g \right) = 0 \qquad \text{(A-6)}$$

$$\frac{\partial \rho_p}{\partial t} + \text{div} \left(\rho_p \bar{q}_p \right) = 0 \qquad \text{(A-7)}$$

The momentum flux through A in the ith direction is

$$\int_A \left[\left(\rho_g u_{gi} \right) \bar{q}_g \cdot \bar{n} + \left(\rho_p u_{pi} \right) \bar{q}_p \cdot \bar{n} \right] dA \qquad \text{(A-8)}$$

The time rate of change of momentum in V in the ith direction is

$$\int_V \left[\frac{\partial}{\partial t} \left(\rho_g u_{gi} \right) + \frac{\partial}{\partial t} \left(\rho_p u_{pi} \right) \right] dV \qquad \text{(A-9)}$$

Through the assumption that all body forces except the pressure of the gas and the drag are negligible, there are no viscous or body forces acting on surface A, and the only forces present are pressure forces. The component of this pressure force in the ith direction is

$$- \int_A P_g n_i dA \tag{A-10}$$

A momentum balance for V gives

$$\sum \bar{F} = \frac{d}{dt} \left(\overline{\text{Momentum}} \right)$$

$$- \int_A P_g n_i dA = \int_A \left[\left(\rho_g u_{gi} \right) \bar{q}_g \cdot \bar{n} + \left(\rho_p u_{pi} \right) \bar{q}_p \cdot \bar{n} \right] dA \tag{A-11}$$

$$+ \int_V \left[\frac{\partial}{\partial t} \left(\rho_g u_{gi} \right) + \frac{\partial}{\partial t} \left(\rho_p u_{pi} \right) \right] dV$$

When the divergence theorem is applied to Equation A-11, the expression for the ith component of the momentum balance becomes

$$\int_V \left[\frac{\partial}{\partial t} \left(\rho_g u_{gi} + \rho_p u_{pi} \right) + \text{div} \left(\rho_g u_{gi} \bar{q}_g + \rho_p u_{pi} \bar{q}_p \right) \right. \tag{A-12}$$

$$\left. + \frac{\partial P_g}{\partial x_i} \right] dV = 0$$

Since this equation must hold for any volume, the momentum balance becomes

$$\frac{\partial}{\partial t} \left(\rho_g u_{gi} + \rho_p u_{pi} \right) + \text{div} \left(\rho_g u_{gi} \bar{q}_g + \rho_p u_{pi} \bar{q}_p \right) + \frac{\partial P_g}{\partial x_i} = 0 \tag{A-13}$$

The flux of enthalpy and kinetic energy through A is

$$\int_A \left\{ \left[h_g + \frac{1}{2} \left| \bar{q}_g \right|^2 \right] \rho_g \bar{q}_g \cdot \bar{n} + \left[h_p + \frac{1}{2} \left| \bar{q}_p \right|^2 \right] \rho_p \bar{q}_p \cdot \bar{n} \right\} dA, \text{ and} \qquad \text{(A-14)}$$

the time rate of change of enthalpy and kinetic energy in V is

$$\int_V \left\{ \frac{\partial}{\partial t} \left[\rho_g \left(h_g + \frac{1}{2} \left| \bar{q}_g \right|^2 \right) \right] + \frac{\partial}{\partial t} \left[\rho_p \left(h_p + \frac{1}{2} \left| \bar{q}_p \right|^2 \right) \right] \right\} dV \qquad \text{(A-15)}$$

The time rate of heat addition to V is

$$\int_V \frac{\partial Q}{\partial t} \, dV \qquad \text{(A-16)}$$

An energy balance for V gives

$$\int_V \frac{\partial Q}{\partial t} \, dV = \int_V \left\{ \frac{\partial}{\partial t} \left[\rho_g \left(h_g + \frac{1}{2} \left| \bar{q}_g \right|^2 \right) \right] + \frac{\partial}{\partial t} \left[\rho_p \left(h_p + \frac{1}{2} \left| \bar{q}_p \right|^2 \right) \right] \right\} dV \qquad \text{(A-17)}$$

$$+ \int_A \left\{ \left[h_g + \frac{1}{2} \left| \bar{q}_g \right|^2 \right] \rho_g \bar{q}_g \cdot \bar{n} + \left[h_p + \frac{1}{2} \left| \bar{q}_p \right|^2 \right] \rho_p \bar{q}_p \cdot \bar{n} \right\} dA$$

When the divergence theorem is applied to Equation A-17

$$\int_V \left\{ \frac{\partial}{\partial t} \left[\rho_g \left(h_g + \frac{1}{2} \left| \bar{q}_g \right|^2 \right) + \rho_p \left(h_p + \frac{1}{2} \left| \bar{q}_p \right|^2 \right) - Q \right] \right.$$

$$\left. + \operatorname{div} \left[\rho_g \left(h_g + \frac{1}{2} \left| \bar{q}_g \right|^2 \right) \bar{q}_g + \rho_p \left(h_p + \frac{1}{2} \left| \bar{q}_p \right|^2 \right) \bar{q}_p \right] \right\} dV = 0 \qquad \text{(A-18)}$$

Since this equation must hold for any volume, the energy balance becomes

$$\frac{\partial Q}{\partial t} = \frac{\partial}{\partial t}\left[\rho_g\left(h_g + \frac{1}{2}|\bar{q}_g|^2\right) + \rho_p\left(h_p + \frac{1}{2}|\bar{q}_p|^2\right)\right]$$

$$+ \text{div}\left[\rho_g\left(h_g + \frac{1}{2}|\bar{q}_g|^2\right)\bar{q}_g + \rho_p\left(h_p + \frac{1}{2}|\bar{q}_p|^2\right)\bar{q}_p\right] \qquad \text{(A-19)}$$

With the assumption that the gas obeys the perfect gas law and has a constant molecular weight and constant specific heat, the equation of state of the gas can be written as

$$P_g = \rho_g R T_g \qquad \text{(A-20)}$$

Next, a spherical particle of constant size is considered in the gas flow field as shown in Figure A-2.

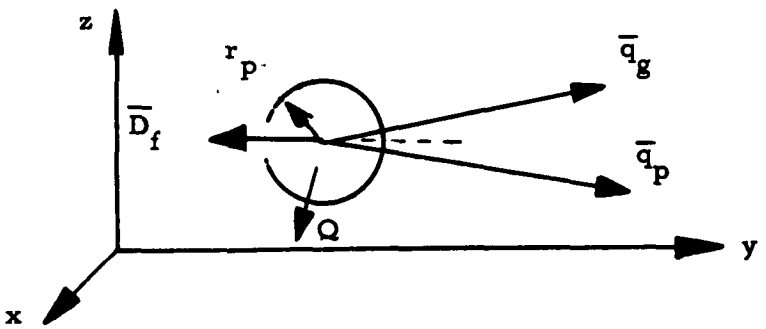

Figure A-2. Particle Momentum and Heat Transfer Model

Remembering the assumption that all body forces except for pressure of the gas and particle drag are negligible, the only force exerted on the particle is a drag force, $\bar{D}_f$, due to the relative motion between the gas and particle. A particle momentum balance gives

$$\bar{D}_f = \frac{d}{dt}\left(m_p \frac{4}{3}\pi r_p^3 \bar{q}_p\right) \qquad \text{(A-21)}$$

where m_p is the particle density per unit volume of particle. The drag on a spherical particle is given by

$$\bar{D}_f = C_D \pi r_p^2 \frac{1}{2} \rho_g \left(\overline{\Delta q}\right) \left|\overline{\Delta q}\right| \tag{A-22}$$

where $(\overline{\Delta q}) = (\bar{q}_g - \bar{q}_p)$

Equating Equations A-21 and A-22 results in

$$\frac{d\bar{q}_p}{dt} = \frac{3\rho_g C_D}{8 m_p r_p} \left(\overline{\Delta q}\right) \left|\overline{\Delta q}\right| \tag{A-23}$$

To simplify the particle momentum and energy balances, the following relations with Stokes' flow regime (where the Reynolds number is less than 1) are defined as:

$$f = \frac{C_D}{(C_D)_{\text{Stokes}}} \tag{A-24}$$

$$g = \frac{Nu}{(Nu)_{\text{Stokes}}} \tag{A-25}$$

In Stokes' flow regime, $C_D = 24/Re$, and $Nu = 2$. Therefore,

$$C_D = \frac{24f}{Re} = \frac{24f\mu_g}{2 r_p \rho_g} \frac{1}{\left|\overline{\Delta q}\right|} \tag{A-26}$$

$$Nu = Z_g \tag{A-27}$$

$$\frac{d\bar{q}_p}{dt} = \frac{9}{2} \frac{\mu_g f}{m_p r_p^2} \left(\overline{\Delta q}\right) \tag{A-28}$$

An energy balance for the particle gives

$$\frac{dQ_p}{dt} = -h4\pi r_p^2 \left(T_p - T_g\right) \tag{A-29}$$

$$h = \frac{k_g}{2r_p} Nu = \frac{k_g g}{r_p} \tag{A-30}$$

$$Q_p = m_p \frac{4}{3}\pi r_p^3 h_p \tag{A-31}$$

$$\frac{dh_p}{dt} = -3 \frac{\mu_g g}{m_p r_p^2} \frac{c_{pg}}{Pr} \left(T_p - T_g\right) \tag{A-32}$$

The temperature of the particle depends on its state; either a liquid, a liquid in the process of solidifying, or a solid, and is uniquely related to the enthalpy,

$$T_p = f\left(h_p\right) \tag{A-33}$$

The gas-particle system is now completely defined by Equations A-6, A-7, A-13, A-19, A-20, A-28, A-32, and A-33. For adiabatic steady flow, the two-dimensional and axisymmetric forms of these equations are obtained by dropping all time derivatives and expanding the above system of equations. By letting $\sigma = 1$ for two-dimensional flow, $\sigma = y$ for axisymmetric flow, x denote the longitudinal axis, and y denote the vertical or radial axis, these equations reduce to the following:

$$\rho_g (u_g)_x + \rho_g (v_g)_y + u_g(\rho_g)_x + v_g (\rho_g)_y = -\sigma_y \frac{\rho_g v_g}{\sigma} \tag{A-34}$$

$$\rho_p (u_p)_x + \rho_p (v_p)_y + u_p(\rho_p)_x + v_p (\rho_p)_y = -\sigma_y \frac{\rho_p v_p}{\sigma} \tag{A-35}$$

Expanding Equation A-13 and combining with the expanded form of Equation A-28 gives

$$\rho_g \left[u_g (u_g)_x + v_g (u_g)_y \right] + A\rho_p (u_g - u_p) + (P_g)_x = 0 \qquad (A-36)$$

$$\rho_g \left[u_g (v_g)_x + v_g (v_g)_y \right] + A\rho_p (v_g - v_p) + (P_g)_y = 0 \qquad (A-37)$$

$$A = \frac{9}{2} \frac{\mu_g f}{m_p r_p^2} \qquad (A-38)$$

The particle momentum and energy equations become

$$u_p (u_p)_x + v_p (u_p)_y = A (u_g - u_p) \qquad (A-39)$$

$$u_p (v_p)_x + v_p (v_p)_y = A (v_g - v_p) \qquad (A-40)$$

$$u_p (h_p)_x + v_p (h_p)_y = -\frac{2}{3} AC (T_p - T_g) \qquad (A-41)$$

$$C = \frac{g}{f} \frac{c_{pg}}{Pr} \qquad (A-42)$$

Expanding the system energy equation (Equation 19) and combining with the gas and particle continuity equations, the gas equation of state, the expanded form of the system momentum equation, and the following gas enthalpy-temperature relationship gives

$$h_g = c_{pg} T_g + \text{Constant} \qquad (A-43)$$

$$u_g (P_g)_x + v_g (P_g)_y - a^2 \left[u_g (\rho_g)_x + v_g (\rho_g)_y \right] - A\rho_p B = 0 \qquad (A-44)$$

$$a^2 = \gamma_g R T_g \qquad (A-45)$$

$$B = (\gamma_g - 1) \left[(u_g - u_p)^2 + (v_g - v_p)^2 + \frac{2}{3} C (T_p - T_g) \right] \qquad (A-46)$$

The gas equation of state and particle enthalpy-temperature relationship are the same.

The equations governing a gas-particle flow field are thus found to be a system of eight, quasi-linear, nonhomogeneous partial differential equations of the first order, shown as Equations A-34, A-35, A-36, A-37, A-39, A-40, A-41, and A-44. The constants A, B, and C in these equations are defined by Equations A-38, A-42, and A-46. The gas equation of state is given by Equation A-20, and the particle equation of state by Equation A-33.

APPENDIX B

METHOD OF CHARACTERISTICS

The governing differential equations often reduce to quasi-linear partial-differential equations of the first order for functions of two independent variables. A quasi-linear partial differential equation of the first order is defined as one that is nonlinear in the dependent variables but linear in the first partial derivatives of the dependent variables. Such a system of n equations can be written as:*

$$L_i = a_{ij} \frac{\partial u^j}{\partial x} + b_{ij} \frac{\partial u^j}{\partial y} + c_i = 0 \quad \begin{pmatrix} i = 1, \ldots, n \\ j = 1, \ldots, n \end{pmatrix} \tag{B-1}$$

where the superscript j identifies a particular dependent variable, and the coefficients a_{ij}, b_{ij}, and c_i depend on x, y, u^1, . . . , u^j. When expanded, this system of equations becomes:

$$\left.\begin{aligned} L_1 &= a_{11} u_x^1 + a_{12} u_x^2 + \ldots + a_{1n} u_x^n + b_{11} u_y^1 + b_{12} u_y^2 + \ldots + b_{1n} u_y^n + c_1 = 0 \\ L_2 &= a_{21} u_x^1 + a_{22} u_x^2 + \ldots + a_{2n} u_x^n + b_{21} u_y^1 + b_{22} u_y^2 + \ldots + b_{2n} u_y^n + c_2 = 0 \\ &\vdots \\ L_n &= a_{n1} u_x^1 + a_{n2} u_x^2 + \ldots + a_{nn} u_x^n + b_{n1} u_y^1 + b_{n2} u_y^2 + \ldots + b_{nn} u_y^n + c_n = 0 \end{aligned}\right\} \tag{B-2}$$

When such systems are hyperbolic, the method of characteristics can be used to obtain the desired solution. A treatise on the method of characteristics applied to fluid-flow problems has been written by Courant and Friedrichs,** and this discussion is based on that treatise. The simplify presentation, the theory will first be developed for a system of two equations, and then the results will be applied to systems of n equations.

---

* In accordance with accepted convention, when an index is repeated, the summation is carried out with respect to that index.

** Courant, R., and K.O. Friedrichs, Supersonic Flow and Shock Waves, New York, Interscience Publishers, 1948.

The concept of characteristics arises from the following relationships. A linear combination $af_x + bf_y$ of the two partial derivatives of a function f can be considered as the derivative of f in a direction given by dx:dy = a:b. Figure B-1 illustrates this point. In the figure, the curve $C(\sigma)$ is given in

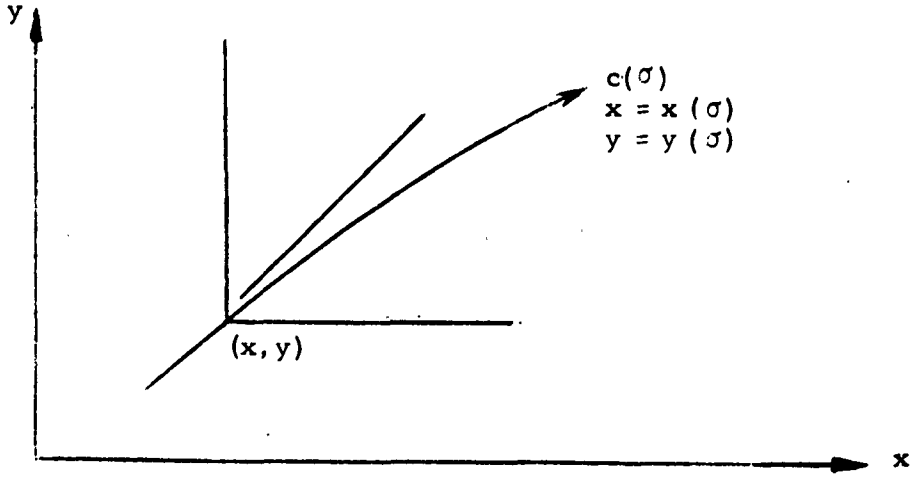

Figure B-1 Characteristic Curve

parametric representation as a function of some parameter σ. Thus, at any point (x, y), x_σ and y_σ are the direction cosines of the curve C (σ). If x_σ: y_σ: = a:b, then $df/d\sigma = f_x (dx/d\sigma) + f_y (dy/d\sigma) = f_x X_\sigma + f_y Y_\sigma$, and $af_x + bf_y$ is the total derivative of f along this curve.

Next, a system of two equations for the two dependent variables u(x, y) and v(x, y) is considered:

$$L_1 = A_1 u_x + B_1 u_y + C_1 v_x + D_1 v_y + E_1 = 0$$
$$L_2 = A_2 u_x + B_2 u_y + C_2 v_x + D_2 v_y + E_2 = 0 \qquad \text{(B-3)}$$

In addition to these equations, there are two additional equations,

$$du = u_x dx + u_y dy$$
$$dv = v_x dx + v_y dy \qquad \text{(B-4)}$$

that are valid for continuous functions having continuous derivatives. The equations of B-4 are applicable to the functions considered here because these functions are assumed to be continuous and have continuous derivatives. A linear combination, L, of L_1 and L_2 is sought:

$$L = \lambda_1 L_1 + \lambda_2 L_2 = 0 \qquad \text{(B-5)}$$

so that, in this differential expression for L, the partial derivatives of u and v combine to give total derivatives of u and v in the same direction. Such a direction, if it exists, depends on the point (x, y), as well on the values of u and v at that point, and is called characteristic. Expanding L as indicated in Equation B-5 results in the following:

$$(\lambda_1 A_1 + \lambda_2 A_2) u_x + (\lambda_1 B_1 + \lambda_2 B_2) u_y + (\lambda_1 C_1 + \lambda_2 C_2) v_x$$
$$+ (\lambda_1 D_1 + \lambda_2 D_2) v_y + (\lambda_1 E_1 + \lambda_2 E_2) = 0 \qquad \text{(B-6)}$$

Suppose the characteristic direction is given by curve C (σ) with direction cosines x_σ and y_σ. Then, for u and v in the expression for L to be differentiated in the direction of C (σ) only, by the analysis above concerning $af_x + bf_y$, the following proportionality must be satisfied:

$$(\lambda_1 A_1 + \lambda_2 A_2) : (\lambda_1 B_1 + \lambda_2 B_2) = (\lambda_1 C_1 + \lambda_2 C_2) : (\lambda_1 D_1 + \lambda_2 D_2) = x_\sigma : y_\sigma \qquad \text{(B-7)}$$

since the coefficients of the derivatives u_x, u_y, v_x, and v_y in L are given by the respective members of the above proportion.

If the functions u and v satisfy the differential equations L_1 and L_2 at the point (x, y), the following two homogeneous linear equations for λ_1 and λ_2 are obtained:

$$\lambda_1(A_1 y_\sigma - B_1 x_\sigma) + \lambda_2 (A_2 y_\sigma - B_2 x_\sigma) = 0$$
$$\lambda_1(C_1 y_\sigma - D_1 x_\sigma) + \lambda_2 (C_2 y_\sigma - D_2 x_\sigma) = 0 \qquad \text{(B-8)}$$

For B-8 to have a nontrivial solution, the determinant of the coefficients of λ_1 and λ_2 in the above equations must vanish.

$$\begin{vmatrix} (A_1 y_\sigma - B_1 x_\sigma) & (A_2 y_\sigma - B_2 x_\sigma) \\ (C_1 y_\sigma - D_1 x_\sigma) & (C_2 y_\sigma - D_2 x_\sigma) \end{vmatrix} = 0 \qquad \text{(B-9)}$$

$$(A_1 C_2 - A_2 C_1) y_\sigma^2 - \left[(A_1 D_2 - A_2 D_1) + (B_1 C_2 - B_2 C_1)\right] x_\sigma y_\sigma + (B_1 D_2 - B_2 D_1) x_\sigma^2 = 0 \qquad \text{(B-10)}$$

$$a y_\sigma^2 - 2b x_\sigma y_\sigma + c x_\sigma^2 = 0. \qquad \text{(B-11)}$$

If $ac - b^2 > 0$, then no real solutions for $\frac{y_\sigma}{x_\sigma} = \frac{dy}{dx}$ exist, and the characteristic curves C (σ) are imaginary. Differential equations that result in imaginary characteristic curves are called elliptic. If $ac - b^2 = 0$, one real characteristic direction exists through each point, and the system is called parabolic. If $ac - b^2 <$, two real characteristic directions exist through each point, and the system is called hyperbolic. From here on, only hyperbolic systems are considered. Introducing the slope

$$\zeta = \frac{y_\sigma}{x_\sigma} = \frac{dy}{dx} \qquad \text{(B-12)}$$

Equation B-11 can be written as

$$a\zeta^2 - 2b\zeta + c = 0 \qquad \text{(B-13)}$$

which, for hyperbolic systems, has two distinct real solutions $\zeta +$ and $\zeta -$. Hence, the two characteristic curves C (σ) satisfy the two ordinary differential equations

$$\frac{dy}{dx} = \zeta + \quad \text{and} \quad \frac{dy}{dx} = \zeta - \qquad \text{(B-14)}$$

Since the roots $\zeta +$ and $\zeta -$ are functions of x, y, u, and v, the hyperbolic character of the system depends on the particular functions u (x, y) and v (x, y) under consideration. When a solution u (x, y) and v (x, y) is inserted into Equation B-14, the equations $dy/dx = \zeta +$ (u, v, x, y) and $dy/dx = \zeta -$ (u, v, x, y) are two ordinary differential equations of the first order that define two families of characteristic curves, or simply characteristics, C+ and C- in the (x, y) plane.

In the case of two dependent variables u and v, four equations were found relating u_x, u_y, v_x, and v_y.

$$L_1 = A_1u_x + B_1u_y + C_1v_x + D_1v_y + E_1 = 0$$
$$L_2 = A_2u_x + B_2u_y + C_2v_x + D_2v_y + E_2 = 0 \qquad \text{(B-15)}$$

$$u_x dx + u_y dy = du$$
$$v_x dx + v_y dy = dv$$

By using Cramer's Rule for a system of n nonhomogeneous linear equations in n unknowns, the partial derivatives of u and v may be determined. Cramer's Rule states that if the determinant of the coefficients of the unknowns, D, is

different from zero, each unknown has a unique solution given by $k_i = \frac{D_i}{D}$, where D_i is the determinant obtained from D by replacing the ith column of D by the nonhomogeneous terms, and k_i is any one of the partial derivatives of u and v. In the present case of two dependent variables discussed above, D is found to be

$$D = \begin{vmatrix} A_1 & B_1 & C_1 & D_1 \\ A_2 & B_2 & C_2 & D_2 \\ dx & dy & 0 & 0 \\ 0 & 0 & dx & dy \end{vmatrix} = \begin{vmatrix} (A_1dy - B_1dx) & (C_1dy - D_1dx) & B_1 & D_1 \\ (A_2dy - B_2dx) & (C_2dy - D_2dx) & B_2 & D_2 \\ (dydx - dydx) & 0 & dy & 0 \\ 0 & (dxdy - dydx) & 0 & dy \end{vmatrix}$$

$$D = \begin{vmatrix} (A_1dy - B_1dx) & (C_1dy - D_1dx) \\ (A_2dy - B_2dx) & (C_2dy - D_2dx) \end{vmatrix} (dy)^2 \qquad \text{(B-16)}$$

By comparing this solution for D with Equation B-9, it is found that D = 0 along characteristic curves. This result is valid along only the characteristic curves. Thus, the solution for $k_i = D_i/D$ will not exist along the characteristic curves unless $D_i = 0$, thus placing k_i into the indeterminant form:

$$k_i = \frac{D_i}{D} = \frac{0}{0} \qquad \text{(B-17)}$$

Solving the determinants $D_i = 0$ results in a system of compatibility equations equal in number to the number of partial derivatives in the original system of equations. The number of compatibility equations that are independent equals at most the number of dependent variables in the original system. By observing the nonhomogeneous term in the equations of B-15, it can be seen that these compatibility equations will contain only total derivatives of u and v. Thus, the system of partial differential equations has been replaced by a system of total differential equations valid along the characteristic curves.

So far, a fixed solution u (x, y) and v (x, y) has been assumed. However, the equations of B-15 no longer depend explicitly on this solution, since all the coefficients are known functions of x, y, u, and v. By a slight change in interpretation, the equations of B-15 and the compatibility equations can be considered as a system of four equations for the determination of x, y, u, and v. Replacing the original system (equations of B-3) by this characteristic system is the basis of the method of characteristics.

The method of characteristics can now be extended to a system of n differential equations by analogy to the above case of two equations. Equation B-1 for such a system is repeated here as

$$L_i = a_{ij} \frac{\partial u^j}{\partial x} + b_{ij} \frac{\partial u^j}{\partial y} + c_i = 0 \quad \begin{pmatrix} i = 1, \ldots, n \\ j = 1, \ldots, n \end{pmatrix}$$

As in the case of two equations, the following equations result from the continuous nature of the assumed solution for u^j:

$$du^j = u_x{}^j dx + u_y{}^j dy \quad (j = 1, \ldots, n) \tag{B-18}$$

Again, a specific solution u^j is assumed, and curves C (σ) are sought so that a linear combination $\lambda_i L_i$ of the differential equations can be formed in which differentiations occur only along the curves C (σ).

$$L = \lambda_i L_i = \lambda_1 L_1 + \lambda_2 L_2 + \ldots + \lambda_n L_n = 0 \tag{B-19}$$

Expanding L as indicated in Equation B-19 yields the following:

$$\begin{aligned} &(\lambda_1 a_{11} + \lambda_2 a_{21} + \ldots + \lambda_n a_{n1})\, u_x{}^1 + (\lambda_1 b_{11} + \lambda_2 b_{21} + \ldots + \lambda_n b_{n1})\, u_y{}^1 \\ &+ (\lambda_1 a_{12} + \lambda_2 a_{22} + \ldots + \lambda_n a_{n2})\, u_x{}^2 + (\lambda_1 b_{12} + \lambda_2 b_{22} + \ldots + \lambda_n b_{n2})\, u_y{}^2 \\ &+ \ldots + (\lambda_1 a_{1n} + \lambda_2 a_{2n} + \ldots + \lambda_n a_{nn})\, u_x^n + (\lambda_1 b_{1n} + \lambda_2 b_{2n} + \ldots + \lambda_n b_{nn})\, u_y^n = 0 \end{aligned} \tag{B-20}$$

As in the case of two equations, the coefficients of u_x^j and u_y^j must be in direct proportion to the direction cosines x_σ and y_σ of C (σ) if L is to be differentiated only along C (σ). This proportionality takes the form

$$\begin{aligned}
&(\lambda_1 a_{11} + \lambda_2 a_{21} + .. + \lambda_n a_{n1}) : (\lambda_1 b_{11} + \lambda_2 b_{21} + .. + \lambda_n b_{n1}) = x_\sigma : y_\sigma \\
&(\lambda_1 a_{12} + \lambda_2 a_{22} + .. + \lambda_n a_{n2}) : (\lambda_1 b_{12} + \lambda_2 b_{22} + .. + \lambda_n b_{n2}) = x_\sigma : y_\sigma \\
&\quad\vdots \qquad\quad \vdots \qquad\qquad \vdots \qquad\quad \vdots \qquad\quad \vdots \qquad\quad \vdots \qquad \vdots \\
&(\lambda_1 a_{1n} + \lambda_2 a_{2n} + .. + \lambda_n a_{nn}) : (\lambda_1 b_{1n} + \lambda_2 b_{2n} + .. + \lambda_n b_{nn}) = x_\sigma : y_\sigma
\end{aligned} \tag{B-21}$$

Equation B-21, when rearranged with λ_i as the unknown, takes the form

$$\begin{aligned}
&\lambda_1(a_{11}y_\sigma - b_{11}x_\sigma) + \lambda_2(a_{21}y_\sigma - b_{21}x_\sigma) + .. + \lambda_n(a_{n1}y_\sigma - b_{n1}x_\sigma) = 0 \\
&\lambda_1(a_{12}y_\sigma - b_{12}x_\sigma) + \lambda_2(a_{22}y_\sigma - b_{22}x_\sigma) + .. + \lambda_n(a_{n2}y_\sigma - b_{n2}x_\sigma) = 0 \\
&\quad\vdots \qquad\qquad\qquad\quad \vdots \qquad\qquad\qquad\quad \vdots \qquad\qquad \vdots \\
&\lambda_1(a_{1n}y_\sigma - b_{1n}x_\sigma) + \lambda_2(a_{2n}y_\sigma - b_{2n}x_\sigma) + .. + \lambda_n(a_{nn}y_\sigma - b_{nn}x_\sigma) = 0
\end{aligned} \tag{B-22}$$

which can be written as

$$\lambda_i\,(a_{ij}y_\sigma - b_{ij}x_\sigma) = 0 \quad (j = 1, \ldots, n) \tag{B-23}$$

For the solution of the system of equations defined by Equation B-23 to be other than zero, the determinant of the coefficients of λ_i must vanish:

$$\left|\,(a_{ij}y_\sigma - b_{ij}x_\sigma)\,\right| = 0 \tag{B-24}$$

When expanded, the determinant takes the form

$$\begin{vmatrix}
(a_{11}y_\sigma - b_{11}x_\sigma) & (a_{12}y_\sigma - b_{12}x_\sigma) & \cdots & (a_{1n}y_\sigma - b_{1n}x_\sigma) \\
(a_{21}y_\sigma - b_{21}x_\sigma) & (a_{22}y_\sigma - b_{22}x_\sigma) & \cdots & (a_{2n}y_\sigma - b_{2n}x_\sigma) \\
\vdots & \vdots & \vdots & \vdots \\
(a_{n1}y_\sigma - b_{n1}x_\sigma) & (a_{n2}y_\sigma - b_{n2}x_\sigma) & \cdots & (a_{nn}y_\sigma - b_{nn}x_\sigma)
\end{vmatrix} = 0 \tag{B-25}$$

The expanded determinant results in an algebraic equation of the nth degree for $\zeta = y_\sigma / x_\sigma = dy/dx$, giving n roots ζ_n, which determine n characteristic directions. If all n roots are distinct and real, the system is totally hyperbolic. There are then n families of characteristics $C_n(\sigma)$ satisfying the ordinary differential equations

$$\frac{dy}{dx} = \zeta_n \qquad \text{(B-26)}$$

each family covering the domain of the (x, y) plane under consideration. As in the case of two equations, the following equations relating the x and y partial derivatives of u^j were found:

$$L_i = a_{ij} u^j_x + b_{ij} u^j_y + c_i = 0 \qquad \begin{pmatrix} i=1, \ldots, n \\ j=1, \ldots, n \end{pmatrix} \qquad \text{(From Equation B-1)}$$

$$u^j_x\, dx + u^j_y\, dy = du^j \qquad (j = 1, \ldots, n) \qquad \text{(From Equation B-18)}$$

Again, by using Cramer's Rule for the system of 2n linear nonhomogeneous equations in 2n unknowns, the partial derivatives of u^j can be determined. By denoting any of the partial derivatives of u^j by k_i, the solution becomes $k_i = D_i/D$, where D is the determinant of the coefficients of the equations of B-1 and B-18, and D_i is the determinant obtained from D by replacing the ith column of D by the nonhomogenous terms. Exactly as in the case of two equations, D is found to be the same as the determinant of Equation B-24, which is equal to zero, and defines the characteristic curves $C_n(\sigma)$. Thus, for k_i to exist, D_i must be zero, and a system of 2n compatibility equations in terms of the total derivatives u^j are obtained, of which at most n are independent. Thus the general system of n partial differential equations for n variables has been replaced by a system of n total differential equations valid along the n characteristic curves, $C_n(\sigma)$.

Next, the initial value problem is formulated for the above system of hyperbolic differential equations. Assume a curve Γ_o is given in the (x, y)

plane, and continuous values of u^j arbitrarily prescribed along Γ_o. Then, the problem is to determine, in the neighborhood of Γ_o, a solution u^j of the system that takes on the prescribed initial values along Γ_o. By replacing the original system by the characteristic system, the system reduces to total differential equations along the characteristic curves. In general, these equations are non-linear, and each is coupled with some of the others. For this reason, a solution by a numerical iteration technique becomes necessary. The compatibility equations, each valid along one or more of the characteristic curves, can be put in finite difference form, and the equations of the characteristic curves themselves can also be put in this form. Then, by moving along a characteristic curve, the initial values of u^j along Γ_o can be extended into the domain enclosed by the outermost characteristic curves passing through the initial data curve Γ_o. By continuing in small steps along the length of Γ_o, a new curve, Γ_1, can be obtained with all the values of u^j determined along this curve, as shown in Figure B-2.

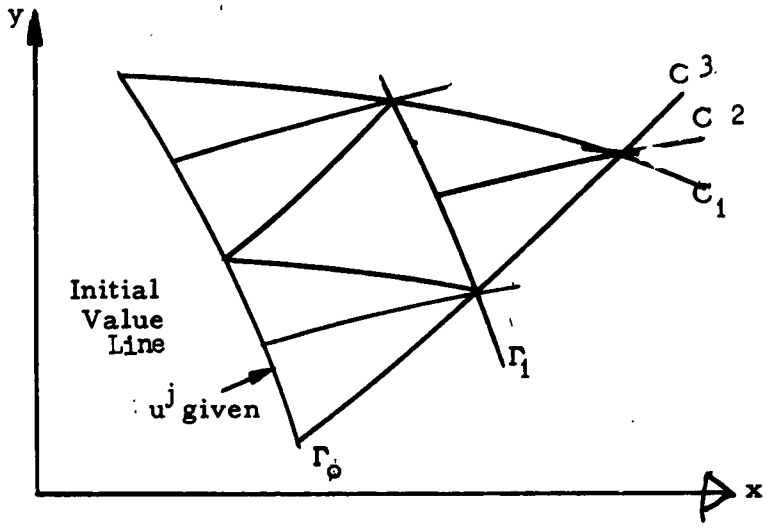

Figure B-2. Characteristic Initial Value Line and Solution Net

The above considerations result in the concepts of domain of dependence and range of influence. The domain of dependence of a point P is the region in the (x, y) plane, bounded by the outermost characteristics passing through the initial data line, in which the solution of the initial value problem can be established. The range of influence of a point Q on the initial value line is the totality of points in the (x, y) plane which are influenced by the initial data at point Q. This region consists of all points whose domain of dependence contain the point Q; therefore, it is the region between the two outermost characteristics passing through the initial point Q. The range of influence and domain of dependence are illustrated in Figures B-3 and B-4.

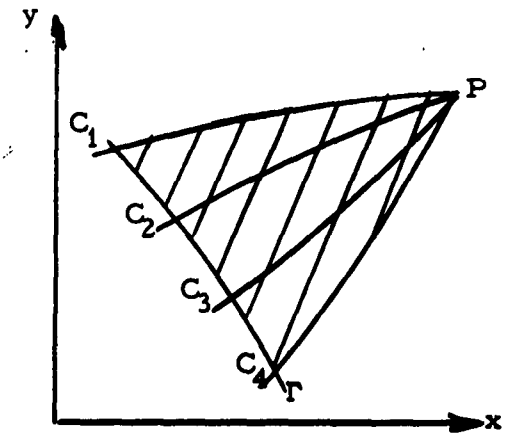

Figure B-3
Domain of Dependence

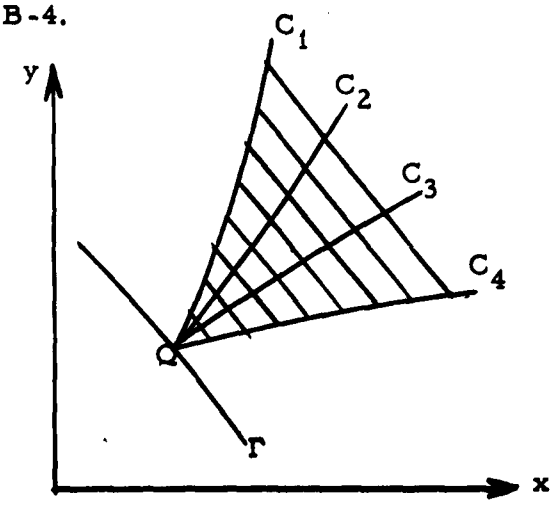

Figure B-4
Range of Influence

For a solution to be possible, the initial data line cannot be characteristic at any place unless initial data are given along two intersecting characteristic curves. Several types of domain with different types of initial data lines can be solved; however, only the domain in which the initial data line is nowhere characteristic is of interest in the present discussion.

By means of the method of characteristics just described, many complicated systems of partial differential equations can be solved, if the system is found to be quasi-linear and hyperbolic. These conditions are frequently encountered in fluid flow problems.

APPENDIX C

DETERMINATION OF THE CHARACTERISTICS OF A GAS-PARTICLE MIXTURE

The complexity of the equations describing a gas-particle mixture requires that a solution be obtained by other than conventional methods. The system of eight first-order, quasi-linear, nonhomogeneous, partial-differential equations can generally be solved by using the general theory of the method of characteristics as outlined in Appendix B. After an initial effort to solve the entire system of eight equations, it was found that four distinct characteristics curves did exist, but only seven distinct compatibility relationships were found. Therefore, the particle continuity equation was solved separately by the introduction of a particle stream function. The resulting relationship was then considered to define the particle density ρ_p throughout the flow field, since there was no compatibility equation describing the variation of ρ_p. The solution was then found for the particle continuity equation as follows:

$$(\rho_p u_p)_x + \frac{1}{\sigma} (\sigma \rho_p v_p)_y = 0 \qquad \text{(C-1)}$$

The definition of the stream function was chosen as

$$(\psi_p)_y = \sigma \rho_p u_p \qquad \text{(C-2)}$$

$$(\psi_p)_x = -\sigma \rho_p v_p \qquad \text{(C-3)}$$

where $\sigma = 1$ for two-dimensional flow, $\sigma = y$ for axisymmetric flow, x is the longitudinal axis direction, and y is the vertical or radial direction for two-dimensional or axisymmetic flow, respectively. The definition of a particle

streamline is

$$\frac{dy}{dx} = \frac{v_p}{u_p} \tag{C-4}$$

The total derivative of Ψ_p is

$$d\Psi_p = \Psi_x dx + \Psi_y dy \tag{C-5}$$

$$d\Psi_p = \sigma \rho_p u_p dy - \sigma \rho_p v_p dx \tag{C-6}$$

Along particle streamlines, therefore,

$$d\Psi_p = 0 \tag{C-7}$$

The remaining seven equations form a system of equations that can be solved by the method of characteristics. The characteristic curves are found to be the gas streamline, the particle streamline, and the two conventional gas Mach lines. For supersonic flow, the system is totally hyperbolic, and for subsonic flow partially hyperbolic.

Since the seven quantities under consideration are assumed to be continuous functions, there also exist seven equations of the form

$$du^j = u_x{}^j dx + u_y{}^j dy \quad (j = 1, \ldots, 7) \tag{C-8}$$

where u^j represents u_g, v_g, ρ_g, P_g, u_p, v_p, and h_p. Thus, there exist the following fourteen equations for the determination of the fourteen partial derivatives of the seven dependent variables:

$$\rho_g (u_g)_x + \rho_g (v_g)_y + u_g (\rho_g)_x + v_g (\rho_g)_y = -\sigma_y \frac{\rho_g v_g}{\sigma} \quad \text{(C-9)}$$

$$\rho_g u_g (u_g)_x + \rho_g v_g (u_g)_y + (P_g)_x = -A\rho_p (u_g - u_p) \quad \text{(C-10)}$$

$$\rho_g u_g (v_g)_x + \rho_g v_g (v_g)_y + (P_g)_y = -A\rho_p (v_g - v_p) \quad \text{(C-11)}$$

$$u_g (P_g)_x + v_g (P_g)_y - a^2 u_g (\rho_g)_x - a^2 v_g (\rho_g)_y = A\rho_p B \quad \text{(C-12)}$$

$$u_p (u_p)_x + v_p (u_p)_y = A(u_g - u_p) \quad \text{(C-13)}$$

$$u_p (v_p)_x + v_p (v_p)_y = A(v_g - v_p) \quad \text{(C-14)}$$

$$u_p (h_p)_x + v_p (h_p)_y = -\frac{2}{3} AC (T_p - T_g) \quad \text{(C-15)}$$

$$(u_g)_x dx + (u_g)_y dy = du_g \quad \text{(C-16)}$$

$$(v_g)_x dx + (v_g)_y dy = dv_g \quad \text{(C-17)}$$

$$(\rho_g)_x dx + (\rho_g)_y dy = d\rho_g \quad \text{(C-18)}$$

$$(P_g)_x dx + (P_g)_y dy = dP_g \quad \text{(C-19)}$$

$$(u_p)_x dx + (u_p)_y dy = du_p \quad \text{(C-20)}$$

$$(v_p)_x dx + (v_p)_y dy = dv_p \quad \text{(C-21)}$$

$$(h_p)_x dx + (h_p)_y dy = dh_p \quad \text{(C-22)}$$

where

$$A = \frac{9}{2} \frac{\mu_g f}{m_p r_p^2} \tag{C-23}$$

$$B = (\gamma_g - 1) \left[(u_g - u_p)^2 + (v_g - v_p)^2 + \frac{2}{3} C (T_p - T_g) \right] \tag{C-24}$$

$$C = \frac{g}{f} \frac{c_{pg}}{Pr} \tag{C-25}$$

The gas and particle equations of state are

$$P_g = \rho_g R T_g \tag{C-26}$$

$$T_p = f(h_p) \quad \text{(Tabulated)} \tag{C-27}$$

As discussed in Appendix B, the characteristic directions themselves are found by solving the determinant

$$\left| a_{ij} \frac{dy}{dx} - b_{ij} \right| = 0 \tag{C-28}$$

where a_{ij} and b_{ij} are the coefficients of the x and y derivatives of the seven dependent variables in the seven original system equations,

$$L_i = a_{ij} u_x^j + b_{ij} u_y^j + c_i = 0 \; (i = 1, .., 7) \tag{C-29}$$

$$a_{ij} = \begin{vmatrix} \rho_g & 0 & u_g & 0 & 0 & 0 & 0 \\ \rho_g u_g & 0 & 0 & 1 & 0 & 0 & 0 \\ 0 & \rho_g u_g & 0 & 0 & 0 & 0 & 0 \\ 0 & 0 & -a^2 u_g & u_g & 0 & 0 & 0 \\ 0 & 0 & 0 & 0 & u_p & 0 & 0 \\ 0 & 0 & 0 & 0 & 0 & u_p & 0 \\ 0 & 0 & 0 & 0 & 0 & 0 & u_p \end{vmatrix} \qquad \text{(C-30)}$$

$$b_{ij} = \begin{vmatrix} 0 & \rho_g & v_g & 0 & 0 & 0 & 0 \\ \rho_g v_g & 0 & 0 & 0 & 0 & 0 & 0 \\ 0 & \rho_g v_g & 0 & 1 & 0 & 0 & 0 \\ 0 & 0 & -a^2 v_g & v_g & 0 & 0 & 0 \\ 0 & 0 & 0 & 0 & v_p & 0 & 0 \\ 0 & 0 & 0 & 0 & 0 & v_p & 0 \\ 0 & 0 & 0 & 0 & 0 & 0 & v_p \end{vmatrix} \qquad \text{(C-31)}$$

When Equations (30) and (31) are used, Equation (28) becomes

$$\begin{vmatrix} \rho_g \frac{dy}{dx} & -\rho_g & (u_g \frac{dy}{dx} - v_g) & 0 & 0 & 0 & 0 \\ \rho_g(u_g \frac{dy}{dx} - v_g) & 0 & 0 & \frac{dy}{dx} & 0 & 0 & 0 \\ 0 & \rho_g(u_g \frac{dy}{dx} - v_g) & 0 & -1 & 0 & 0 & 0 \\ 0 & 0 & -a^2(u_g \frac{dy}{dx} - v_g) & (u_g \frac{dy}{dx} - v_g) & 0 & 0 & 0 \\ 0 & 0 & 0 & 0 & (u_p \frac{dy}{dx} - v_p) & 0 & 0 \\ 0 & 0 & 0 & 0 & 0 & (u_p \frac{dy}{dx} - v_p) & 0 \\ 0 & 0 & 0 & 0 & 0 & 0 & (u_p \frac{dy}{dx} - v_p) \end{vmatrix} = 0 \qquad \text{(C-32)}$$

Expanding Equation (32) and solving for $\frac{dy}{dx}$ gives

$$(u_g \frac{dy}{dx} - v_g)^2 \left(\frac{dy}{dx} - \frac{u_g v_g \pm a^2\sqrt{M^2-1}}{u_g^2 - a^2}\right) \left(u_p \frac{dy}{dx} - v_p\right)^3 = 0 \qquad \text{(C-33)}$$

From Equation (33), seven characteristic directions were obtained, the following four being distinct:

a) Gas streamlines,

$$\frac{dy}{dx} = \frac{v_g}{u_g} \qquad \text{(C-34)}$$

b) Gas Mach lines,

$$\frac{dy}{dx} = \frac{u_g v_g \pm a^2\sqrt{M^2 - 1}}{u_g^2 - a^2} \qquad \text{(C-35)}$$

c) Particle streamlines,

$$\frac{dy}{dx} = \frac{v_p}{u_p} \qquad \text{(C-36)}$$

To determine the compatibility equations that must be valid along the characteristic curves, the determinant of the coefficients of the 14 equations of the complete system was modified by replacing one column at a time by the nonhomogeneous terms, c_i. The system of Equations (C-9) through (C-22) in matrix form is shown in Figure C-1.

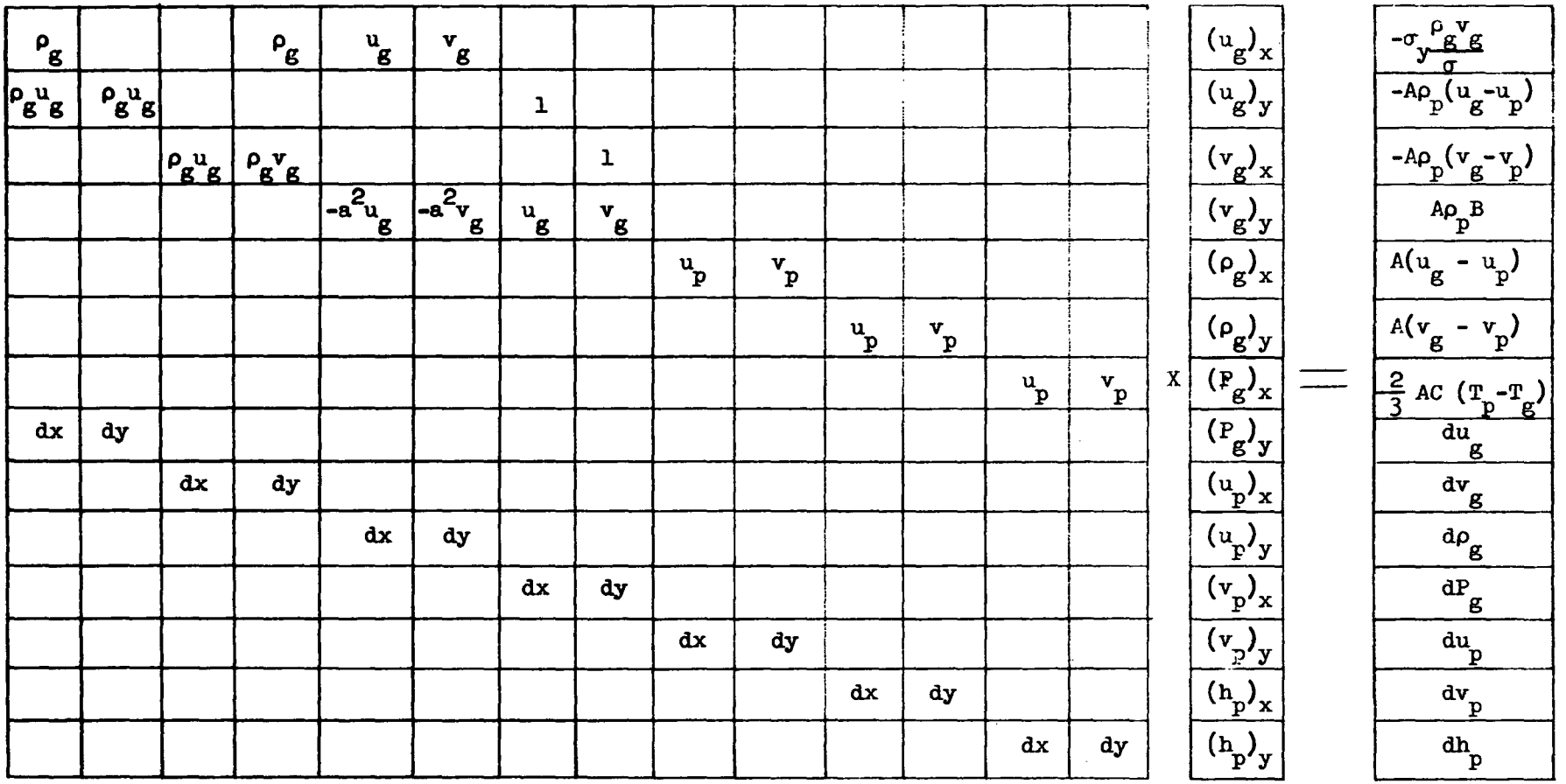

ρ_g			ρ_g	u_g	v_g								
$\rho_g u_g$	$\rho_g u_g$					1							
		$\rho_g u_g$	$\rho_g v_g$				1						
				$-a^2 u_g$	$-a^2 v_g$	u_g	v_g						
								u_p	v_p				
										u_p	v_p		
												u_p	v_p
dx	dy												
		dx	dy										
				dx	dy								
						dx	dy						
								dx	dy				
										dx	dy		
												dx	dy

X

$(u_g)_x$
$(u_g)_y$
$(v_g)_x$
$(v_g)_y$
$(\rho_g)_x$
$(\rho_g)_y$
$(P_g)_x$
$(P_g)_y$
$(u_p)_x$
$(u_p)_y$
$(v_p)_x$
$(v_p)_y$
$(h_p)_x$
$(h_p)_y$

=

$-\sigma_y \frac{\rho_g v_g}{\sigma}$
$-A\rho_p(u_g - u_p)$
$-A\rho_p(v_g - v_p)$
$A\rho_p B$
$A(u_g - u_p)$
$A(v_g - v_p)$
$\frac{2}{3} AC\,(T_p - T_g)$
du_g
dv_g
$d\rho_g$
dP_g
du_p
dv_p
dh_p

Figure C-1. Matrix of Equations C-9 Through C-22

All blank spaces represent zeros. By replacing the columns one at a time with the nonhomogeneous terms, seven compatibility equations were obtained, each valid along a particular characteristic curve. Along gas streamlines:

$$\frac{dy}{dx} = \frac{v_g}{u_g} \tag{C-37}$$

$$\rho_g \left[u_g du_g + v_g dv_g \right] + dP_g = -A\rho_p \left[(u_g - u_p)\, dx + (v_g - v_p)\, dy \right] \tag{C-38}$$

$$\frac{dP_g}{P_g} - \gamma_g \frac{d\rho_g}{\rho_g} = \frac{A\rho_p B dx}{P_g u_g} \tag{C-39}$$

Along gas Mach lines,

$$\frac{dy}{dx} = \frac{u_g v_g \pm a^2 \sqrt{M^2 - 1}}{u_g^2 - a^2} \tag{C-40}$$

$$\left(u_g dy - v_g dx\right)\left[A\rho_p B dx - u_g dP_g \right] + a^2 \left\{ A\rho_p \left[\left(u_g - u_p \right) dy - \left(v_g - v_p \right) dx \right] dx + \rho_g \left[v_g du_g - u_g dv_g - \sigma_y \frac{v_g}{\sigma} \left(u_g dy - v_g dx \right) \right] dx + dP_g dy \right\} = 0 \tag{C-41}$$

Along particle streamlines,

$$\frac{dy}{dx} = \frac{v_p}{u_p} \tag{C-42}$$

$$u_p du_p = A(u_g - u_p) dx \tag{C-43}$$

$$v_p dv_p = A(v_g - v_p)\, dy \tag{C-44}$$

$$u_p dh_p = -\frac{2}{3} AC\, (T_p - T_g)\, dx \tag{C-45}$$

These seven compatibility equations were found when solving for the following partial derivatives:

$(u_g)_x$: (C-38) on gas streamlines and (C-41) on gas Mach lines

$(u_g)_y$: (C-38) on gas streamlines and (C-41) on gas Mach lines

$(v_g)_x$: (C-38) on gas streamlines and (C-41) on gas Mach lines

$(v_g)_y$: (C-38) on gas streamlines and (C-41) on gas Mach lines

$(\rho_g)_x$: (C-39) on gas streamlines and (C-41) on gas Mach lines

$(\rho_g)_y$: (C-39) on gas streamlines and (C-41) on gas Mach lines

$(P_g)_x$: (C-41) on gas Mach lines

$(P_g)_y$: (C-41) on gas Mach lines

$(u_p)_x$: (C-43) on particle streamlines

$(u_p)_y$: (C-43) on particle streamlines

$(v_p)_x$: (C-44) on particle streamlines

$(v_p)_y$: (C-44) on particle streamlines

$(h_p)_x$: (C-45) on particle streamlines

$(h_p)_y$: (C-45) on particle streamlines

When the flow is supersonic, ($M > 1$), the system is totally hyperbolic. The original system of eight partial differential equations can be replaced by the system of seven total differential equations valid along the characteristics and by the definition of the particle stream function Ψ_p.

In the subsonic flow regime where $M < 1$, the gas Mach lines are imaginary. However, the gas and particle streamlines are still real and can be used to determine the gas and particle properties if the gas velocity components u_g and v_g can be determined by some other procedure. A simplification of the original system is thus obtained even in the subsonic and transonic flow regimes.

APPENDIX D

GENERAL ONE-DIMENSIONAL FLOW OF A GAS-PARTICLE MIXTURE

In the application of the method of characteristics to the supersonic portion of a nozzle, a starting line is required across the flow field in the supersonic region. To determine the starting line, the solution for the entire flow field in the subsonic and transonic portions of the nozzle must first be derived. Since all the characteristic curves do not exist in the regions with Mach numbers less than 1, a different approach is necessary in these regions.

The only feasible approach is a general one-dimensional analysis in the subsonic portion of the nozzle and a constant-lag one-dimensional analysis in the transonic portion of the nozzle. The general one-dimensional analysis is discussed in this appendix, and the constant-lag analysis is discussed in Appendix E. The assumptions that pertain to the following discussion are the same as those made for the axisymmetric case with the additional restriction of one-dimensional flow.

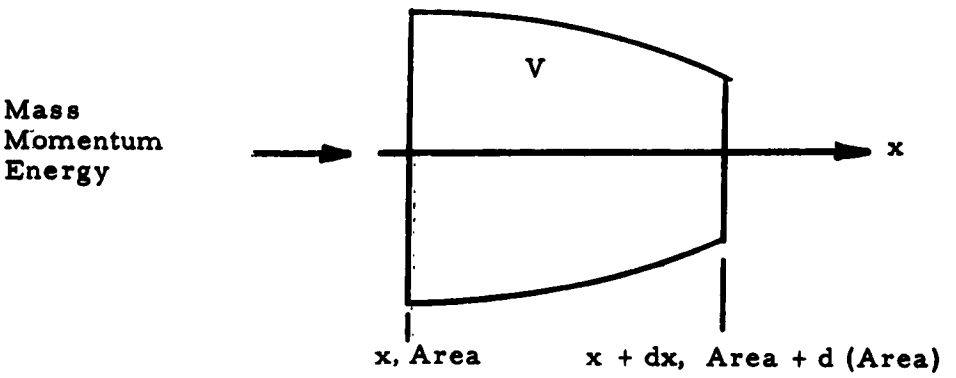

Figure D-1. General One-Dimensional Gas-Particle Model

In the one-dimensional control volume shown in Figure D-1, a mass balance results in

$$\dot{w}_g = \rho_g u_g \text{ Area} \qquad \text{(D-1)}$$

$$\dot{w}_g = \rho_p u_p \text{ Area} \qquad \text{(D-2)}$$

A momentum balance on V yields the equation

$$\rho_g u_g (u_g)_x + \rho_p u_p (u_p)_x + (P_g)_x = 0 \qquad \text{(D-3)}$$

An energy balance on V results in the relationship

$$\dot{w}_g \left[C_{pg}(T_g - T_{go}) + \frac{1}{2} u_g^2 \right] + \dot{w}_p \left[(h_p - h_{po}) + \frac{1}{2} u_p^2 \right] = 0 \qquad \text{(D-4)}$$

where the subscript o denotes chamber stagnation conditions. The equation of state of the gas is

$$P_g = \rho_g R T_g \qquad \text{(D-5)}$$

A momentum balance on a spherical particle yields the relationship

$$u_p (u_p)_x = \frac{3}{8} \frac{C_D \rho_g}{m_p r_p} (u_g - u_p) \mid u_g - u_p \mid \qquad \text{(D-6)}$$

and an energy balance on a spherical particle results in

$$u_p (h_p)_x = - \frac{3h}{m_p r_p} (T_p - T_g) \qquad \text{(D-7)}$$

where

$$C_D = f(Re)$$

$$Re = \frac{2 r_p \mid u_g - u_p \mid \rho_g}{\mu_g}$$

$$h = \frac{k_g Nu}{2 r_p}$$

The equation of state of the particle was expressed in tabular form by the relationship

$$T_p = f(h_p) \qquad \text{(Tabulated)} \qquad \text{(D-8)}$$

When the system energy equation (Equation D-4) is solved for the gas temperature T_g in terms of the remaining flow variables, the result is

$$T_g = T_{go} - \frac{\dot{w}_p}{\dot{w}_g} \frac{1}{C_{pg}} \left[(h_p - h_{po}) + \frac{1}{2} u_p^2 \right] - \frac{1}{2} \frac{u_g^2}{C_{pg}} \qquad \text{(D-9)}$$

By means of the gas and particle continuity equations, the gas equation of state, the system energy equation given in Equation D-9, and the multiplier $\frac{u_g \text{ Area}}{\dot{w}_g}$, the system momentum balance can be rewritten as

$$\frac{RT_g}{u_g} (M^2 - 1) (u_g)_x + \frac{\dot{w}_p}{\dot{w}_g} \left[(u_g - \frac{R}{C_{pg}} u_p)(u_p)_x - \frac{R}{C_{pg}} (h_p)_x \right] - \frac{RT_g}{\text{Area}} (\text{Area})_x = 0 \qquad \text{(D-10)}$$

where

$$M^2 = \frac{u_g^2}{a^2}$$

As in the axisymmetric case, the following definitions apply:

$$f = \frac{C_D}{(C_D)_{\text{Stokes}}} = \frac{C_D \, Re}{24} \quad \text{and} \qquad \text{(D-11)}$$

$$g = \frac{Nu}{(Nu)_{\text{Stokes}}} = \frac{Nu}{2} \qquad \text{(D-12)}$$

Equations D-6 and D-7 can then be solved for $(u_p)_x$ and $(h_p)_x$

$$\frac{du_p}{dx} = A \left(\frac{u_g - u_p}{u_p} \right) \qquad \text{(D-13)}$$

$$\frac{dh_p}{dx} = - \frac{2}{3} AC \left(\frac{T_p - T_g}{u_p} \right) \text{ where} \qquad \text{(D-14)}$$

$$A = \frac{9}{2} \frac{\mu_g f}{m_p r_p 2} \quad \text{and} \tag{D-15}$$

$$C = \frac{g}{f} \frac{C_{pg}}{Pr} \tag{D-16}$$

Substituting Equations D-13 and D-14 in Equation D-10 results in

$$\frac{du_g}{dx} = \left(\frac{1}{M^2-1}\right)\left\{\left(\frac{u_g}{Area}\frac{d(Area)}{dx}\right) - \left(\frac{\dot{w}_p}{\dot{w}_g}\right)\left(\frac{u_g}{u_p}\right)\frac{1}{a^2}\left[\frac{2}{3}(\gamma_g-1)AC(T_p-T_g) + A\left\{\gamma_g\left(u_g-u_p\right)^2 + u_p\left(u_g-u_p\right)\right\}\right]\right\} \tag{D-17}$$

$$a^2 = \gamma_g R T_g.$$

Solving Equations D-1 and D-2 for ρ_g and ρ_p results in the following relationships

$$\rho_g = \frac{\dot{w}_g}{u_g Area} \tag{D-18}$$

$$\rho_p = \frac{\dot{w}_p}{u_p Area} \tag{D-19}$$

The gas pressure is found from the gas equation of state

$$P_g = \rho_g R T_g \tag{D-20}$$

The shape of the nozzle determines the function

$$Area = f(x) \tag{D-21}$$

the cross-sectional area of the nozzle.

Thus, the general one-dimensional flow of a gas-particle system is represented by the following system of equations.

$$\frac{du_p}{dx} = A \left(\frac{u_g - u_p}{u_p}\right) \tag{D-22}$$

$$\frac{dh_p}{dx} = -\frac{2}{3} AC \left(\frac{T_p - T_g}{u_p}\right) \tag{D-23}$$

$$\frac{du_g}{dx} = \left(\frac{1}{M^2-1}\right) \left\{ \frac{u_g}{area} \frac{d\,(Area)}{dx} - \left(\frac{\dot{w}_p}{\dot{w}_g}\right) \left(\frac{u_g}{u_p}\right) \frac{1}{a^2} \left[\frac{2}{3} \left(\gamma_g - 1\right) AC \left(T_p - T_g\right) + A \left\{ \gamma_g (u_g - u_p)^2 + u_p (u_g - u_p) \right\} \right] \right\} \tag{D-24}$$

$$a^2 = \gamma_g R\, T_g$$

$$M^2 = \frac{u_g^2}{a^2}$$

$$Area = f(X) \qquad \text{(Given)} \tag{D-25}$$

$$C = \frac{g}{f} \frac{c_{pg}}{Pr} \tag{D-26}$$

$$A = \frac{9}{2} \frac{\mu_g f}{m_p r_p^2} \tag{D-27}$$

$$f = f(Re) \qquad \text{(Given)}$$

$$g = g(Re) \qquad \text{(Given)}$$

$$\rho_g = \frac{\dot{w}_g}{u_g\, Area} \tag{D-28}$$

$$\rho_p = \frac{\dot{w}_p}{u_p\, Area} \tag{D-29}$$

$$T_p = f(hp) \qquad \text{(Tabulated)} \tag{D-30}$$

$$T_g = T_{go} - \frac{\dot{W}_p}{\dot{W}_g} \frac{1}{c_{pg}} \left[\left(h_p - h_{po} \right) + \frac{1}{2} u_p^2 \right] - \frac{1}{2} \frac{u_g^2}{c_{pg}} \tag{D-31}$$

$$P_g = \rho_g R T_g \tag{D-32}$$

$$\gamma_g = f(T_g) \quad \text{and} \quad c_{pg} = f(T_g) \quad \text{(Tabulated)} \tag{D-33}$$

$$\mu_g = \mu_o T_g^{\alpha} \tag{D-34}$$

In Equations D-22 through D-34, the quantities

Pr, m_p, r_p, $\dot{W}_g$, $\dot{W}_p$, T_{go}, h_{po}, R, μ_o, and α are all given constant parameters.

Equations D-22, D-23, and D-24 can be solved numerically in the subsonic regime for u_p, h_p, and u_g by any of several standard techniques, such as the Adams' or the Runge-Kutta method, provided that starting values are assumed at some location where the flow velocities are small and gas-particle equilibrium can be assumed. The remaining flow variables, ρ_g, ρ_p, T_p, T_g, and P_g, then can be calculated from Equations D-28 through D-32, respectively. Thus, the entire one-dimensional subsonic flow field is determined up to some value of $M < 1$. Near $M = 1$, the numerical solution begins to diverge as a result of the $\left(\frac{1}{M^2 - 1} \right)$ term in Equation D-24.

Because of this divergence, it becomes necessary to consider a constant lag one-dimensional gas-particle system to obtain solutions in the transonic regions.

APPENDIX E

CONSTANT-LAG ONE-DIMENSIONAL FLOW OF A GAS-PARTICLE MIXTURE

To obtain a transonic solution for a one-dimensional gas-particle mixture, it was necessary to assume that the particle kinetic and thermal lags are constant throughout the transonic regime. The particle kinetic and thermal lags were defined:

$$K = \frac{u_p}{u_g}, \quad 0 < K \leq 1 \tag{E-1}$$

$$L = \frac{T_{go} - T_p}{T_{go} - T_g}, \quad 0 < L \leq 1 \tag{E-2}$$

It was also assumed that the particles do not change phase in the transonic portion of the nozzle. The particle equation of state was then expressed as

$$(h_p - h_{po}) = c_{pl} (T_p - T_{go}) \tag{E-3}$$

where $T_{go} = T_{po}$ in the chamber.

The temperature of the gas, T_g, was found to be

$$T_g = T_{go} - \frac{\dot{w}_p}{\dot{w}_g} \frac{1}{c_{pg}} \left[(h_p - h_{po}) + \frac{1}{2} u_p^2 \right] - \frac{1}{2} \frac{u_g^2}{c_{pg}} \tag{E-4}$$

Substituting Equations (E-1), (E-2), and (E-3) in Equation (E-4) results in the following expression for T_g:

$$T_g = T_{go} - \frac{D}{2} \frac{u_g^2}{c_{pg}} \tag{E-5}$$

where:
$$D = \left[\frac{1 + \frac{\dot{w}_p}{\dot{w}_g} K^2}{1 + \frac{\dot{w}_p}{\dot{w}_g} \frac{c_{pl}}{c_{pg}} L} \right]$$

The system momentum balance was found to be

$$\frac{RT_g}{u_g}(M^2-1)(u_g)_x + \frac{\dot{w}_p}{\dot{w}_g}\left[(u_g - \frac{R}{c_{pg}} u_p)(u_p)_x - \frac{R}{c_{pg}}(h_p)_x\right] - \frac{RT_g}{(Area)}(Area)_x = 0 \quad (E-6)$$

Substituting Equations (E-1), (E-2), (E-3), and (E-5) in Equation (E-6) gives, for the system momentum balance,

$$\frac{d(Area)}{(Area)} = (\bar{M}^2 - 1) \frac{du_g}{u_g} \quad (E-7)$$

$$\bar{M}^2 = EM^2 \quad (E-8)$$

$$E = 1 + \frac{\dot{w}_p}{\dot{w}_g}\left\{K\left[\gamma_g(1-K) + K\right] + (\gamma_g - 1)\frac{c_{pl}}{c_{pg}} L D\right\} \quad (E-9)$$

The particle momentum balance was found to be

$$\frac{du_p}{dx} = A\left(\frac{u_g - u_p}{u_p}\right) \quad (E-10)$$

Substituting Equation (E-1) in Equation (E-10) gives

$$\frac{du_g}{dx} = A\frac{(1-K)}{K^2} \quad (E-11)$$

The particle energy balance was found to be

$$\frac{dh_p}{dx} = -\frac{2}{3} \quad A\ C \left(\frac{T_p - T_g}{u_p} \right) \tag{E-12}$$

Substituting Equations (E-1), (E-2), (E-3), and (E-5) in Equation (E-12) gives

$$\frac{du_g}{dx} = \frac{1}{3} \quad A\ C \quad \frac{(1-L)}{c_{pl}\ K\ L} \tag{E-13}$$

Equating Equations (E-11) and (E-13) gives

$$L = \frac{1}{1 + 3 \frac{c_{pl}}{C} \left(\frac{1-K}{K} \right)} \tag{E-14}$$

Equation (E-14) determines the relationship between the particle thermal and kinetic lags in a constant-lag situation.

Equation (E-5) was solved for the ratio T_{go}/T_g to give

$$\frac{T_{go}}{T_g} = \left[1 + \frac{(\bar{\gamma}_g - 1)}{2} \bar{M}^2 \right] \tag{E-15}$$

$$\bar{\gamma}_g = 1 + (\gamma_g - 1) \frac{D}{E} \tag{E-16}$$

Equation (E-7) was considered at the geometric throat where

$$\frac{d(\text{Area})}{(\text{Area})} = \frac{d\,(\text{Area})}{dx} \frac{dx}{(\text{Area})} = 0$$

and $$\frac{du_g}{u_g} = \frac{du_g}{dx} \frac{dx}{u_g} > 0$$

Therefore $\bar{M}_t^2 - \left|1\right| = 0$ and $\bar{M}_t = 1$ at the throat. (E-17)

Therefore, from Equation (E-15) at the throat, where conditions are denoted by *,

$$T_g^* = \frac{2}{(\bar{\gamma}_g + 1)} T_{go} \qquad \text{(E-18)}$$

Equation (E-7) was integrated in the following manner:

$$\frac{d\,(\text{Area})}{(\text{Area})} = (\bar{M}^2 - 1) \frac{du_g}{u_g} \quad \text{(Equation E-7)}$$

$$\bar{M}^2 = EM^2 = \frac{Eu_g^2}{\gamma_g R T_g}$$

$$T_g = T_{go} - \frac{1}{2} \frac{u_g^2}{c_{pg}} D$$

$$\bar{M}^2 = \frac{Eu_g^2}{\gamma_g R(T_{go} - \frac{1}{2} \frac{u_g^2}{c_{pg}} D)}$$

$$\frac{d(\text{Area})}{(\text{Area})} = \frac{Eu_g du_g}{\gamma_g R(T_{go} - \frac{1}{2} \frac{u_g^2}{c_{pg}} D)} - \frac{du_g}{u_g}$$

$$\ln A = -\frac{E}{(\gamma_g - 1)} D \ln T_g - \ln u_g + \text{Constant} \qquad \text{(E-19)}$$

Evaluating the above expression between a general point and the throat where $T_g = T_g^*$ and $\bar{M} = 1$ gives

$$\frac{(\text{Area})}{(\text{Area})^*} = \frac{1}{\bar{M}} \left[\frac{2}{(\bar{\gamma}_g + 1)} \left(1 + \frac{\bar{\gamma}_g - 1}{2} \bar{M}^2 \right) \right]^{\frac{(\bar{\gamma}_g + 1)}{2(\bar{\gamma}_g - 1)}} \qquad \text{(E-20)}$$

The gas continuity equation, the perfect gas law, and the system momentum equation were combined to determine the following pressure relationship:

$$\dot{w}_g = \rho_g u_g \text{ Area} \tag{E-21}$$

$$\frac{d\rho_g}{\rho_g} + \frac{du_g}{u_g} + \frac{d(\text{Area})}{(\text{Area})} = 0$$

$$P_g = \rho_g R T_g \tag{E-22}$$

$$\frac{dP_g}{P_g} - \frac{d\rho_g}{\rho_g} - \frac{dT_g}{T_g} = 0$$

$$\frac{d(\text{Area})}{(\text{Area})} = (\bar{M}^2 - 1)\frac{du_g}{u_g} \tag{E-23}$$

Combining the above gives

$$\frac{dP_g}{P_g} + \bar{M}^2 \frac{du_g}{u_g} - \frac{dT_g}{T_g} = 0 \tag{E-24}$$

In the same manner as Equation (E-7) was integrated, Equation (E-24) was solved and evaluated between the general condition and the stagnation chamber condition where $P_g = P_{go}$ and $T_g = T_{go}$ to give

$$\frac{P_{go}}{P_g} = \left[1 + \frac{\bar{\gamma}_g - 1}{2} \bar{M}^2\right]^{\frac{\bar{\gamma}_g}{\bar{\gamma}_g - 1}} \tag{E-25}$$

Substituting Equations (E-15) and (E-25) into the perfect gas law gives

$$\frac{\rho_{go}}{\rho_g} = \left[1 + \frac{\bar{\gamma}_g - 1}{2} \bar{M}^2 \right]^{\frac{1}{\bar{\gamma}_g - 1}} \tag{E-26}$$

Combining the gas and particle continuity equations gives

$$\rho_p = \frac{1}{K} \frac{\dot{w}_p}{\dot{w}_g} \rho_g \tag{E-27}$$

The solution of a one-dimensional gas-particle system under constant-lag conditions is thus given by

$$\frac{(\text{Area})}{(\text{Area})^*} = \frac{1}{\bar{M}} \left[\left(\frac{2}{\bar{\gamma}_g + 1} \right) \left(1 + \frac{\bar{\gamma}_g - 1}{2} \bar{M}^2 \right) \right]^{\frac{(\bar{\gamma}_g + 1)}{2(\bar{\gamma}_g - 1)}} \tag{E-28}$$

$$\frac{T_{go}}{T_g} = \left[1 + \frac{\bar{\gamma}_g - 1}{2} \bar{M}^2 \right] \tag{E-29}$$

$$\frac{\rho_{go}}{\rho_g} = \left[1 + \frac{\bar{\gamma}_g - 1}{2} \bar{M}^2 \right]^{\frac{1}{\bar{\gamma}_g - 1}} \tag{E-30}$$

$$\frac{P_{go}}{P_g} = \left[1 + \frac{\bar{\gamma}_g - 1}{2} \bar{M}^2 \right]^{\frac{\bar{\gamma}_g}{\bar{\gamma}_g - 1}} \tag{E-31}$$

$$\overline{M}^2 = E\,M^2 \tag{E-32}$$

$$u_g^2 = M^2 a^2 \tag{E-33}$$

$$a^2 = \gamma_g R T_g \tag{E-34}$$

$$u_p = K u_g \tag{E-35}$$

$$T_p = (1 - L)\,T_{go} + L\,T_g \tag{E-36}$$

$$\rho_p = \frac{1}{K}\,\frac{\dot{w}_p}{\dot{w}_g}\,\rho_g \tag{E-37}$$

$$L = \frac{1}{1 + 3\,\frac{c_{pl}}{C}\left(\frac{1-K}{K}\right)} \tag{E-38}$$

$$\overline{\gamma}_g = 1 + (\gamma_g - 1)\,\frac{D}{E} \tag{E-39}$$

$$D = \left[\frac{1 + \frac{\dot{w}_p}{\dot{w}_g}\,K^2}{1 + \frac{\dot{w}_p}{\dot{w}_g}\,\frac{c_{pl}}{c_{pg}}\,L}\right] \tag{E-40}$$

$$E = 1 + \frac{\dot{w}_p}{\dot{w}_g}\left\{K\left[\gamma_g\left(1 - K\right) + K\right] + \left(\gamma_g - 1\right)\frac{c_{pl}}{c_{pg}}\,L\,D\right\} \tag{E-41}$$

Equations E-28 through E-31 are seen to be the one-dimensional isentropic gas-dynamic relationships with γ_g and M replaced by the modified parameters $\overline{\gamma}_g$ and $\overline{M}$, respectively. A gas-particle mixture in a constant-lag nozzle with no phase change can thus be considered as a perfect gas with appropriately modified specific heat ratio and Mach number.

From Equation (E-11) it is seen that, for constant lag nozzles,

$$\frac{du_g}{dx} = \frac{A\,(1 - K)}{K^2} = \text{Constant}$$

Thus, the assumption of constant lag imposes the restriction of constant axial velocity gradient. Such a condition is approximated in the throat region of most nozzles. The solution for constant-lag flow, therefore, shows that in the throats of most nozzles the gas-particle mixture may be treated as a perfect gas with the appropriately modified specific heat ratio and Mach number.

APPENDIX F

TRANSONIC FLOW APPROXIMATION

By using the analysis of a one-dimensional gas-particle mixture under constant-lag conditions, it was found that the gas-particle mixture could be treated as a perfect gas with appropriately modified specific heat ratio and Mach number. The solutions for transonic flow can therefore be obtained in the same manner as for a perfect gas, since the two-dimensional gas-particle flow in the throat region can be treated approximately as a one-dimensional flow, and the actual specific heat ratio and Mach number of the two-dimensional flow can be approximated by the modified parameters $\bar{\gamma}_g$ and $\bar{M}$ based on the one-dimensional approximations. Several methods have been proposed for analyzing transonic perfect-gas flow. Methods proposed by Sauer, Oswatitsch and Rothstein, and Kliegel (References F-1, F-2, and F-3, respectively) appear to be practicable. Sauer's method will be used until a better solution is available.

Figure F-1 illustrates the geometry of the model considered by Sauer.

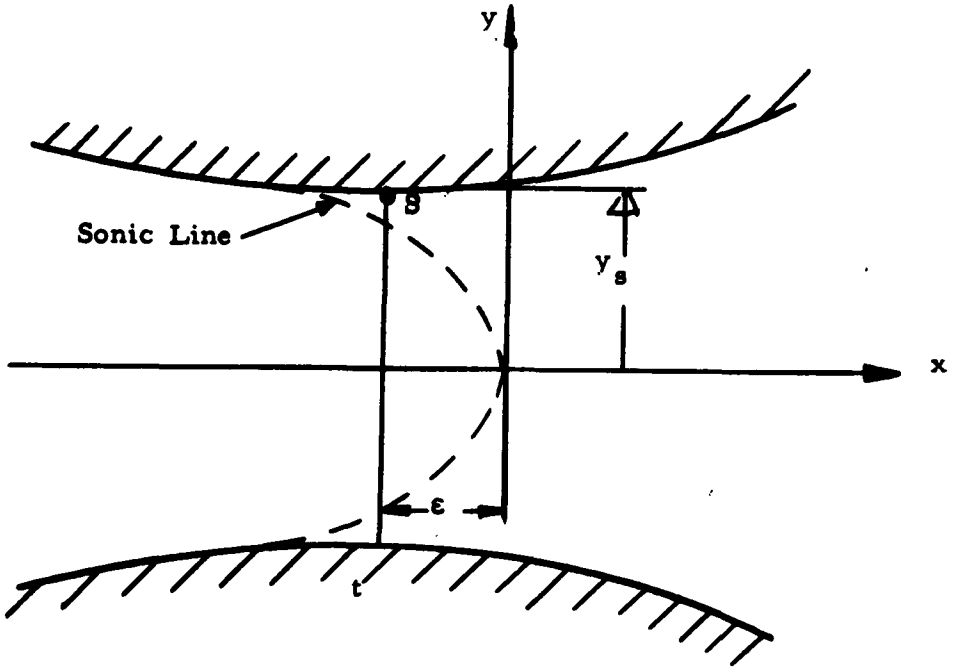

Figure F-1. Transonic-Flow Model

The assumptions made for the model are as follows:

1. The gas is a perfect gas.

2. The flow is irrotational.

3. The flow is two-dimensional ($\delta = 0$) or axisymmetric ($\delta = 1$).

4. The specific heats are constant.

By combining the continuity, momentum, and speed-of-sound equations for such a flow field, the following equation was obtained:

$$\tilde{u}_x (a^2 - \tilde{u}^2) + \tilde{v}_y (a^2 - \tilde{v}^2) - 2\,\tilde{u}\,\tilde{v}\,\tilde{u}_y + \delta a^2 \frac{\tilde{v}}{y} = 0 \qquad \text{(F-1)}$$

where $\tilde{u}$ and $\tilde{v}$ are the x and y components of velocity, and a is the speed of sound. The energy equation is

$$\frac{1}{2}(\tilde{u}^2 + \tilde{v}^2) + h = \text{constant} \qquad \text{(F-2)}$$

$$\left(\frac{\bar{\gamma}_g}{\quad}\right)\left(\tilde{u}^2 + \tilde{v}^2\right) + a^2 = \text{constant} \qquad \text{(F-3)}$$

Defining a^* as the speed of sound where $(\tilde{u}^2 + \tilde{v}^2) = a^2$, Equation (F-3) becomes

$$a^2 = \left(\frac{\bar{\gamma}_g + 1}{2}\right) a^{*2} - \left(\frac{\bar{\gamma}_g - 1}{2}\right)\left(\tilde{u}^2 + \tilde{v}^2\right) \qquad \text{(F-4)}$$

The dimensionless velocity components are defined by

$$U = \frac{\tilde{u}}{a^*} \quad \text{and} \quad V = \frac{\tilde{v}}{a^*} \qquad \text{(F-5)}$$

In terms of $\overline{U}$ and $\overline{V}$, (F-1) becomes

$$\overline{U}_x \left[1 - \overline{U}^2 - \frac{\overline{\gamma}_g - 1}{\overline{\gamma}_g + 1} \overline{V}^2 \right] + \overline{V}_y \left[1 - \left(\frac{\overline{\gamma}_g - 1}{\overline{\gamma}_g + 1} \right) \overline{U}^2 - \overline{V}^2 \right] - \frac{4}{\overline{\gamma}_g - 1} \overline{UVU}_y$$

$$+ \delta \left[1 - \frac{\overline{\gamma}_g - 1}{\overline{\gamma}_g + 1} (\overline{U}^2 + \overline{V}^2) \right] = 0 \qquad \text{(F-6)}$$

By limiting the investigation to the vicinity of the sonic condition where $\overline{U} \approx 1$ and $\overline{V} \approx 0$, $\overline{U}$ and $\overline{V}$ can be expressed in terms of perturbation velocities as

$$\overline{U} = 1 + u \quad \text{and} \quad \overline{V} = v \qquad \text{(F-7)}$$

where u and v are much smaller than 1. In terms of u and v, Equation (F-6) becomes

$$u_x \left[2u + u^2 + \frac{\overline{\gamma}_g - 1}{\overline{\gamma}_g + 1} v^2 \right] - v_y \left[\frac{2}{\overline{\gamma}_g + 1} - 2 \left(\frac{\overline{\gamma}_g - 1}{\overline{\gamma}_g + 1} \right) u - \frac{\overline{\gamma}_g - 1}{\overline{\gamma}_g + 1} u^2 + v^2 \right]$$

$$+ \frac{4}{\overline{\gamma}_g + 1} u_y (1 + u) v - \delta \left[\frac{2}{\overline{\gamma}_g + 1} - 2 \left(\frac{\overline{\gamma}_g - 1}{\overline{\gamma}_g + 1} \right) u - \left(\frac{\overline{\gamma}_g - 1}{\overline{\gamma}_g + 1} \right) (u^2 + v^2) \right] \frac{v}{y} = 0$$

(F-8)

As x and y approach zero, u and v approach zero. However, u_x should not approach zero. Equation (F-8) shows that as x and y approach zero, $\frac{v}{y}$ and v_y approach zero. From the symmetry about the x axis, u_y approaches zero at y = 0. Substituting these limiting values into Equation (F-8) and neglecting terms of higher order than the first in quantities which approach zero as x and y approach zero, Equation (F-8) becomes

$$(\bar{\gamma}_g + 1)\, u\, u_x - v_g - \delta\, \frac{v}{y} = 0 \qquad \text{(F-9)}$$

For irrotational flow,

$$\frac{\partial u}{\partial y} = \frac{\partial v}{\partial x} \qquad \text{(F-10)}$$

Hence, a velocity potential $\phi\ (x, y)$ can be defined such that

$$u = \phi_x \text{ and } v = \phi_y \qquad \text{(F-11)}$$

The velocity potential can be defined as a power series in y, containing only even powers of y because u is symmetrical about the x axis.

$$\phi\ (x, y) = f_o\ (x) + f_2\ (x)\, y^2 + f_4\ (x)\, y^4 + \ldots \qquad \text{(F-12)}$$

$$u\ (x, y) = \phi_x = f_o'(x) + f_2'(x)\, y^2 + f_4'(x)\, y^4 + \ldots \qquad \text{(F-13)}$$

$$v\ (x, y) = \phi_y = 2f_2\ (x)\, y + 4f_4\ (x)\, y^3 + \ldots \qquad \text{(F-14)}$$

where the primes denote ordinary differentiation with respect to x.

Substituting the power series for u and v into Equation (F-9), equating the sum of like powers of y to zero, and solving for $f_2(x)$ and $f_4(x)$ gives

$$f_2(x) = \frac{(\bar{\gamma}_g + 1) f_0' f_0''}{2(1+\delta)} \tag{F-15}$$

$$f_4(x) = \frac{(\bar{\gamma}_g + 1)(f_0' f_2'' + f_0'' f_2')}{2(3+\delta)} \tag{F-16}$$

When $y = 0$, $u(x, 0) = f_0'(x)$, where $u(x, 0)$ is the axial perturbation velocity distribution along the x axis. If $u(x, 0)$ is known, $f_2(x)$ and $f_4(x)$ can be determined, and the flow field would be established. For a linear axial perturbation velocity distribution,

$$u(x, 0) = a\,x \tag{F-17}$$

$$f_2(x) = \frac{(\bar{\gamma}_g + 1)\, a^2\, x}{2(1+\delta)} \tag{F-18}$$

$$f_4(x) = \frac{(\bar{\gamma}_g + 1)^2\, a^3}{8(1+\delta)(3+\delta)} \tag{F-19}$$

$$u(x, y) = a\,x + \frac{(\bar{\gamma}_g + 1)\, a^2}{2(1+\delta)}\, y^2 + \ldots \tag{F-20}$$

$$v(x, y) = \frac{(\bar{\gamma}_g + 1)\, a^2\, x}{(1+\delta)}\, y + \frac{(\bar{\gamma}_g + 1)^2\, a^3}{2(1+\delta)(3+\delta)}\, y^3 + \ldots \tag{F-21}$$

The critical curve where $\bar{M} = 1$ and $(\tilde{u}^2 + \tilde{v}^2) = a^{*2}$ can be determined as follows:

$$\tilde{u}^2 + \tilde{v}^2 = a^{*2} = \bar{U}^2 a^{*2} + \bar{V}^2 a^{*2}$$

$$(1+u)^2 + v^2 = 1$$

$$u = 0 \tag{F-22}$$

Therefore, the critical curve is found from Equation (F-20) to be

$$x = - \frac{(\bar{\gamma}_g + 1)\, a}{2\,(1 + \delta)}\, y^2 \qquad \text{(F-23)}$$

To locate the coordinate system in the nozzle, let y at x = 0 be equal to y_s, and solve for ϵ from Equation (F-23):

$$\epsilon = - \frac{(\bar{\gamma}_g + 1)\, a}{2\,(3 + \delta)}\, y_s^2 \qquad \text{(F-24)}$$

ϵ is the distance from the geometrical throat downstream to the gas dynamic throat where $\bar{M} = 1$.

Next, by using Figure F-2, determine the curvature of the nozzle wall at the narrowest cross section. Curvature is defined as the change of direction of the tangent to a curve per unit distance along the curve, and the radius of curvature is denoted by ρ_s.

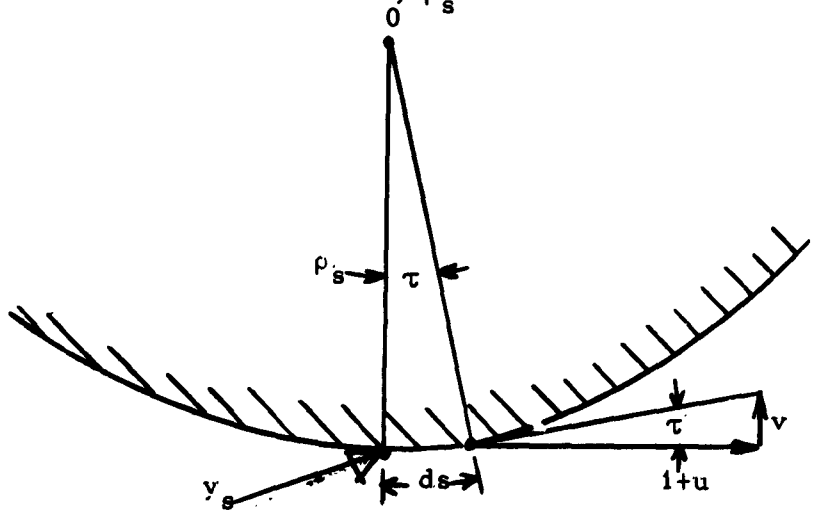

Figure F-2. Radius-of-Curvature Model

$$\tan \tau = \frac{v}{1+u} \approx v$$

$$\frac{1}{\rho_s} = \frac{d}{ds}\left(\tan \tau\right)_{y_s} = \frac{dv}{ds}_{y_s}$$

$$v = \frac{(\bar{\gamma}_g + 1)\, a^2 x}{(1+\delta)}\, y + \frac{(\bar{\gamma}_g + 1)^2 a^3}{2(1+\delta)(3+\delta)}\, y^3$$

$$\frac{\partial v}{\partial s} = \frac{\partial v}{\partial x}\,\frac{dx}{ds} \approx \frac{\partial v}{\partial x}$$

$$\frac{\partial v}{\partial x} = \frac{(\bar{\gamma}_g + 1)\, a^2}{(1+\delta)}\, y$$

$$\frac{1}{\rho_s} = \frac{(\bar{\gamma}_g + 1)\, a^2}{(1+\delta)}\, y_s \qquad \text{(F-25)}$$

Until now, u (x, 0) was assumed known, and a nozzle-wall curve was calculated to give this u (x, 0). Now, by inverting the above equations, u (x, 0) can be determined from the wall properties at the narrowest cross section. From Equation (F-25),

$$a = \sqrt{\frac{(1+\delta)}{(\bar{\gamma}_g + 1)\,\rho_s\, y_s}} \qquad \text{(F-26)}$$

From Equation (F-24),

$$\varepsilon = -\frac{y_s}{2(3+\delta)} \sqrt{\frac{(\bar{\gamma}_g + 1)(1+\delta)\, y_s}{\rho_s}} \qquad \text{(F-27)}$$

The flow field near the sonic line in the throat of a nozzle is thus determined by the following relationships:

$$u(x,y) = a\,x + \frac{(\bar{\gamma}_g + 1)\,a^2}{2(1+\delta)}\,y^2 \qquad \text{(F-28)}$$

$$v(x,y) = \frac{(\bar{\gamma}_g + 1)\,a^2\,x}{(1+\delta)}\,y + \frac{(\bar{\gamma}_g + 1)^2\,a^3}{2(1+\delta)(3+\delta)}\,y^3 \qquad \text{(F-29)}$$

$$\varepsilon = -\frac{y_s}{2(3+\delta)}\sqrt{\frac{(\bar{\gamma}_g + 1)(1+\delta)\,y_s}{\rho_s}} \qquad \text{(F-30)}$$

$$a = \sqrt{\frac{(1+\delta)}{(\bar{\gamma}_g + 1)\,\rho_s\,y_s}} \qquad \text{(F-31)}$$

where y_s and ρ_s are geometric properties of the nozzle.

By using the modified specific heat ratio and Mach number defined for gas-particle flow under constant lag with linear velocity gradient and no phase change, the above equations can be used to determine the two-dimensional or axisymmetric flow of a gas-particle system in transonic flow,

$$\tilde{u}(x,y) = a^*(1+u) \qquad \text{(F-32)}$$

$$\tilde{v}(x,y) = a^*\,v \qquad \text{(F-33)}$$

$$a^* = \frac{2\bar{\gamma}_g\,R\,T_{go}}{(\bar{\gamma}_g + 1)} \qquad \text{(F-34)}$$

$$u_g = (E)^{-\frac{1}{2}} \tilde{u} \qquad \text{(F-35)}$$

$$v_g = (E)^{-\frac{1}{2}} \tilde{v} \qquad \text{(F-36)}$$

where E and $\overline{\gamma}_g$ are defined in Appendix of this report.

REFERENCES

F-1. R. Sauer, General Characteristics of the Flow Through Nozzles at Near Critical Speeds, NACA TM No. 1147, June 1947.

F-2. K. Oswatitsch and W. Rothstein, Flow Pattern in a Converging-Diverging Nozzle, NACA TM No. 1215, March 1949.

F-3. J. R. Kliegel, Higher Order Approximations to the Transonic Flow in a Nozzle Throat, STL Report 7106-0016-RV-000, March 1961.

APPENDIX G

DERIVATION OF THE FINITE-DIFFERENCE EQUATIONS

Seven total differential equations were derived that are valid along the four characteristic curves. Because of the nonlinear nature of these equations, numerical techniques had to be used to obtain a solution. The seven compatibility equations were put into finite-difference form and are presented in this appendix. The remaining equations necessary to carry out the numerical solution by use of a high-speed digital computer were also put into a form suitable for computation.

Three equations for particle properties were derived for a constant particle size. To account for the possibility of more than one particle size or species, six discrete particles were allowed for in the numerical solution. This was accomplished by considering the streamline of each additional particle as an additional characteristic curve and by applying the particle compatibility equations independently for each particle along its streamline.

The equations were put into a form suitable for calculation of an interior point in the flow field. For special points, such as the nozzle axis, the nozzle wall, the limiting particle streamline, and a free boundary, the same equations apply; but the procedure for obtaining a solution must be modified. The characteristic net for such an interior point is bounded by the initial data line and the two Mach lines, as illustrated in Figure G-1.

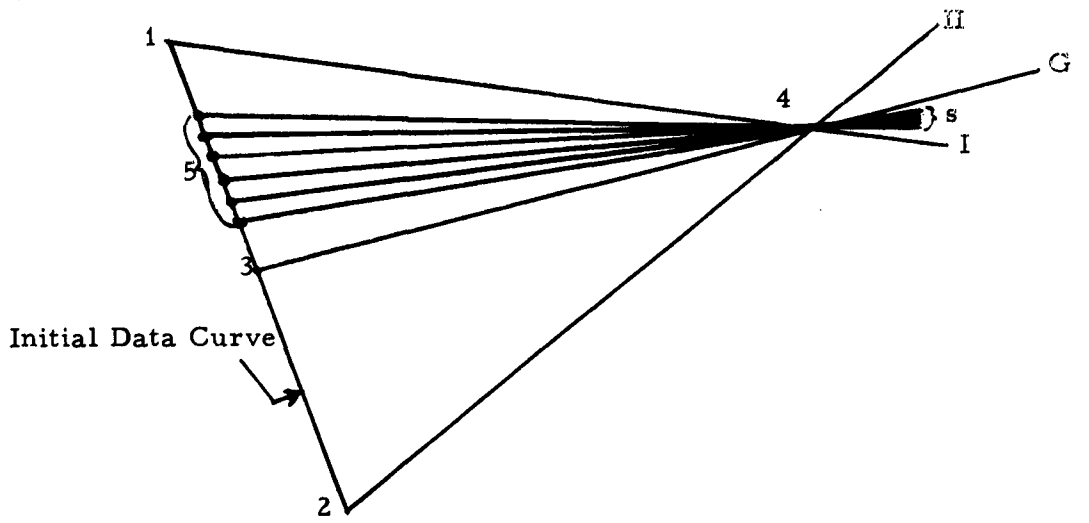

Figure G-1. Interior-Point Characteristic Net

In Figure G-1, functions evaluated along gas Mach lines are designated by subscripts I and II, corresponding to right and left running Mach lines, respectively; and functions evaluated along gas and particle streamlines are designated by G (gas) and s (solid), respectively.

Along right and left running Mach lines, the characteristic and compatibility equations are:

$$\left(\frac{dy}{dx}\right)_{I,\,II} = \frac{u_g v_g \pm a^2\sqrt{M^2-1}}{u_g^2 - a^2} \quad (I,-)\ (II,+) \tag{G-1}$$

$$(u_g dy - v_g dx)\left[\sum_{i=1}^{6}(A\rho_p B)dx - u_g dP_g\right] + a^2\left[\sum_{i=1}^{6}\left\{A\rho_p\left[(u_g-u_p)dy-(v_g-v_p)dx\right]\right\}dx\right.$$

(G-2)

$$\left. + \rho_g\left\{v_g du_g - u_g dv_g - \sigma_y\frac{v_g}{\sigma}(u_g dy - v_g dx)\right\}dx + dP_g dy\right] = 0$$

To integrate these equations, all properties were assumed to be constant at the average value of the property along the line of integration. Equations G-1 and G-2 then became

$$\left(\frac{\Delta y}{\Delta x}\right)_{I,\,II} = \frac{\bar{u}_g \bar{v}_g \pm \bar{a}^2\sqrt{\bar{M}^2 - 1}}{\bar{u}_g^2 - \bar{a}^2} \quad (I, -)\ (II, +) \tag{G-3}$$

$$M\Delta P_g + Q\Delta u_g + R\Delta v_g = S \tag{G-4}$$

where the bar denotes average values, and

$$\bar{a} = \gamma_g R \bar{T}_g,$$

$$\bar{M}^2 = \frac{(\bar{u}_g^2 + \bar{v}_g^2)}{\bar{a}^2}$$

$$M = \left[\bar{a}^2 \Delta y - \bar{u}_g K\right]$$

$$Q = \bar{a}^2 \bar{\rho}_g \bar{v}_g \Delta x$$

$$R = -\bar{a}^2 \bar{\rho}_g \bar{u}_g \Delta x$$

$$S = \left\{\sigma_y \frac{\bar{\rho}_g \bar{v}_g}{\sigma} \bar{a}^2 K - K \sum_{i=1}^{6} (A\bar{\rho}_p B) - \bar{a}^2 \sum_{i=1}^{6} \left[A\bar{\rho}_p \left\{ (\bar{u}_g - \bar{u}_p)\Delta y - (\bar{v}_g - \bar{v}_p)\Delta x \right\} \right] \right\} \Delta x$$

$$K = \left[\bar{u}_g \Delta y - \bar{v}_g \Delta x\right]$$

$$A = \frac{9}{2} \frac{\bar{\mu}_g \bar{r}}{m_p r_p^2}$$

$$B = (\bar{\gamma}_g - 1)\left[(\bar{u}_g - \bar{u}_p)^2 + (\bar{v}_g - \bar{v}_p)^2 + \frac{2}{3} C (\bar{T}_p - \bar{T}_g) \right]$$

$$C = \frac{\bar{g}}{\bar{f}} \quad \frac{\bar{c}_{pg}}{Pr}$$

$$\left.\begin{array}{lll} \bar{\gamma}_g = f(\bar{T}_g) & \text{and} & \bar{c}_{pg} = f(\bar{T}_g) \\ \bar{f} = f(Re) & \text{and} & \bar{g} = g(Re) \end{array}\right\} \text{Tabulated}$$

$$Re = \frac{2 r_p \bar{\rho}_g}{\bar{\mu}_g} \sqrt{(\bar{u}_g - \bar{u}_p)^2 + (\bar{v}_g - \bar{v}_p)^2}$$

$$Pr = \text{Constant}$$

$$\bar{\mu}_g = \mu_o \bar{T}_g^{\,a}$$

where μ_o and a are constants,

$$P_g = \rho_g R T_g \qquad \text{(G-5)}$$

Since Equation (G-4) is valid along both Mach lines, two equations relating ΔP_g, Δu_g, and Δv_g were obtained:

$$M_I \Delta P_{gI} + Q_I \Delta u_{gI} + R_I \Delta v_{gI} = S_I \qquad \text{(G-6)}$$

$$M_{II} \Delta P_{gII} + Q_{II} \Delta u_{gII} + R_{II} \Delta v_{gII} = S_{II} \qquad \text{(G-7)}$$

Along the gas streamlines, the characteristic and compatibility equations are

$$\left(\frac{dy}{dx}\right)_G = \frac{v_g}{u_g} \tag{G-8}$$

$$\rho_g \left[u_g du_g + v_g dv_g \right] + dP_g = -\sum_{i=1}^{6} \left\{ A\rho_p \left[(u_g - u_p)dx + (v_g - v_p)dy \right] \right\} \tag{G-9}$$

$$\frac{dP_g}{P_g} - \gamma_g \frac{d\rho_g}{\rho_g} = \sum_{i=1}^{6} \left[\frac{A\rho_p B dx}{P_g u_g} \right] \tag{G-10}$$

In integrated form, these equations are

$$\left(\frac{\Delta y}{\Delta x}\right)_G = \frac{\bar{v}_g}{\bar{u}_g} \tag{G-11}$$

$$\Delta P_{gG} + \bar{U}_G \Delta u_{gG} + \bar{V}_G \Delta v_{gG} = D_G \tag{G-12}$$

$$\Delta \rho_{gG} = \frac{1}{\bar{a}^2} \Delta P_{gG} + T_G \tag{G-13}$$

$$\bar{U} = \bar{\rho}_g \bar{u}_g$$

$$\bar{V} = \bar{\rho}_g \bar{v}_g$$

$$D_G = -\sum_{i=1}^{6} \left\{ A\bar{\rho}_p \left[(\bar{u}_g - \bar{u}_p) \Delta x + (\bar{v}_g - \bar{v}_p) \Delta y \right] \right\}$$

$$T_G = -\sum_{i=1}^{6} \left\{ A\bar{\rho}_p B \left| \frac{\bar{\rho}_g}{\bar{v}_g \bar{P}_g \bar{u}_g} \right| \right\} \Delta x$$

Along the particle streamlines, the characteristic and compatibility equations for each particle are

$$\left(\frac{dy}{dx}\right)_S = \frac{v_p}{u_p} \tag{G-14}$$

$$u_p du_p = A\,(u_g - u_p)\,dx \tag{G-15}$$

$$v_p dv_p = A\,(v_g - v_p)\,dy \tag{G-16}$$

$$u_p dh_p = -\frac{2}{3} AC\,(T_p - T_g)\,dx \tag{G-17}$$

In integrated form, these equations are

$$\left(\frac{\Delta y}{\Delta x}\right)_S = \frac{\bar{v}_p}{\bar{u}_p} \tag{G-18}$$

$$\Delta u_{pS} = \bar{A}_S\ \Delta x \tag{G-19}$$

$$\Delta v_{pS} = \bar{B}_S\ \Delta y \tag{G-20}$$

$$\Delta h_{pS} = \bar{C}_S\ \Delta x \tag{G-21}$$

$$\bar{A} = A\left(\frac{\bar{u}_g - \bar{u}_p}{\bar{u}_p}\right)$$

$$\bar{B} = A\left(\frac{\bar{v}_g - \bar{v}_p}{\bar{v}_p}\right)$$

$$\bar{C} = -\frac{2}{3} A\,C\left(\frac{\bar{T}_p - \bar{T}_g}{\bar{u}_p}\right)$$

The particle-stream function equation, when solved for ρ_p, becomes

$$\rho_p = \frac{d\psi_p}{\sigma(u_p dy - v_p dx)}$$

In integrated form, this equation becomes

$$\rho_{p4} = \frac{\psi_{p2} - \psi_{p1} - L_1 \rho_{p1} - L_2 \rho_{p2}}{(L_1 + L_2)} \qquad \text{(G-22)}$$

$$L_1 = \sigma_1 \left[\bar{u}_p (y_4 - y_1) - \bar{v}_p (x_4 - x_1) \right]$$

$$L_2 = \sigma_2 \left[\bar{u}_p (y_4 - y_2) - \bar{v}_p (x_4 - x_2) \right]$$

$$\psi_{p4} = \psi_{p2} + L_2 (\rho_{p2} + \rho_{p4})$$

where, for two-dimensional flow,

$$\sigma_1 = \sigma_2 = 1$$

and, for axisymmetric flow,

$$\sigma_1 = \tfrac{1}{2}(y_1 + y_4)$$

$$\sigma_2 = \tfrac{1}{2}(y_2 + y_4)$$

Equations G-6, G-7, and G-12, relating the gas pressure and velocity components, can be solved for these properties at the intersection of the Mach lines to give

$$u_{g4} = \frac{(Y-M_I X)(R_{II}-M_{II}\bar{V}_G) - (Z-M_{II}X)(R_I - M_I \bar{V}_G}{(Q_I - M_I \bar{U}_G)(R_{II} - M_{II}\bar{V}_G) - (Q_{II} - M_{II}\bar{V}_G)(R_I - M_I \bar{V}_G)} \qquad (G\text{-}23)$$

$$v_{g4} = \frac{(Q_I - M_I \bar{U}_G)(Z-M_{II}X) - (Q_{II} - M_{II}\bar{V}_G)(\bar{Y} - M_I X)}{(Q_I - M_I \bar{U}_G)(R_{II} - M_{II}\bar{V}_G) - (Q_{II} - M_{II}\bar{V}_G)(R_I - M_I \bar{V}_G)} \qquad (G\text{-}24)$$

$$P_{g4} = X - \bar{U}_G u_{g4} - \bar{V}_G v_{g4} + P_{g3} \qquad (G\text{-}25)$$

$$X = D_G + \bar{V}_G u_{g3} + \bar{V}_G v_{g3}$$

$$Y = S_1 + M_I (P_{g1} - P_{g3}) + Q_I u_{g1} + R_I v_{g1}$$

$$Z = S_{II} + M_{II} (P_{g2} - P_{g3}) + Q_{II} u_{g2} + R_{II} v_{g2}$$

The gas density at point 4 from Equation G-13 is given by

$$\rho_{g4} = \rho_{g3} + \frac{(P_{g4} - P_{g3})}{\gamma_g R \bar{T}_g} + T_G \qquad (G\text{-}26)$$

where T_G is defined above.

Equations (G-19), (G-20), and (G-21) were solved for the particle velocity components and enthalpy at point 4 to give

$$u_{p4} = u_{p5} + \overline{A}_S \, \Delta x \tag{G-27}$$

$$v_{p4} = v_{p5} + \overline{B}_S \, \Delta y \tag{G-28}$$

$$h_{p4} = h_{p5} + \overline{C}_S \, \Delta x \tag{G-29}$$

The particle density at point 4, ρ_{p4}, is given by Equation (G-22).

Thus, the original system of characteristic total-differential equations has been put into finite-difference form, and expressions for all the flow properties at point 4 have been obtained in a form suitable for computation.

APPENDIX H

NUMERICAL-SOLUTION PROCEDURE FOR COMPUTER PROGRAM

I. GENERAL

The equations governing a gas-particle system have been derived, the characteristic equations have been determined, and the characteristic equations put into finite-difference form in the preceding appendixes. In this appendix, the use of these equations is demonstrated for determining the flow properties at an interior point in the flow field: any general point that is not on a solid or free boundary, on the nozzle axis, or in the region between the limiting particle streamline and the nozzle wall. For these, slight modifications to the procedure are necessary.

This procedure has been programed for the IBM 7090 computer. The computer program follows the solution procedure outlined in this section.

The units of the physical parameters appearing in the solution are shown in Table H-1. The given data and the solution are both expressed in these units.

Two types of data are needed for this solution: general and specific. The general data (Table H-2) pertains to the entire nozzle calculation, and the specific data (Table H-3) pertain only to the flow properties at the point under consideration. The properties found at point 4 consist of:

1. Location of point 4 (x and y)
2. Gas properties; the same as the initial data
3. Particle properties; the same as the initial data.

The numerical solution is based on the characteristic net shown in Figure H-1.

II. SOLUTION PROCEDURE

The detailed solution procedure for the location of point 4 and the calculation of the flow properties at that point is in the following sequence:

TABLE H-1

UNITS OF PHYSICAL PARAMETERS

C_p	specific heat at constant pressure	Btu/lbm-°R
γ_g	specific heat ratio of the gas	dimensionless
f	ratio of C_D to C_D for Stokes' flow	dimensionless
g	ratio of N_u to N_u for Stokes' flow	dimensionless
h_p	particle enthalpy	Btu/lbm
m_p	particle density per unit volume of particle	lbm/ft^3
P_g	gas static pressure	$lbf/in.^2$
Pr	Prandtl number	dimensionless
r_p	particle radius, based on spherical particles	micron
R	gas constant	Btu/lbm-°R
Re	Reynolds number	dimensionless
T_g	gas static temperature	°R
T_p	particle static temperature	°R
u_g	axial gas velocity component	ft/sec
u_p	axial particle velocity component	ft/sec
v_g	normal or radial gas velocity component	ft/sec
v_p	normal or radial particle velocity component	ft/sec
x	axial coordinate	ft
y	normal coordinate	ft
α	component of gas viscosity expression	dimensionless
μ_g	gas viscosity	lbm/ft-sec
μ_o	coefficient of gas viscosity expression	$lbm/ft\text{-}sec\text{-}(°R)^{\alpha}$
ρ_g	gas density	lbm/ft^3
ρ_p	particle density per unit volume of gas	lbm/ft^3

TABLE H-2

GENERAL INITIAL DATA

1. Two-dimensional or axisymmetric flow specification ($\delta = 0$ or $\delta = 1$)
2. Number of particles and the density m_p, and radius r_p of each
3. Tabulated values of f as a function of Re
4. Tabulated values of g as a function of Re
5. Tabulated values of γ_g, R, C_{pg}, μ_g, and Pr as a function of T_g
6. Tabulated values of T_p as a function of h_p for each particle species
7. The solidfication temperature, T_{pm}, of each particle species
8. The iteration accuracy criteria, K and L

TABLE H-3

SPECIFIC INITIAL DATA
(given at both points 1 and 2)

1. Location of points 1 and 2, (x and y).

2. Gas properties at points 1 and 2:

   u_g - axial velocity component

   v_g - normal velocity component

   ρ_g - density

   P_g - pressure

   T_g - temperature

3. Particle properties for each particle at points 1 and 2:

   u_p - axial velocity component

   v_p - normal velocity component

   ρ_p - density

   h_p - enthalpy

   T_p - temperature

   Ψ_p - stream function

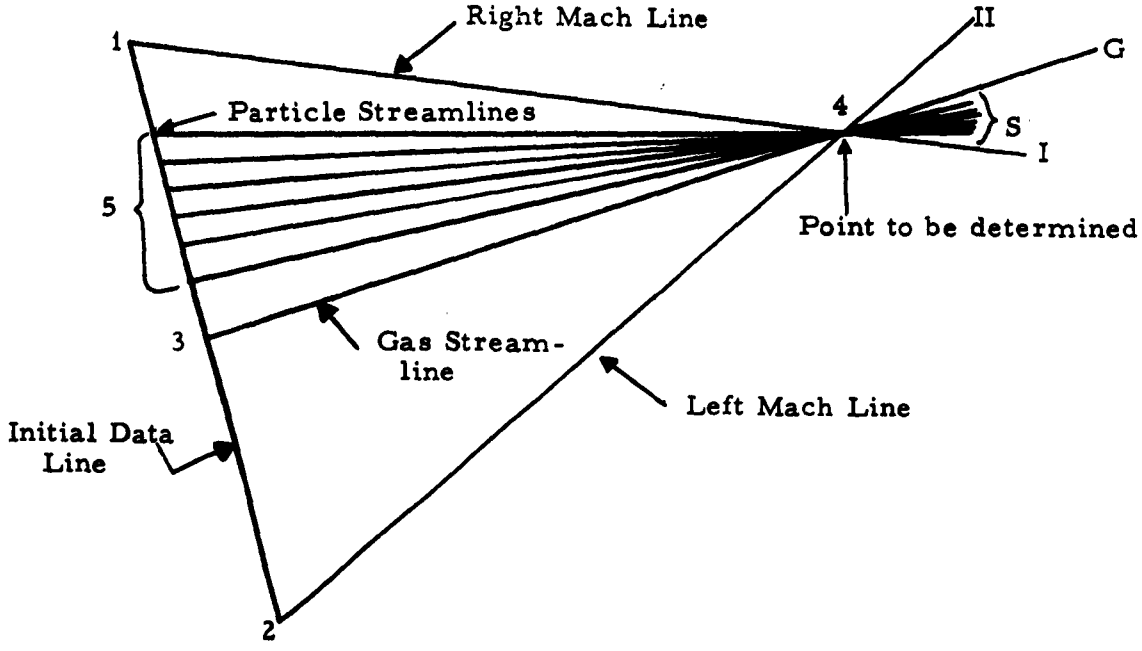

Figure H-1. Numerical-Solution Characteristic Net

1. Determine the location of points 1 and 2, and the gas and particle properties at points 1 and 2:

$$(x_1, y_1) \qquad \begin{bmatrix} u_{g1}, & u_{g2} \\ v_{g1}, & v_{g2} \\ \rho_{g1}, & \rho_{g2} \\ P_{g1}, & P_{g2} \\ T_{g1}, & T_{g2} \end{bmatrix} \qquad \begin{bmatrix} u_{p1}, & u_{p2} \\ v_{p1}, & v_{p2} \\ \rho_{p1}, & \rho_{p2} \\ h_{p1}, & h_{p2} \\ T_{p1}, & T_{p2} \\ \Psi_{p1}, & \Psi_{p2} \end{bmatrix}$$

$$(x_2, y_2)$$

2. Determine T_{gm} at the midpoint of line 1-2, and, from tables of γ_g and C_{pg} vs T_g, determine c_{pg} and γ_g at this temperature. This c_{pg} and γ_g are then considered as the constant values of c_{pg} and γ_g for the entire net.

3. Calculate u_g, v_g, u_p, v_p, and μ_g at the midpoint of line 1-2,

$$P_m = \frac{1}{2}(P_1 + P_2)$$

where P is any of the above properties. Calculate the gas viscosity at the midpoint of line 1-2.

$$\mu_{gm} = \mu_o T_{gm}^{a}$$

4. Calculate Re for each of the 6 particles at the midpoint of Line 1-2.

$$Re = 6.5602 \times 10^{-6} \frac{\rho_{gm}}{\mu_{gm}} \left\{ r_p \sqrt{(u_{gm} - u_{pm})^2 + (v_{gm} - v_{pm})^2} \right\}$$

From tabulated values of f and g vs Re, f and g for each of the particles may be determined. Calculate A and C of the particles.

$$A = 4.1806 \times 10^{11} \frac{\mu_{gm}^{f}}{m_p r_p^2}$$

$$C = 25 \times 10^{3} \frac{g}{f} \frac{c_{pgm}}{Pr}$$

5. In the following steps, note that the value of any flow property P at point i on the initial data line 1-2 can be found as follows:

$$P_i = P_2 + \left(\frac{x_i - x_2}{x_1 - x_2}\right)(P_1 - P_2)$$

6. Locate point 4. For the first overall approximation of point 4, base the location on properties at points 1 and 2 only. For subsequent approximations, base the location on the average of properties at points 1, 2, and 4.

$$a_1^2 = 32.139\, \gamma_g R T_{g1} \qquad a_2^2 = 32.139\, \gamma_g R T_{g2}$$

$$M_1 = \left[\frac{u_{g1}^2 + v_{g1}^2}{a_1^2}\right]^{\frac{1}{2}} \qquad M_2^2 = \left[\frac{u_{g2}^2 + v_{g2}^2}{a_2^2}\right]^{\frac{1}{2}}$$

$$\theta_{g1} = \tan^{-1}(v_{g1}/u_{g1}) \qquad \theta_{g2} = \tan^{-1}(v_{g2}/u_{g2})$$

$$\alpha_{g1} = \sin^{-1}(1/M_1) \qquad \alpha_{g2} = \sin^{-1}(1/M_2)$$

$$\mu_{I1} = (\theta_{g1} - \alpha_1) \qquad \mu_{II2} = (\theta_{g2} + \alpha_2)$$

For the first overall trial on point 4, set $\mu_{I4} = \mu_{I1}$ and $\mu_{II4} = \mu_{II2}$.

On subsequent trials, μ_{I4} and μ_{II4} will be known from flow properties at point 4.

$$\bar{\mu}_{14} = \frac{1}{2}(\mu_{I1} + \mu_{I4}) \quad \mu_{24} = \frac{1}{2}(\mu_{II2} + \mu_{II4})$$

$$\bar{m}_{14} = \tan \bar{\mu}_{14} \qquad \bar{m}_{24} = \tan \bar{\mu}_{24}$$

$$x_4 = \left[\frac{x_2 \bar{m}_{24} - x_1 \bar{m}_{14} + (y_1 - y_2)}{(\bar{m}_{24} - \bar{m}_{14})}\right]$$

$$y_4 = y_2 + \bar{m}_{24}(x_4 - x_2)$$

7. Locate point 3. For the first overall trial for point 4, $\mu_{G4} = \frac{1}{2}(\mu_{II2} + \mu_{I1})$. On subsequent trials, μ_{G4} will be known from flow properties at point 4. Calculate μ_{G3}. During the first overall trial on point 4, assume $x_3 = \frac{1}{2}(x_1 + x_2)$ as a first approximation. During subsequent overall trials on point 3, assume that x_3 is the final value of x_3 from the previous overall trial on point 4.

$$\mu_{G3} = \tan^{-1}(v_{g3}/u_{g3}) \qquad \mu_{G4} = \tan^{-1}(v_{g4}/u_{g4})$$

$$\bar{\mu}_{34} = \frac{1}{2}(\mu_{G3} + \mu_{G4}) \qquad \bar{m}_{34} = \tan \bar{\mu}_{34}$$

Pass a line through point 4 with the average slope $\bar{m}_{34}$ and determine a new location for point 3 as the intersection of this line with 1-2. Note that $m_{12} = (y_1 - y_2)/(x_1 - x_2)$ is constant.

$$x_3 = \left[\frac{m_{12} x_2 - \bar{m}_{34} x_4 + (y_4 - y_2)}{(m_{12} - \bar{m}_{34})}\right]$$

$$y_3 = y_2 + m_{12}(x_3 - x_2)$$

Repeat the above steps, obtaining even more refined values of x_3 and y_3, each time using the last location of point 3 to calculate μ_{G3} until

$$\left| \frac{\text{Distance } [3(n+1) \quad -3(n)]}{\text{Distance } [1-2]} \right| \leq K$$

where K is an accuracy criterion and n denotes the nth trial. When the above equality is satisfied, point 3 is located.

8. In all the equations which follow, all flow properties must be expressed as average values. This is accomplished by replacing each property, P, by the relationship

$$\overline{P} = \frac{1}{2}(P_i + P_{i4})$$

where P_i is the value of the property at point i and P_{i4} is the value of the property at point 4 where $\overline{P}$ is evaluated along line i-4. On the first over-all trial on point 4, all values of P_{i4} are set equal to P_i. On subsequent trials, actual values of properties at point 4 will be used.

9. Set two-dimensional or axisymmetric flow parameters.

If $\sigma_y = 0.0$,	If $\sigma_y = 1.0$,
SIGK = 0.0	SIGK = 1.0
SIG1 = 1.0	SIG1 = $(y_1 + y_4)$
SIG2 = 1.0	SIG2 = $(y_2 + y_4)$
SIG3 = 1.0	SIG3 = $(y_1 + y_2)$

10. Locate point 5 and calculate ρ_{p4} and Ψ_{p4}

$$L_1 = \frac{1}{8} \text{SIG1} \left\{ \left[v_{p1} + v_{p14} \right] (x_1 - x_4) + \left[u_{p1} + u_{p14} \right] (y_4 - y_1) \right\}$$

$$L_2 = \frac{1}{8} \text{SIG2} \left\{ \left[v_{p2} + v_{p24} \right] (x_4 - x_2) + \left[u_{p2} + u_{p24} \right] (y_2 - y_4) \right\}$$

$$\rho_{p4}(I) = \left[\frac{\Psi_{p2} - \Psi_{p1} - L_1 \rho_{p1} - L_2 \rho_{p2}}{(L_1 + L_2)} \right]$$

$$\Psi_{p4}(I) = \Psi_{p2} - L2 \left[\rho_{p2} + \rho_{p4} \right]$$

$$\bar{\Psi} = \left[\frac{\Psi_{p4} - \Psi_{p2}}{\Psi_{p1} - \Psi_{p2}} \right]$$

$$y_5 = y_2 + \bar{\Psi} (y_1 - y_2)$$

$$x_5 = x_2 + \bar{\Psi} (x_1 - x_2)$$

By use of the above steps, point 5 is located and ρ_{p4} and Ψ_{p4} are calculated. This procedure must be repeated for each particle.

11. Evaluate the gas properties at point 4:

$$\bar{U} = \frac{1}{4} (\rho_{g3} + \rho_{g34}) (u_{g3} + u_{g34})$$

$$\bar{V} = \frac{1}{4} (\rho_{g3} + \rho_{g34}) (v_{g3} + v_{g34})$$

$$K_I = \frac{1}{2} \left[(u_{g1} + u_{g14}) (y_4 - y_1) - (v_{g1} + v_{g14}) (x_4 - x_1) \right]$$

$$K_{II} = \frac{1}{2} \left[(u_{g2} + u_{g24}) (y_4 - y_2) - (v_{g2} + v_{g24}) (x_4 - x_2) \right]$$

$$M_I = \left[16.069 \gamma_g R (T_{g1} + T_{g14}) (y_4 - y_1) - \frac{1}{2} K_I (u_{g1} + u_{g14}) \right]$$

$$M_{II} = \left[16.069 \gamma_g R (T_{g2} + T_{g24}) (y_4 - y_2) - \frac{1}{2} K_{II} (u_{g2} + u_{g24}) \right]$$

$$Q_I = 4.0174\ \gamma_g R\ (T_{g1} + T_{g14})\ (\rho_{g1} + \rho_{g14})\ (v_{g1} + v_{g14})\ (x_4 - x_1)$$

$$Q_{II} = 4.0174\ \gamma_g R\ (T_{g2} + T_{g24})\ (\rho_{g2} + \rho_{g24})\ (v_{g2} + v_{g24})\ (x_4 - x_2)$$

$$R_I = -4.0174\ \gamma_g R\ (T_{g1} + T_{g14})\ (\rho_{g1} + \rho_{g14})(u_{g1} + u_{g14})\ (x_4 - x_1)$$

$$R_{II} = -4.0174\ \gamma_g R\ (T_{g2} + T_{g24})\ (\rho_{g2} + \rho_{g24})(u_{g2} + u_{g24})\ (x_4 - x_2)$$

$$D = -\frac{1}{4} \sum_{i=1}^{6} \Big\{ A\ (\rho_{p3} + \rho_{p34}) \Big[(u_{g3} + u_{g34} - u_{p3} - u_{p34})\ (x_4 - x_3) + (v_{g3} + v_{g34} - v_{p3} - v_{p34})\ (y_4 - y_3) \Big] \Big\}$$

$$B_I = \frac{(\gamma_g - 1)}{4} \Big[(u_{g1} + u_{g14} - u_{p1} - u_{p14})^2 + (v_{g1} + v_{g14} - v_{p1} - v_{p14})^2 + 1.33333\ C\ (T_{p1} + T_{p14} - T_{g1} - T_{g14}) \Big]$$

$$B_{II} = \frac{(\gamma_g - 1)}{4} \Big[(u_{g2} + u_{g24} - u_{p2} - u_{p24})^2 + (v_{g2} + v_{g24} - v_{p2} - v_{p24})^2 + 1.33333\ C\ (T_{p2} + T_{p24} - T_{g2} - T_{g24}) \Big]$$

$$B_G = \frac{(\gamma_g - 1)}{4} \Big[(u_{g3} + u_{g34} - u_{p3} - u_{p34})^2 + (v_{g3} + v_{g34} - v_{p3} - v_{p34})^2 + 1.33333\ C\ (T_{p3} + T_{p34} - T_{g3} - T_{g34}) \Big]$$

$$S_I = \left\{ \frac{8.0348 KSIG}{SIG\ 1} \right. (\rho_{g1} + \rho_{g14})(v_{g1} + v_{g14})\gamma_g R (T_{g1} + T_{g14}) K_I$$

$$- \frac{1}{2} K_I \sum_{i=1}^{6} \left[A B_I (\rho_{p1} + \rho_{p14}) \right] \quad -4.0174 \gamma_g R (T_{g1} + T_{g14}) X$$

$$\sum_{i=1}^{6} A (\rho_{p1} + \rho_{p14}) \left\{ (u_{g1} + u_{g14} - u_{p1} - u_{p14})(y_4 - y_1) \right.$$

$$\left. \left. - (v_{g1} + v_{g14} - v_{p1} - v_{p14})(x_4 - x_1) \right\} \right\} (x_4 - x_1)$$

$$S_{II} = \left\{ \frac{8.0348 KSIG}{SIG\ 2} \right. (\rho_{g2} + \rho_{g24})(v_{g2} + v_{g24})\gamma_g R (T_{g2} + T_{g24}) K_{II}$$

$$- \frac{1}{2} K_{II} \sum_{i=1}^{6} \left[A B_{II} (\rho_{p2} + \rho_{p24}) \right] - 4.0174 \gamma_g R (T_{g2} + T_{g24}) x$$

$$\sum_{i=1}^{6} A (\rho_{p2} + \rho_{p24}) \left\{ (u_{g2} + u_{g24} - u_{p2} - u_{p24})(y_4 - y_2) \right.$$

$$\left. \left. - (v_{g2} + v_{g24} - v_{p2} - v_{p24})(x_4 - x_2) \right\} \right\} (x_4 - x_2)$$

$$Y = S_I + 4,628\ M_I (P_{g1} - P_{g3}) + Q_I u_{g1} + R_I v_{g1}$$

$$Z = S_{II} + 4,628\ M_{II} (P_{g2} - P_{g3}) + Q_{II} u_{g2} + R_{II} v_{g2}$$

$$X = D + \overline{U} u_{g3} + \overline{V} v_{g3}$$

$$T = -2.1608 \times 10^{-4} \left[\frac{(\rho_{g3} + \rho_{g34})(x_4 - x_3)}{\gamma_g (P_{g3} + P_{g34})(u_{g3} + u_{g34})} \right] \sum_{i=1}^{6} \left[A B_G (\rho_{p3} + \rho_{p34}) \right]$$

$$DENOM = \left[(Q_I - M_I \overline{U})(R_{II} - M_{II} \overline{U}) - (Q_{II} - M_{II} \overline{v})(R_I - M_I \overline{V}) \right]$$

$$u_{g4} = \left[\frac{(Y - M_I X)(R_{II} - M_{II}\overline{V}) - (Z - M_{II}X)(R_I - M_I\overline{V})}{\text{DENOM}} \right]$$

$$v_{g4} = \left[\frac{(Q_I - M_I\overline{U})(Z - M_{II}X) - (Q_{II} - M_{II}\overline{U})(Y - M_I X)}{\text{DENOM}} \right]$$

$$P_{g4} = P_{g3} + 2.160 \times 10^{-4} (X - \overline{U}u_{g4} - \overline{V}v_{g4})$$

$$\rho_{g4} = \rho_{g3} + T + \left[\frac{288.0 (P_{g4} - P_{g3})}{\gamma_g R(T_{g3} + T_{g34})} \right]$$

$$T_{g4} = \frac{144 P_{g4}}{R\rho_{g4}}$$

12. **Evaluate the particle properties at point 4.**

$$\overline{A} = A \left[\frac{(u_{g4} + u_{g5} - u_{p45} - u_{p5})}{(u_{p45} + u_{p5})} \right]$$

$$\overline{B} = A \left[\frac{(v_{g4} + v_{g5} - v_{p45} - v_{p5})}{(v_{p45} + v_{\rho 5})} \right]$$

$$\overline{C} - 2.6667 \times 10^{-5} \; AC \left[\frac{(T_{p45} + T_{p5} - T_{g4} - T_{g5})}{(u_{p45} + u_{p4})} \right]$$

$$u_{p4} = u_{p5} + \overline{A}(x_4 - x_5)$$

$$v_{p4} = v_{p5} + \overline{B}(y_4 - y_5)$$

$$h_{p4} = h_{p5} + \overline{C}(x_4 - x_5)$$

$$T_{p4} = f(h_{p4})$$

13. Thus, the location of point 4, and all the flow properties at point 4, are known approximately. To improve the accuracy of the approximation, point 4 must be relocated, based on the average values of flow properties, by using the last-determined values of the flow properties at point 4. Then, all the flow properties can be recalculated by using these same average values.

14. Repeat step 6 to relocate point 4. Repeat step 7 to relocate point 3. Repeat step 8 to set all $P_{i4} = P_4$ as just determined. Repeat step 9 to recalculate SIG 1, SIG 2, and SIG 3. Repeat step 10 to recalculate ρ_{p4}, Ψ_{p4}, and to locate point 5. Repeat step 11 to recalculate gas properties at point 4. Repeat step 12 to recalculate particle properties at point 4. Thus, point 4 is relocated, and all the flow properties at point 4 have been recalculated. Apply the following convergence test on all flow properties:

$$\left| \frac{P\ (n+1) - P(n)}{P(n+1)} \right| \leq L.$$

When the test has been satisfied by all flow properties, the solution for the location and properties at point 4 is complete. If the solution does not converge, the entire procedure must be repeated until convergence is achieved.

EXAMPLE CALCULATION FOR VERIFICATION OF COMPUTER PROGRAM

To check the general validity of both the theory and accuracy of the computer program, a numerical example was calculated for a general interior point. A solid propellant that contains aluminum was chosen. The exhaust gases contained 0.48 lb of aluminum oxide per lb of gas.

Particle properties were defined listing six discrete particle sizes (Table I-1). The transport properties of the gas phase at chamber stagnation conditions were defined and are given in Table I-2. T_g, γ_g, and C_{pg} are given as functions of gas temperature in Table I-3. The temperature-enthalpy relationship for solid and liquid aluminum oxide is shown in Table I—4 with other particle properties needed for the solution. The f and g parameters as functions of Reynolds number were obtained from current studies and are presented in Table I-5. Values listed in this table may be considered as permanent values of f and g for all subsequent work. Units of physical parameters are shown in Table I-6.

The general and specific data, outlined in Appendix H, are shown in Tables I-7 and -8, respecitvely. The example calculation is based on the characteristic net shown in Figure I-1 and the location and properties for the general interior point 4 are given in Table I-9.

The gas viscosity for several propellants was found to satisfy the relationship.

$$\mu_g = \mu_o \, T_g^{0.787}$$

Hence, if μ_g is known at any temperature, μ_o may be determined. Usually μ_g is known at the flame temperature as a result of thermochemical calculations.

In comparison of results, u_g and v_g decreased, and ρ_g and P_g remained about the same, and T_g increased, which is almost opposite to the trend expected in a perfect-gas flow. However, in the example calculation, u_p and v_p increased,

and ρ_p and h_p decreased, which was the expected trend. The apparent inconsistencies in the gas properties are due to the fact that this problem was artificially conceived. An actual problem beginning at the supersonic starting line should behave in a more normal manner.

The example calculation appears to verify the theory developed in the preceeding appendixes and authenticate the correctness of the computer program.

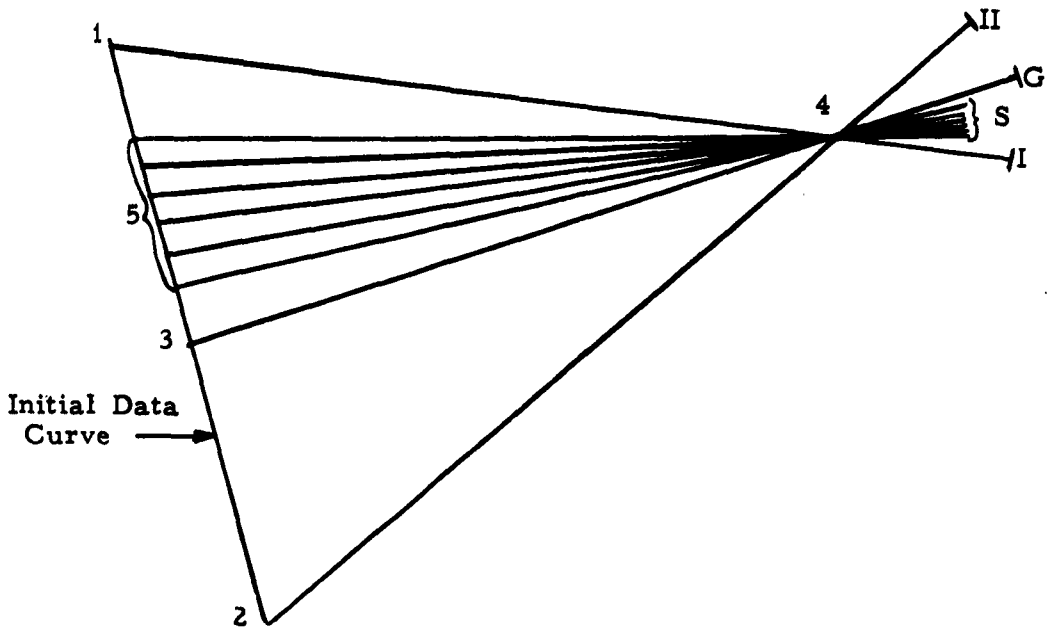

Figure I-1

Characteristic Net and Point 4

Table I-1

PARTICLE PROPERTIES

Chemical Species = Al_2O_3

$$\frac{\text{Mass flow rate of particles}}{\text{Mass flow rate of gas}} = 0.46$$

Particle Radii, microns

$r_{p1} = 0.45$

$r_{p2} = 0.72$

$r_{p3} = 0.90$

$r_{p4} = 1.15$

$r_{p5} = 1.42$

$r_{p6} = 1.75$

Table I-2

GAS TRANSPORT PROPERTIES

Pressure, P_g	1,000.0 psia
Temperature, Tg	6,650.0 °R
Molecular Weight (Gas)	20.99
Gas Constant, R	72.8 $\frac{\text{ft-lbf}}{\text{lbm-°R}}$
Specific Heat Ratio, γ_g	1.20
Constant Pressure Specific Heat, c_{pg}	0.4776 $\frac{\text{Btu}}{\text{lbm-°R}}$
Viscosity, μ_g	0.2416 $\frac{\text{lbm}}{\text{ft-hr}}$
Density, ρ_g	0.2940 $\frac{\text{lbm}}{\text{ft}^3}$
Prandtl Number, Pr	0.4996
Thermal Conductivity, k_g	0.2307 $\frac{\text{Btu}}{\text{ft-hr-°R}}$

Table I-3

γ_g AND C_{pg} VS TEMPERATURE

T_g, °R	γ_g	C_{pg}, $\frac{Btu}{lbm-°R}$
200	1.366	0.2860
500	1.365	0.2870
1,000	1.344	0.3130
2,000	1.297	0.3730
3,000	1.257	0.4210
4,000	1.244	0.4520
5,000	1.228	0.4700
6,000	1.212	0.4750
6,650	1.200	0.4776

Table I-4

PROPERTIES OF ALUMINUM OXIDE

$T_{pm} = 4,172.4\ °R$

$h_{ps} = 1,051.4\ \frac{Btu}{lbm}$

$h_{pl} = 1,695.5\ \frac{Btu}{lbm}$

Solid		Liquid	
h_p, $\frac{Btu}{lbm}$	T_p, °R	h_p, $\frac{Btu}{lbm}$	T_p, °R
-42.26	0	1,695.5	4,172.4
-40.89	180	1,745.6	4,320
0.62	540	1,807.2	4,500
37.90	720	3,043.0	8,100
80.80	900		
175.5	1,260		
276.9	1,620		
435.6	2,160		
598.6	2,700		
874.7	3,600		
1,051.4	4,172.4		

Table I-5

f AND g PARAMETERS AS FUNCTIONS OF REYNOLDS NUMBER*

Re	f	Re	g
0	1.0000	0	1.0000
1	1.0000	3	1.0000
4	1.4167	10	1.3750
10	1.7917	20	1.7000
40	3.1667	30	2.0000
70	4.0800	40	2.1500
100	4.7917	70	2.8000
200	6.6667	100	2.9300
500	12.1000		
1,000	16.6670		
	For Re ≥ 1,000, $f = 0.016667\ Re$		For Re ≥ 100, $g = 0.185\ (Re)^{0.60}$

* f data taken from Boundary Layer Theory by Schlichting
g data taken from Heat Transmission by McAdams

TABLE I-6

UNITS OF PHYSICAL PARAMETERS

C_p	specific heat at constant pressure	Btu/lbm-°R
c_{pg}	specific heat ratio of the gas	dimensionless
f	ratio of Nu to Nu for Stokes' flow	dimensionless
g	ratio of Nu to Nu for Stokes' flow	dimensionless
h_p	particle enthalpy	Btu/lbm
m_p	particle density per unit volume of particle	lbm/cu ft
P_g	gas static pressure	lbf/sq in.
Pr	Prandtl number	dimensionless
r_p	particle radius, based on spherical particles	micron
R	gas constant	Btu/lbm- °R
Re	Reynolds number	dimensionless
T_g	gas static temperature	°R
T_p	particle static temperature	°R
u_g	axial gas velocity component	ft/sec
u_p	axial particle velocity component	ft/sec
v_g	normal or radial gas velocity component	ft/sec
v_p	normal or radial particle velocity component	ft/sec
x	axial coordinate	ft
α	component of gas viscosity expression	dimensionless
μ_g	gas viscosity	lbm/ft-sec
μ_o	coefficient of gas viscosity expression	lbm/ft-sec(°R)$^{\alpha}$
ρ_g	gas density	lbm/cu ft
ρ_p	particle density per unit volume of gas	lbm/cu ft

TABLE I-7

GENERAL DATA

1. Axisymmetric flow, $\sigma_y = 1$
2. Six aluminum-oxide particles, $m_p = 247.61$, with the radii given in Table I-1.
3. f is given in Table I-5
4. g is given in Table I-5
5. γ is given in Table I-3
6. c_{pg} is given in Table I-3
7. T_p vs h_p is given in Table I-4
8. $T_{pm} = 4,172.4$
9. Pr = 0.4996
10. $\mu_o = 6.6 \times 10^{-8}$ and $\alpha = 0.787$
11. R = 72.8
12. K = L = 0.0001

TABLE I-8

SPECIFIC DATA AT INITIAL POINTS 1 AND 2*

1. $x_1 = 1.00000$

$y_1 = 0.60000$

2. $u_{g1} = 8,960.0$

$v_{g1} = 2,460.0$

$\rho_{g1} = 0.00022444$

$P_{g1} = 0.45500$

$T_{g1} = 4,010.0$

3. $u_{p1}(1) = 8,050$

$v_{p1}(1) = 2,140$

$\rho_{p1}(1) = 0.0000195$

$h_{p1}(1) = 1,035.2$

$T_{p1}(1) = 4,120.0$

$u_{p1}(2) = 7,650$

$v_{p1}(2) = 1,880$

$\rho_{p1}(2) = 0.0000862$

$h_{p1}(2) = 1,054.0$

$T_{p1}(2) = 4,172.4$

$u_{p1}(3) = 7,220$

$v_{p1}(3) = 1,640$

$\rho_{p1}(3) = 0.0000502$

$h_{p1}(3) = 1,300.0$

$T_{p1}(3) = 4,172.4$

$x_2 = 1.02500$

$y_2 = 0.50000$

$u_{g2} = 9,060.0$

$v_{g2} = 2,370.0$

$\rho_{g2} = 0.00018289$

$P_{g2} = 0.36800$

$T_{g2} = 3,980.0$

$u_{p2}(1) = 8,100$

$v_{p2}(1) = 2,200$

$\rho_{p2}(1) = 0.0000160$

$h_{p2}(1) = 1,029.1$

$T_{p2}(1) = 4,100.0$

$u_{p2}(2) = 7,710$

$v_{p2}(2) = 1,940$

$\rho_{p2}(2) = 0.0000710$

$h_{p2}(2) = 1,052.0$

$T_{p2}(2) = 4,172.4$

$u_{p2}(3) = 7,280$

$v_{p2}(3) = 1,700$

$\rho_{p2}(3) = 0.0000412$

$h_{p2}(3) = 1,295.0$

$T_{p2}(3) = 4,172.4$

TABLE I-8 (cont.)

u_{p1} (4) = 6,790
v_{p1} (4) = 1,420
ρ_{p1} (4) = 0.0000302
h_{p1} (4) = 1,696.0
T_{p1} (4) = 4,173.9

u_{p2} (4) = 6,850
v_{p2} (4) = 1,480
ρ_{p2} (4) = 0.0000249
h_{p2} (4) = 1,694.5
T_{p2} (4) = 4,172.4

u_{p1} (5) = 6,380
v_{p1} (5) = 1,225
ρ_{p1} (5) = 0.0000211
h_{p1} (5) = 1,697.3
T_{p1} (5) = 4,177.7

u_{p2} (5) = 6,420
v_{p2} (5) = 1,265
ρ_{p2} (5) = 0.0000173
h_{p2} (5) = 1,696.0
T_{p2} (5) = 4,173.9

u_{p1} (6) = 5,930
v_{p1} (6) = 1,030
ρ_{p1} (6) = 0.0000118
h_{p1} (6) = 1,779.8
T_{p1} (6) = 4,420.0

u_{p2} (6) = 5,970
v_{p2} (6) = 1,070
ρ_{p2} (6) = 0.0000097
h_{p2} (6) = 1,773.0
T_{p2} (6) = 4,400.0

* The location and properties of point 4 (Figure I-1 and Table I-8) for the above case are given in Table I-9 in the format printed out by the computer.

TABLE I-9

TRIAL CASE FOR A SUPERSONIC INTERIOR POINT OF A GAS PARTICLE FLOW

X-COORDINATE	Y-COORDINATE	MACH NUMBER	MACH ANGLE
1.1365	0.5811	2.5794	22.8104

GAS PROPERTIES

U	V	TEMPERATURE	FLOW DIRECTION	PRESSURE	DENSITY
8666.9	2044.0	4094.3	13.2702	4.1134E-01	1.9872E-04

PARTICLE PROPERTIES

PARTICLE	U	V	TEMPERATURE	ENTHALPY	FLOW DIRECTION	DENSITY
1	8658.5	2215.2	4038.0	1009.9	14.3506	1.5576E-05
2	8151.7	2040.1	4090.8	1026.2	14.0505	6.9926E-05
3	7719.1	1835.0	4172.4	1270.9	13.3721	4.0774E-05
4	7230.2	1607.7	4172.4	1677.9	12.5362	2.4889E-05
5	6758.9	1389.2	4172.4	1679.3	11.6142	1.7519E-05
6	6258.4	1174.7	4344.8	1754.1	10.6306	4.4466E-05

Aerojet-General Corporation
Sacramento, California

ANALYSIS OF THE FLOW OF GAS-PARTICLE MIXTURES IN TWO-DIMENSIONAL AND AXI-SYMMETRIC NOZZLES, by J. D. Hoffman.
September 1962. 34 PP 5 Illus.
9 Appendixes. Technical Report
AFBSD-TN-BSD-TDR-62-144

UNCLASSIFIED REPORT

From theoretical studies of two-phase flow of gas-particle mixtures in rocket nozzles, the governing equations for two-dimensional and axisymmetrical flows have been derived. A mathematical model has been developed for a general interior point in the supersonic field. The subsonic and transonic fields have been investigated. To integrate the subsonic, transonic, and supersonic solutions, a mathematical model will be programed for the IBM 7090 computer that will determine nozzle performance for given nozzle contour and motor contour and motor conditions.

UNCLASSIFIED

1. Analysis of the Flow of Gas-Particle Mixtures in Two-Dimensional Axisymmetric Nozzles

I. Aerojet-General Corporation

II. Air Force Ballistic Systems Division, Air Force Systems Command, USAF

III. Contract No. AF 33(600)-36610

UNCLASSIFIED

Aerojet-General Corporation
Sacramento, California

ANALYSIS OF THE FLOW OF GAS-PARTICLE MIXTURES IN TWO-DIMENSIONAL AND AXI-SYMMETRIC NOZZLES, by J. D. Hoffman.
September 1962. 34 PP 5 Illus.
9 Appendixes. Technical Report
AFBSD-TN-BSD-TDR-62-144

UNCLASSIFIED REPORT

From theoretical studies of two-phase flow of gas-particle mixtures in rocket nozzles, the governing equations for two-dimensional and axisymmetrical flows have been derived. A mathematical model has been developed for a general interior point in the supersonic field. The subsonic and transonic fields have been investigated. To integrate the subsonic, transonic, and supersonic solutions, a mathematical model will be programed for the IBM 7090 computer that will determine nozzle performance for given nozzle contour and motor contour and motor conditions.

UNCLASSIFIED

1. Analysis of the Flow of Gas-Particle Mixtures in Two-Dimensional Axisymmetric Nozzles

I. Aerojet-General Corporation

II. Air Force Ballistic Systems Division, Air Force Systems Command, USAF

III. Contract No. AF 33(600)-36610

UNCLASSIFIED

Aerojet-General Corporation
Sacramento, California

ANALYSIS OF THE FLOW OF GAS-PARTICLE MIXTURES IN TWO-DIMENSIONAL AND AXI-SYMMETRIC NOZZLES, by J. D. Hoffman.
September 1962. 34 PP 5 Illus.
9 Appendixes. Technical Report
AFBSD-TN-BSD-TDR-62-144

UNCLASSIFIED REPORT

From theoretical studies of two-phase flow of gas-particle mixtures in rocket nozzles, the governing equations for two-dimensional and axisymmetrical flows have been derived. A mathematical model has been developed for a general interior point in the supersonic field. The subsonic and transonic fields have been investigated. To integrate the subsonic, transonic, and supersonic solutions, a mathematical model will be programed for the IBM 7090 computer that will determine nozzle performance for given nozzle contour and motor contour and motor conditions.

UNCLASSIFIED

1. Analysis of the Flow of Gas-Particle Mixtures in Two-Dimensional Axisymmetric Nozzles

I. Aerojet-General Corporation

II. Air Force Ballistic Systems Division, Air Force Systems Command, USAF

III. Contract No. AF 33(600)-36610

UNCLASSIFIED

Aerojet-General Corporation
Sacramento, California

ANALYSIS OF THE FLOW OF GAS-PARTICLE MIXTURES IN TWO-DIMENSIONAL AND AXI-SYMMETRIC NOZZLES, by J. D. Hoffman.
September 1962. 34 PP 5 Illus.
9 Appendixes. Technical Report
AFBSD-TN-BSD-TDR-62-144

UNCLASSIFIED REPORT

From theoretical studies of two-phase flow of gas-particle mixtures in rocket nozzles, the governing equations for two-dimensional and axisymmetrical flows have been derived. A mathematical model has been developed for a general interior point in the supersonic field. The subsonic and transonic fields have been investigated. To integrate the subsonic, transonic, and supersonic solutions, a mathematical model will be programed for the IBM 7090 computer that will determine nozzle performance for given nozzle contour and motor contour and motor conditions.

UNCLASSIFIED

1. Analysis of the Flow of Gas-Particle Mixtures in Two-Dimensional Axisymmetric Nozzles

I. Aerojet-General Corporation

II. Air Force Ballistic Systems Division, Air Force Systems Command, USAF

III. Contract No. AF 33(600)-36610

UNCLASSIFIED